DISSERTATION

CLINICAL IMPORTANCE OF AUTOPHAGY DEPENDENCY AND INHIBITION IN CANCER TREATMENT

Submitted By

Kristen M. Van Eaton

School of Biomedical Engineering

In partial fulfillment of the requirements

For the Degree of Doctor of Philosophy

Colorado State University

Fort Collins, Colorado

Summer 2021

Doctoral Committee:

Advisor: Daniel L. Gustafson

Brian Munsky
Douglas Thamm
Andrew Thorburn
TingTing Yao

ABSTRACT

CLINICAL IMPORTANCE OF AUTOPHAGY DEPENDENCY AND INHIBITION IN CANCER TREATMENT

Autophagy, a lysosomal degradation recycling process, has a complex and context-dependent role in cancer. Certain cancers have been found to be inherently dependent on autophagy for survival regardless of the environment. Autophagy is also implicated as a mechanism of resistance to many chemotherapies. More autophagy dependent tumors are generally more sensitive to autophagy inhibition genetically and pharmacologically. Therefore, determining what tumors are autophagy dependent is important for selecting patients that are viable candidates for autophagy inhibition.

Currently, autophagy inhibition is being tested in over 90 clinical trials using FDA-approved hydroxychloroquine (HCQ) alone or in combination with other therapies. However, responses have been variable, especially in trials where HCQ is used as a monotherapy. Further, the relationship between HCQ pharmacokinetics and pharmacodynamics is not well understood in patients. Pharmacokinetics of HCQ and one of its active metabolites DHCQ was assessed in non-tumor bearing mice. Both parent and metabolite were observed at clinically relevant concentrations after 72 hr and this corresponded with evident autophagy inhibition in various tissues, although autophagy inhibition was inconsistent across the mice. The pharmacokinetic data established 60 mg/kg as the human equivalent dose observed in patients based on HCQ exposure. Cellular responses to HCQ were assessed in 2D cell culture, 3D tumor organoids, and *in*

vivo tumor xenografts using autophagy dependent and autophagy independent tumors. Overall, cellular responses were similar across the *in vitro* and *in vivo* methods. Autophagy was inhibited regardless of autophagy status, but autophagy dependent tumors had increased cell death and decreased cell proliferation at earlier time points and lower doses of HCQ, suggesting autophagy dependency matters for optimal results. Since autophagy inhibition was inconsistent *in vivo*, it is still important to determine better biomarkers and possibly consider using more potent autophagy inhibitors in the clinic.

Since there have not been any major advancements in osteosarcoma survival over the past four decades, autophagy dependency was assessed in osteosarcoma. Osteosarcoma was found to be intermediately to very dependent on autophagy following a genetic screen. Further, initially autophagy dependent tumor cells were able to survive and adapt to autophagy loss. Not all tumor cells adapted in the same way nor were these autophagy deficient tumor cells more sensitive to standard osteosarcoma chemotherapy, highlighting the difficulty of determining what context autophagy inhibition should be used in the clinic. Since some autophagy inhibitors like HCQ are lysosomal inhibitors and do not specifically target autophagy alone, the results of these studies also emphasized the importance of understanding whether autophagy inhibition via lysosomal degradation or autophagy inhibition of the autophagic pathway itself is superior. Overall, these results indicate targeting autophagy in osteosarcoma is a promising therapy.

ACKNOWLEDGEMENTS

I am extremely grateful for all the support I have received that have made this work possible and there are many people I would like to thank. First, to my advisor Dr. Daniel Gustafson, for his time and commitment to this project and to me. His expertise within the scientific community and in laboratory techniques have enabled me to become the scientist I am today. Also, a huge thanks to my committee members, Drs. Brian Munsky, Douglas Thamm, Andrew Thorburn, and TingTing Yao, for offering expertise and advice along the way. Without help and insight from others including Drs. Christina Towers, Daniel Regan, Dawn Duval, Sunetra Das, Ryan Hansen, and Christopher Allen, this project would not be where it is today. Thank you to the members of the Gustafson and Duval labs, most especially Dr. Kathryn Cronise and Rupa Idate, that allowed me to bounce ideas off of them and helped me with lab techniques. I am also grateful for the continuous support I received from the School of Biomedical Engineering including Dr. Stuart Tobet and Sara Mattern.

It cannot be understated the amount of support I have received from family and friends. To my parents- thank you for providing me the means to receive the education I have and for supporting my ambitions when I decided to go to graduate school. Thank you to my siblings, especially my twin sister Sarah, for having my back throughout this graduate school ride. Lastly, a special thank you to my husband Ross, for keeping me sane during the hardest times and reminding me this journey is worth it when I lost sight of that. Without everyone's unwavering presence, I would not be where I am today.

TABLE OF CONTENTS

ABSTRACT ii

ACKNOWLEDGEMENTS iv

Chapter One 1

Literature Review and Project Rationale 1

Molecular Mechanisms and Regulation of Autophagy 1

Overview 1

Regulation of the Pathway 2

Upstream Regulation 9

Autophagy in Cell Death 12

Mechanisms of Autophagy in Cancer 13

Overall Role in Cancer 13

Tumor Suppression 14

Tumor Promotion and Metastasis 16

Autophagy Dependency and Genotype Sensitivity 19

Preclinical and Clinical Targeting of Autophagy in Cancer 23

Pharmacologic Modulation of Autophagy 23

Preclinical Assessment of Autophagy Inhibition 26

Assessing Autophagy in the Clinic 27

Autophagy in Breast Cancer 31

Autophagy in Osteosarcoma 33

Autophagy in Comparative Oncology 36

Summary 38

References 40

Chapter Two 63

PK/PD Assessment of HCQ in Breast Cancer 63
Summary 63
Introduction/Motivation 64
Materials and Methods 66
Results 74
Discussion 97
References 103
Chapter Three 109
Autophagy dependency in osteosarcoma and subsequent clinical implications 109
Summary 109
Introduction/Motivation 110
Materials and Methods 113
Results 124
Discussion 147
References 152
Chapter Four 159
Conclusions and Future Directions 159
Conclusions 159
Future Directions 163

Chapter One

Literature Review and Project Rationale

Molecular Mechanisms and Regulation of Autophagy

Overview

Autophagy, meaning “self-eating” in Greek, is a catabolic process by which cellular components are recycled via lysosomes for energy to help maintain homeostasis [1]. The term autophagy was coined by Nobel Prize winner Christian de Duve in the 1960s [2, 3]. Autophagy is an evolutionarily conserved pathway from yeast to humans, induced by environmental stressors including nutrient deprivation, insufficient oxygen, pathogen infection, and oxidative stress due to reactive oxygen species [3]. Cells undergoing remodeling or differentiation also upregulate autophagy [1, 2]. Therefore, it has implications in growth and development as well as many diseases including cancer, neurodegeneration, and infectious diseases [1, 3, 4].

There are three types of autophagy: macroautophagy, chaperone-mediated autophagy, and microautophagy. Macroautophagy, the most studied form, is the process by which organelles, proteins, and other cytoplasmic components are encircled by a double membrane vesicle called an autophagosome that eventually fuses with a lysosome. Mitophagy, pexophagy, and xenophagy are special types of macroautophagy involved in the breakdown of specific intracellular components including mitochondria, peroxisomes, and intracellular bacteria, respectively [5]. During chaperone-mediated autophagy, soluble substrate proteins are selectively targeted to lysosomes via the

cytosolic chaperone heat-shock cognate of 70 kDA (HSC70), translocating the substrate proteins across the lysosomal membrane by binding to the lysosomal-associated membrane protein type 2A (LAMP-2A) [6, 7]. Microautophagy, the most poorly understood form of autophagy in higher eukaryotes, refers to the direct engulfment of cytosolic components by lysosomes through invaginations in their limiting membrane [3, 4, 7].

Regulation of the Pathway

Macroautophagy, hereafter referred to as autophagy in all following instances, requires four major steps: membrane initiation, membrane elongation, substrate sequestration, and fusion of the autophagosome with a lysosome (**Figure 1.1**). Phagophores, also known as pre-autophagosomal structures, are the beginning structures of autophagosomes thought to arise from the endoplasmic reticulum (ER) [3]. They elongate and fuse together while encapsulating cellular components targeted for autophagy degradation. Autophagosomes then fuse with lysosomes to form autolysosomes. The autophagosome content is degraded and recycled by acid hydrolases located in lysosomes [8].

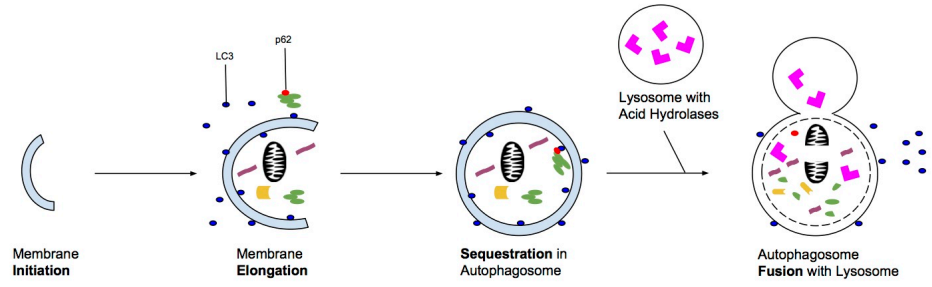

Figure 1.1 Process of autophagy. Steps of autophagy include membrane initiation, membrane elongation, formation of a full autophagosome that sequesters cellular contents, and fusion of the autophagosome to a lysosome with acid hydrolases to form an autolysosome where the contents of the autophagosome are broken down.

Autophagy is one of two mechanisms cells use for degrading proteins. The other pathway used to recycle proteins is the ubiquitin-proteasome system (UPS). The UPS typically degrades short-lived proteins while autophagy is responsible for degrading long-lived proteins [7]. Ultimately, the UPS tags a protein or a protein complex with the co-factor ubiquitin (Ub) which is recognized by catalytic protease complexes that break down proteins to peptides. The UPS uses three enzymatic components to Ub-tag proteins. The first enzyme component, E1, is the Ub-activating enzyme. The second, E2, is the Ub-carrier or conjugating protein that prepares Ub for conjugation to proteins. The third and most important enzymatic component is the E3, which is the Ub-protein ligase that recognizes a specific protein substrate and catalyzes the transfer of activated Ub to it. The Ub linked on proteins is recognized by the 26S proteasome, a catalytic protease complex that completes the degradation process [9]. The UPS shares some characteristics with autophagy. Autophagy contains two ubiquitin-like reactions during membrane elongation [3]. The other big commonality is the use of a Ub-binding protein. Autophagy uses p62, also known as sequestosome 1 (SQSTM1), a substrate that acts similarly to Ub by specifically targeting protein aggregates to autophagosomes for breakdown [3, 10].

More than 30 autophagy-related genes (ATGs) were first discovered in yeast. Since then, homologs have been found in eukaryotic cells [3]. Various autophagy proteins have different functions including interacting proteins, phosphatidylinositol 3-kinases (PI3Ks), serine/threonine kinases (STKs), and BH3-only proteins. PI3Ks are enzymes that positively regulate the PI3K pathway by phosphorylating other players in the pathway which helps control cellular processes such as metabolism, survival, proliferation,

apoptosis, growth, and migration [11]. STKs are enzymes that phosphorylate serine or threonine on transcription factors, cell cycle regulators, and various cytoplasmic and nuclear effectors, thereby functioning as homeostasis regulators [12]. BH3 proteins are a sub-family of BCL-2 family of proteins which are regulators of apoptosis [13].

Many of the autophagy proteins function together in complexes throughout the autophagic process (**Table 1.1 & Figure 1.2**). There are two complexes associated with membrane initiation. The Class III PI3K complex consists of VPS34, Beclin-1, ATG14L, and p150. VPS34 is a PI3K and its activity produces phosphatidylinositol-3-phosphate (PI3P) which is essential for the early stages of autophagy, though the precise role of PI3P in autophagosome formation is unknown. Beclin-1 has multiple binding proteins such as activating molecule in Beclin-1-regulated autophagy protein 1 (AMBRA1), UV radiation resistance-associated gene (UVRAG) product, and Bif-1. When all of these proteins are bound to Beclin-1, autophagy is induced but when their interaction with Beclin-1 is blocked, autophagosome formation is negatively affected. BCL-2, an anti-apoptotic protein, can also bind Beclin-1, causing inhibition of autophagy by sequestering Beclin-1 from the PI3K complex. ATG14L is a Beclin-1 interacting protein required as part of the complex to initiate autophagosome formation. p150 is a STK that is a VPS34 adaptor; the VPS34-p150 subset of the Class III PI3K complex is required for endocytosis. The other complex associated with membrane initiation is the ULK complex, comprised of ULK1/2, FIP200, and ATG13. ULK1 and ULK2 are STK homologs with redundant functions. FIP200 acts as a scaffold for ULK1/2. ATG13 binds ULK1 or ULK2, and this interaction mediates their interaction with FIP200. This complex is regulated in a nutrient-dependent manner. Under nutrient deprivation, ATG13 and ULK1/2 are

dephosphorylated which activates ULK1/2 to phosphorylate FIP200 to induce autophagosome formation [3, 5, 7, 14].

Table 1.1. ATG complexes and their associated proteins and functions.

Complex	**ATG Protein (Mammalian)**	**Features/Functions**
Class III PI3K (membrane initiation)	VPS34	PI3K*, produces PI3P for early-stage autophagy
	p150	STK**, VPS34 adaptor
	Beclin-1	BCL-2 interacting protein, BH3-only protein
	Atg14L	Beclin-1 interacting protein, autophagy inducer
	AMBRA1	Beclin-1 interacting protein, autophagy inducer
	UVRAG	Beclin-1 interacting protein, autophagy inducer
	Bif-1	Beclin-1 interacting protein, autophagy inducer
ULK1/2 (membrane initiation)	ULK1/2	STK**, homologs that interact with FIP200
	ATG13	Binds ULK1/2
	FIP200	Scaffold for ATG13 and ULK1/2
ATG5-ATG12 (membrane elongation)	ATG7	E1-like Ub activating enzyme, activates ATG12
	ATG12	Ub-like protein, covalently tagged to ATG5
	ATG5	Conjugated to ATG12
	ATG10	E2-like Ub conjugating enzyme, conjugates ATG5 to ATG12
	ATG16L1	Interacts with ATG5

LC3-PE (membrane elongation)	LC3	Protein that gets cleaved to form cytosolic LC3-I then cleaved again to form autophagosome membrane-bound LC3-II
	ATG4	Cysteine protease, cleaves LC3 to form cytosolic LC3-I
	ATG7	E1-like Ub activating enzyme, activates LC3-I
	ATG3	E2-like Ub conjugating enzyme, conjugates LC3 to PE to form LC3-II
Other ATG proteins	ATG9L1	Transmembrane protein, carries membrane for phagophore formation
	WIPI1/WIPI2	Colocalize with ATG14 and ATG16L during isolation membrane formation, bind PI3P
	p62	Substrate protein for selectively degrading protein aggregates via autophagy and mitochondria in mitophagy
	VMP1	Beclin-1 interacting protein, required for autophagosome formation
	STX17	Mediates fusion of autophagosome to the lysosome
	LAMP2	Lysosomal receptor, aids in fusion of autophagosomes and lysosomes

* PI3K = phosphatidylinositol 3-kinase, ** STK = serine/threonine kinase

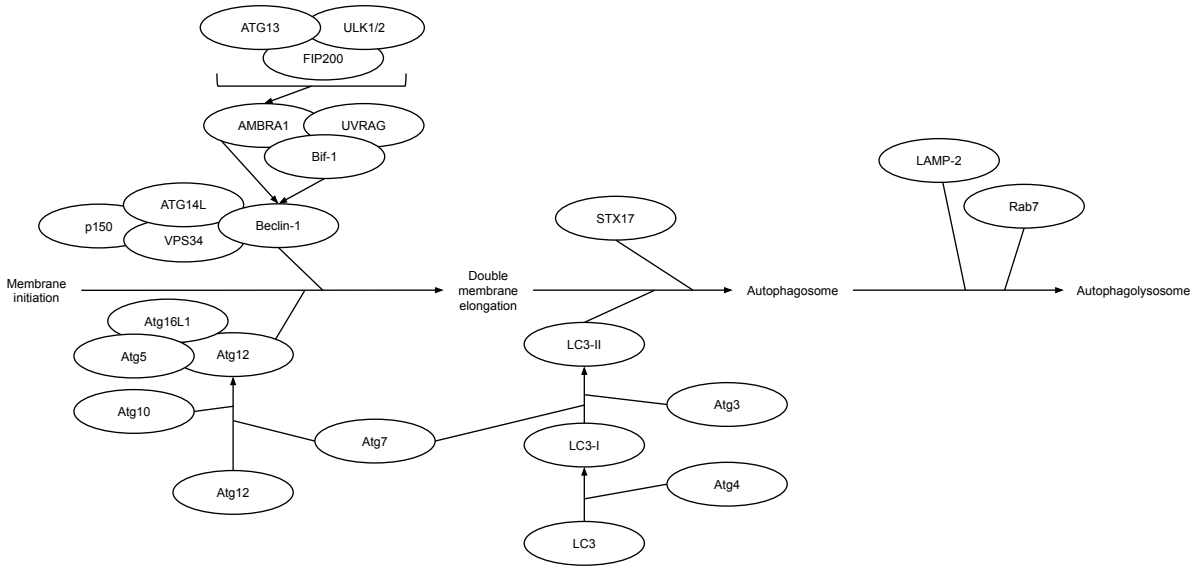

Figure 1.2 Proteins in the autophagy pathway. Many proteins in the autophagic pathway function together in complexes to ultimately help form an autophagosome filled with cargo to be degraded when the autophagosome fuses with an autolysosome.

The ATG5-ATG12 complex and the LC3-PE complex are ubiquitin-like conjugation systems that have vital roles in membrane elongation. In the ATG5-ATG12 complex, the E1 ubiquitin activating enzyme-like ATG7 activates the ubiquitin-like protein ATG12. ATG12 is then transferred to the E2 ubiquitin conjugating enzyme-like ATG10 where ATG12 is linked to ATG5. The ATG12-ATG5 linked proteins form a complex with ATG16L1. This complex aids in the elongation and closure of the autophagosome membrane and dissociates from the membrane immediately before or after complete autophagosome membrane formation. The formation of this complex occurs irrespective of nutrient conditions [3, 5, 7]. ATG5-ATG12-ATG16 is crucial for the in vivo functioning of the other ubiquitin-like conjugation system, called ATG8-PE in yeast but known as LC3-PE in mammalian cells. In yeast, ATG8 is cleaved by the cysteine protease ATG4, activated by E1-like ATG7, transferred to E2-like ATG3, and ultimately conjugated to lipid

phosphatidylethanolamine (PE). The ATG8 homologs in mammalian cells are Golgi-associated ATPase enhancer of 16 kDa (GATE-16), γ-aminobutyric acid type A receptor-associated protein (GABARAP), and microtubule-associated protein 1 light chain 3 (MAP1LC3). Light chain 3 (LC3) is cleaved by ATG4 to form LC3-I then further cleaved and conjugated by ATG3 to lipid PE to form LC3-II. LC3-I is a cytosolic soluble protein while LC3-II is a protein bound on both the inner and outer autophagosome membranes (**Figure 1.1**). The outer membrane-bound LC3-II is delipidated by ATG4 and recycled while the inner membrane-bound LC3-II is degraded following autophagosome-lysosome fusion. The ATG5-ATG12-ATG16L1 complex is critical to the LC3-PE functioning since it interacts with ATG3 and has been suggested to be involved in determining the site of LC3 lipidation [3, 5, 7].

Other ATG proteins important to successful autophagy completion are ATG9L1, WD-repeat proteins interacting with phosphoinositides (WIPI1&2) which are mammalian homologs to yeast ATG18, vacuole membrane protein 1 (VMP1), STX17, and LAMP2. ATG9 is the only known transmembrane protein among the core autophagy proteins. It carries membrane for phagophore expansion between the Golgi network and endosomes and finally localizes to the outer membrane of the autophagosome [3, 5]. WIPI1 and WIPI2 colocalize with ATG14 and ATG16L1 on the isolation membrane during autophagosome formation to help regulate the autophagy pathway through binding with PI3P [5, 14]. VMP1, only found in high eukaryote autophagy, is a transmembrane protein found on the ER and the Golgi. It interacts with Beclin-1 and is required for autophagosome formation via the recruitment and activation of the Class III PI3K complex. VMP1 expression triggers autophagy even in nutrient rich conditions [5, 15]. STX17 is a protein recruited to mature

autophagosomes and mediates their fusion to the lysosome so that incomplete membranes untagged with STX17 do not fuse with lysosomes [16]. LAMP2 is a lysosomal receptor that aids in the fusion of the autophagosome and the lysosome [3].

Beyond the ATG proteins involved in canonical autophagy, there are substrate proteins or adaptors used in selective autophagy. One of the most well-known autophagy substrates is p62. p62 facilitates the autophagic clearance of protein aggregates [3] and has been found to tag mitochondria during mitophagy although its use as a required adaptor for this process is debated [5]. p62 knockout mice exhibit no defect in bulk autophagy, showing that p62 does not seem necessary for the clearance of most autophagic substrates [3]. Although p62 is not required for bulk autophagy, its levels are elevated in autophagy-deficient or autophagy-suppressed situations while levels tend to decrease when autophagy is activated [3, 7].

Upstream Regulation

Multiple upstream proteins and signaling pathways regulate autophagy (**Figure 1.3**). The mammalian target of rapamycin (mTOR) is one of the most important regulators of autophagy. mTOR is a PI3K-related STK that controls metabolic stress signals to drive cellular growth, development, and proliferation when activated by abundant nutrients, growth factors, or hormones such as insulin [7, 17]. Although there are two complexes of mTOR, mTORC1 and mTORC2, only mTORC1 directly regulates autophagy [3, 5]. mTORC1 and autophagy have opposing roles; when mTORC1 is inhibited under nutrient deprivation, autophagy is induced. Autophagy is downregulated when mTORC1 is activated because mTORC1 directly interacts with the ULK1/2-ATG13-FIP200 complex

and phosphorylates (inactivates) ULK1 which inhibits initiation of autophagosome formation [3].

Upstream of mTOR, elevated levels of the PI3K/AKT and mitogen-activated protein kinase (MAPK)/extracellular signal-regulated kinase (ERK) pathways cause autophagy suppression [3, 17, 18]. PIK3K/AKT and MAPK/ERK are stress sensing pathways that function in cell growth, differentiation, survival, and proliferation [19, 20, 21, 22]. PI3K/AKT is a nutrient sensor [22] and MAPK/ERK is a sensor of diverse stimuli such as osmotic stress [21]. In the PI3K/AKT pathway, autophagy is suppressed when a PI3K activates AKT which in turn phosphorylates the tuberous sclerosis complex (TSC) 2, thereby suppressing the repressive action of the TSC complex and allowing mTOR activity [19, 23]. AKT has also been reported to inhibit adenosine monophosphate-activated protein kinase (AMPK) (discussed below), further stimulating mTOR activation [24]. The PI3K/AKT pathway can be inhibited by phosphatase and tensin homolog (PTEN), a tumor suppressor, which leads to autophagy stimulation [7]. The ERK1/2 MAPK-dependent pathway suppresses autophagy by the signaling cascade from MEK1/2 to ERK1/2; phosphorylation of ERK blocks the formation of the TSC1 and TSC2 complex due to phosphorylation of TSC2, allowing mTOR activation [3, 24].

Elevated levels of other upstream mTOR effectors conversely induce autophagy. AMPK mediates cellular metabolism in response to energy stress [25]. It negatively regulates mTOR by phosphorylating TSC2, thus enhancing the repressive function of TSC2 on mTORC1 [7, 25]. Although both AKT and AMPK phosphorylate the TSC complex, their phosphorylation statuses have opposing roles in activation or de-activation of mTOR due to the function of phosphorylating different sites on TSC2; AKT

phosphorylates TSC2 at Ser 939, Ser 1086/Ser 1088, or Thr 1422 which destabilizes TSC2 association with TSC1 [26] while AMPK phosphorylates TSC2 at Thr 1227 or Ser 1387 which enhances TSC2 function [7, 25]. AMPK also negatively regulates mTOR by phosphorylating the mTOR binding partner Raptor which results in the inactivation of Raptor and mTORC1 [7, 25]. Further, AMPK directly induces autophagy via its ability to phosphorylate ULK1 [7]. AMPK is regulated by a couple of tumor suppressors that are activated during metabolic stress and deprivation including liver kinase B1 (LKB1) and p53 [7, 17, 24]. LKB1 is a STK that phosphorylates AMPK at the activation-loop threonine [24, 25]. p53, a transcription factor that activates pro-apoptotic and cell-cycle arresting genes, has juxtaposing roles in autophagy modulation that is location dependent; nuclear p53 stimulates autophagy by activating autophagy-inducing genes such as damage-regulated autophagy modulator (DRAM) while cytoplasmic p53 suppresses autophagy in a poorly understood cell cycle-dependent manner [7, 17].

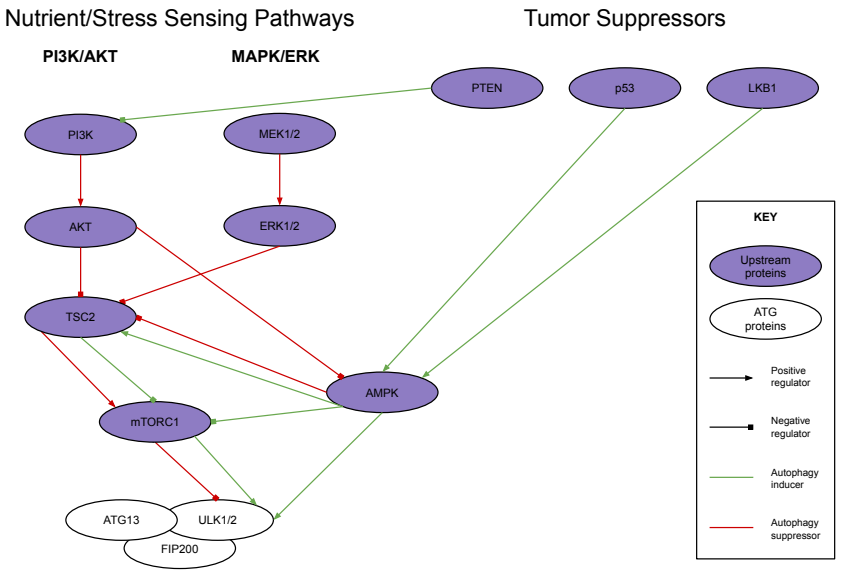

Figure 1.3 Pathways upstream of autophagy. Upstream regulators of autophagy include nutrient and stress sensing pathways and tumor suppressors, most of which act through mTOR to affect autophagic flux.

Autophagy is also regulated in a mTOR independent fashion via the cyclic overlap of intracytosolic calcium ion (Ca^{2+}) and calpain signaling with cyclic adenosine monophosphate (cAMP) and inositol signaling [3, 27]. High intracytosolic Ca^{2+} levels inhibit autophagy by first activating Ca^{2+}-dependent cysteine proteases called calpains. Calpains cleave the α-subunit of heterotrimeric G-proteins ($Gs\alpha$) whose activity ultimately leads to cAMP production. Upregulated cAMP signals one its two targets, Epac, to activate PLC-ε through the small G protein Rap2B which leads to the formation of inositol triphosphate (IP_3). High cAMP and IP_3 levels negatively regulate autophagy [3, 27].

Autophagy in Cell Death

Autophagy is somewhat controversially considered a type of cell death, although recent work suggests that autophagy itself is not the cause of death but rather necessary for cell death in context dependent manners [28, 29]. A few studies demonstrate autophagic cell death in a caspase-independent manner by inhibiting autophagy or knocking down autophagy genes and observing suppressed cell death [30, 31, 32]. However, the evidence of a causal role for autophagy was not established in most of these studies. More recent studies reveal that the role of autophagy cell death is autophagy-mediated, autophagy-associated, or autophagy-dependent in the absence of apoptosis and necrosis [29]. The difficulty of assessing autophagic cell death with respect to programmed cell death is particularly evident due to cross talk and sometimes contradictory overlap between autophagy and apoptosis [13, 33]. Autophagy proteins can regulate apoptosis through direct interaction with proteins in the apoptotic pathway. This includes non-conjugated forms of ATG5 and ATG12 which may have roles in the initiation of apoptosis that are independent of autophagy, as evidenced by no significant

effect on apoptosis following knockdown of essential autophagic genes [34, 35]. Beclin-1 is constitutively bound to the apoptotic factor BCL2 but dissociates under cell stress, suggesting its role in maintaining autophagy at levels appropriate for cell survival [36]. Further, apoptotic proteins can also regulate autophagy. Just as Beclin-1 regulates apoptosis via BCL2, BCL2 also regulates autophagy. One way this occurs is increased autophagy due to JNK1 or ERK phosphorylation of BCL2 [37, 38]. The anti-apoptotic protein MCL1 also regulates autophagy because its degradation induces autophagy [39]. Another way autophagy and apoptosis are connected is via autophagosome roles in apoptosis. Caspase activation occurs by their recruitment to autophagosomes (but not autolysosomes) and therefore the depletion of autophagy genes can lead to inhibition of caspase 8 activation and apoptosis [40]. It is clear that autophagy has important functions in cell death and characterizing its roles in context-dependent manners is vital to a greater understanding of this complexity [29].

Mechanisms of Autophagy in Cancer

Overall Role in Cancer

Since autophagy plays a major role in protein and organelle degradation and subsequent metabolism, it has been implicated in most cancer types and in cancer therapies as a mechanism of therapy resistance [17, 41, 42, 43]. Autophagy is associated with several of the hallmarks of cancer including sustained proliferative signaling, inducing angiogenesis, tissue invasion and metastasis, resisting cell death, and reprogramming energy metabolism [44, 45].

As a natural response to cellular stress, autophagy has a paradoxical role in the progression of cancer. During the early stages of tumor development and under basal conditions, autophagy is a protective mechanism by eliminating reactive oxygen species and potentially harmful organelles and misfolded proteins that can lead to genetic mutations that could ultimately lead to cancer. However, tumor cells may use autophagy to their advantage by providing themselves a means of producing energy to grow, proliferate, and eventually metastasize in a tumor environment with limited to no access to outside nutrients and oxygen for metabolism. It has been speculated that autophagy is a mechanism of tumor cell dormancy, allowing cells to avoid cell death and begin to invade and metastasize when the tumor environment is more ideal for them [44, 45]. There is a balance between the tumor suppressive and progressive roles of autophagy in cancer, but it is still unclear at what disease stage the cells take over autophagy [42, 44, 46]. Overall, the role of autophagy in cancer is complex and context dependent.

Tumor Suppression

Autophagy acts as a tumor suppressor in multiple ways. Directly, autophagy reduces DNA and ROS damage as well as removes damaged proteins and organelles [47]. Autophagy can also prevent centrosome abnormalities, aneuploidy, and chromosomal defects [3]. In one study, it was found that autophagy defective tumors accumulated p62, endoplasmic reticulum chaperones, damaged mitochondria, ROS, and genome damage but upon suppression of ROS or p62, damage resulting from the autophagy deficiency was prevented, suggesting that defective autophagy causing p62 upregulation contributes to tumorigenesis [48]. p62 protein levels are also upregulated in many human cancers, highlighting the role autophagy plays in degrading p62 through

completion of the process since without autophagy, p62 accumulates and contributes to tumorigenesis [49]. Another study revealed that p53, which is normally activated during stress conditions, is degraded by autophagy when it is mutant, showing that autophagy removes oncogenic proteins [50].

Indirectly, circumstantial evidence supports the ability of autophagy to help maintain genomic stability as a tumor suppressive function. This idea is driven by studies where mice with monoallelic loss of Beclin-1 develop spontaneous tumors [51, 52]. Others subsequently demonstrated that the mono-allelic deletion of Beclin-1 occurs in many types of human cancer including hepatocellular carcinoma, breast, ovarian, and prostate [52, 53, 54]. However, there is some doubt that Beclin-1 alone causes this phenomenon since the human homolog of the Beclin-1 gene is adjacent to other tumor suppressors on the same chromosome and therefore the tumorigenesis may be driven by loss of neighboring genes rather than Beclin-1 [55]. Somatic point deletions of ATG5 are also identified in many gastric, colorectal, and hepatocellular carcinoma patients, indicating the importance of autophagy genes in tumor suppression [56]. Frameshift mutations with mononucleotide repeats may be involved in cancer development by deregulating the autophagy process in gastric and colorectal cancer in genes such as ATG2B, ATG9B, ATG12, and ATG16L1 [57]. Further, autophagy attenuates inflammation; defects in autophagy are linked to a pro-inflammatory state that results in cellular dysfunction and death and creates a cancer-prone environment [58, 59]. Autophagy also stimulates anti-tumor immunity by enhancing the processing and presentation of tumor antigens [59].

Tumor Promotion and Metastasis

Conversely, autophagy also acts as a tumor promoter during later stages of cancer. Many of the explanations that describe the role of autophagy as a tumor promoter are opposite from its role as a tumor suppressor. Cancer cells use autophagy to supply nutrients and energy to themselves during various stress conditions including nutrient deprivation, starvation, hypoxia, damaging stimuli, and proteasome inhibition [3, 47, 60]. Knockdown of autophagy in epithelial tumor cells in an ischemic environment sensitized cells to metabolic stress [61]. Hypoxia is a characteristic of many advanced solid tumors [62] and hypoxia-inducible factors (HIFs) activated in these hypoxic environments have been shown to promote autophagy as a survival mechanism [63]. Cancer cells also use autophagy to prevent cell damage by removing damaged mitochondria through mitophagy which in turn reduces ROS production, allows oxygen and nutrients be consumed more efficiently, and promotes tumor cell survival [64]. Further, mice with a genetically distinct population of cells with deleted ATG5 or ATG7 form benign lesions in the liver but not elsewhere, suggesting that autophagy is important for the suppression of spontaneous tumorigenesis in a tissue specific manner [65].

Another role of autophagy in promoting tumor growth occurs during various stages of metastasis. In early stages of metastasis during epithelial-to-mesenchymal transition (EMT), in which intercellular adhesion is lost, the basement membrane and extracellular matrix are destroyed, the cytoskeleton is reconstructed, and cell motility is enhanced, autophagy can be beneficial or unfavorable for the cancer cells. Cells can be dependent on autophagy to survive EMT, demonstrated by one study where renal cell carcinoma with an EMT-like phenotype corresponded to higher autophagic flux [66]. In other studies,

autophagy plays key roles in focal adhesion dynamics, such as one in breast cancer where focal adhesions accumulated in autophagy deficient cells, reflecting the role of autophagy in focal adhesion disassembly [67]. On the other hand, autophagy also can prevent cells from entering EMT, shown in studies such as one in glioblastoma where autophagy induction reversed EMT by down-regulating two master regulators of the EMT process [68]. Further along in the metastatic process, autophagy enhances colonization of detached metastatic cells in destination organs. This was demonstrated in hepatocellular carcinoma where autophagy levels were higher in metastases compared to primary tumor sites and autophagy was only involved in colonization but not invasion, migration, or detachment of cells [69]. Knockdown of ATG12 in glioma cells also significantly reduced cellular invasion but did not affect cell viability, proliferation, or migration in a three-dimensional model [70]. Autophagy has also been shown to induce metastatic cells to enter dormancy to survive the new environment once they arrive [71]. For instance, autophagy was a critical mechanism to the survival of disseminated dormant breast cancer cells in both *in vitro* and *in vivo* models of dormancy [72]. In dormant human ovarian xenografts, high autophagy levels contributed to fast growth of tumors, but tumors were dormant when autophagy was blocked pharmacologically, indicating that autophagy contributed to the survival of dormant cells [73].

Within the tumor microenvironment, autophagy contributes to tumor progression in multiple ways. Autophagy can promote tumors to develop their own blood and lymphatic vessels through the process of angiogenesis to achieve proper oxygenation and nutrient supply [60]. This has been shown in renal cell carcinoma where co-culture with endothelial cells in the presence of upregulated HMGB1 (a nuclear protein implicated

in tumor progression and prognosis) increased autophagic proteins LC3-II and Beclin-1 and also increased angiogenesis factors VEGF and VEGFR2 in the endothelial cells but silencing of HMGB1 in the co-culture downregulated VEGF and VEGFR2, which is in line with another study that showed suppression of HMGB1 attenuated autophagy and enhanced cell death in bladder cancer [74]. Inhibition of autophagy in pancreatic ductal carcinoma cells increased the amount of intratumoral macrophages associated with pro-tumor qualities, causing tumor regression which implicates that autophagy partially regulates macrophage infiltration [75]. Autophagy is also linked to other non-tumor cells that make up the tumor microenvironment. When pancreatic ductal adenocarcinoma cells were co-cultured with pancreatic stellate cells, a specialized type of fibroblast, autophagy was found to be specifically upregulated in the stellate cells but autophagy was not upregulated in the stellate cells when they were co-cultured with normal ductal epithelia [76] This study also showed that the stellate cells use autophagy to secrete alanine which the tumor cells in turn use as an alternative carbon source to fuel the tricarboxylic acid cycle , highlighting the importance of autophagy for tumor cells even in indirect manners [76].

Lastly, autophagy is linked to resistance in tumors. It acts as a protective mechanism against cell death during cancer treatment [60]. For example, there is ample evidence of this in breast cancer treated with chemotherapies including paclitaxel, epirubicin, tamoxifen, and trastuzumab [77, 78, 79, 80]. Further, autophagy has been linked to multidrug resistance (MDR). This was shown where the expression level of MDR-1, a multidrug resistance gene, positively correlated with the expression of LC3 and Beclin-1 and negatively correlated with Raptor, a binding protein in the mTOR pathway,

in colorectal tumor samples, indicating that autophagy plays a role in MDR in the clinical setting [81]. High expression of ATG5 has also been connected to MDR. In human gastric cancer patients, ATG5 was highly expressed, its expression was positively correlated with the multidrug resistance-associated protein-1 (MRP-1), and its expression was significantly correlated to poor overall survival and disease-free survival, suggesting upregulated ATG5 is associated with chemoresistance [82].

Autophagy Dependency and Genotype Sensitivity

Autophagy dependency occurs when some cancer cells are especially dependent on autophagy even in the absence of added stress [83]. Many studies have showed that some, but not all, cancer cells are dependent on autophagy. This has been shown by genetic knockdown of essential autophagy genes as well as by pharmacological inhibition of autophagy. One study in pancreatic ductal adenocarcinoma conducted a CRISPR knockout screen of ATG5 or ATG7 on 17 cell lines and found some were very dependent on autophagy while others were much less dependent on these autophagy genes for survival [84]. Another study conducting a CRISPR screen knocking out essential autophagy genes in multiple types of cancer including breast, lung, colon, osteosarcoma, fibrosarcoma, and central nervous system cancers found that only some cell lines were initially dependent on autophagy for survival [85]. Further, studies have suggested that pharmacological inhibition of autophagy is only synergistic with other anticancer drugs when the cancer cells are autophagy dependent and can actually be antagonistic in autophagy independent tumor cells [83]. One study evaluating brain tumors found those that have high rates of induced autophagy following starvation were sensitive to genetic and pharmacologic inhibition of autophagy but the tumors that did not have highly induced

autophagy were not sensitive [86]. In another study of breast cancer, only autophagy dependent tumors responded to pharmacological inhibition of autophagy [43].

Mutations in multiple oncogenes and tumor suppressors have also been suggested to regulate autophagy dependence and cause increased sensitivity to autophagy inhibition [87]. For instance, mutations in RAS have been linked to autophagy dependency. Three ubiquitously expressed RAS genes HRAS, KRAS, and NRAS help control cell proliferation, differentiation and survival, and mutations of RAS that leave the protein constitutively active are widely observed in cancer [88]. One *in vivo* study in non-small cell lung cancer demonstrated that prior autophagy ablation did not alter the efficiency of cancer initiation but acute systemic ablation of autophagy in mice with pre-existing cancer was selectively destructive to established tumors compared to normal tissue and generated more benign disease [89]. RAS-expressing cells upregulate basal autophagy, and in human cell lines bearing activating mutations in RAS, down-regulating the expression of essential autophagy genes impaired cell growth in multiple cancer types including bladder, lung, pancreatic, colorectal, and prostate carcinomas [90]. Autophagy has also been shown to be essential for oncogenic KRAS-induced malignant cell transformation in human breast epithelial cells where ATG7 mRNA and protein levels were increased in cells overexpressing KRAS and autophagy suppression by ATG5 or ATG7 knockdown *in vitro* and *in vivo* decreased cell growth [91]. With the prevalence of autophagy dependency in RAS-activated cancers, subsequent downstream inhibition of RAS targets is synergistic with autophagy inhibition [87]. This has been shown in pancreatic ductal adenocarcinoma with KRAS activation treated concurrently with autophagy inhibitors and MEK1/2 inhibitors [92]. Another study in colorectal and

pancreatic cancer cell lines with activating KRAS mutations co-targeted MAPK and autophagy inhibition to efficiently eliminate KRAS mutant cells while minimizing toxicity in normal cells [93]. Farther down in the RAS pathway, autophagy is implicated in targeted therapy resistance in BRAF-mutant cancers, especially $BRAF^{V600E}$ mutated cancers [87]. Autophagy is upregulated in BRAF-mutant treatment resistant melanoma cells following treatment with BRAF and/or combined BRAF and MEK inhibitors [94]. When BRAF mutant melanoma cells lose ATG7, tumor growth decreases following BRAF inhibition compared to tumors without the ATG7 deficiency, suggesting autophagy inhibition combined with BRAF inhibition may improve therapeutic outcomes in $BRAF^{V600E}$ cancers [95]. Further, when BRAF mutant brain tumors are resistant to a BRAF inhibitor, genetic and pharmacologic inhibition of autophagy overcomes this resistance [86, 96].

About 50% of human cancers have mutations in the tumor suppressor p53 and p53 modulates autophagy through both its action in the nucleus and the cytoplasm [97]. Mutations in p53 can have contrasting roles on the effect of autophagy. For instance, mutant p53 proteins can counteract autophagy by localizing in the cytoplasm but not in the nucleus [98]. Mutant p53 proteins can also inhibit autophagy by blocking AMPK signaling [99, 100, 101], stimulating the AKT/mTOR pathway [100, 102], suppressing ATG12 [100], and inhibiting expression of multiple autophagy genes [103]. On the other hand, mutant p53 can promote autophagy by certain mutations failing to associate with FIP200 causing the loss of the autophagy inhibitory function [104]. Further, in the context of proteasomal inhibition, cancer cells with mutant p53 displayed activated autophagy [105]. In the presence of mutant p53, KRAS mutated tumors are still addicted to autophagy, indicating that mutant p53 does not always inhibit autophagy [106]. Further,

another study in pancreatic ductal adenocarcinoma found that all cell lines tested were sensitive to genetic and pharmacologic inhibition of autophagy regardless of the differing p53 status [107]. Given these studies, caution must be taken when determining which p53 mutations inhibit or enhance autophagy since the impact of p53 on autophagy is context dependent. Various genes have been suggested to be predictive of autophagy dependency and sensitivity to lysosomal inhibitors. For instance, a nine gene autophagy related signature classified high risk of early relapse colon cancer patients [108]. Another relapse autophagy score was predicted in colorectal cancer using five autophagy genes, suggesting predictivity of patients with high risk can be selected by the signature for more aggressive treatment interventions [109]. Lung and colon cancer cells expressing high levels of aldehyde dehydrogenase 1A1 (ALDH1A1) and concurrent low levels of helicase-like transcription factor (HLTF) or low levels of both ALDH1A1 and HLTF were especially vulnerable to lysosomal inhibitors [110]. These types of predictive signatures can help identify patients that would potentially benefit from autophagy inhibition.

There are some studies that challenge the idea of autophagy dependency because even autophagy dependent cancer cells can still grow as well as parental cells after complete inactivation of ATG7 [111]. This study found that a subset of cancer cell lines was sensitive to lysosomal inhibition but that autophagy genes are dispensable for growth. Studies like this could have discrepancies from studies that suggest autophagy dependency because of the use of short-term 2D assays, reliance on nutrient rich conditions, using only immune incompetent models, adaptations during selection of knockout clones, or an increased reliance on lysosomal scavenging pathways in adapted clones. Some of these discrepancies have recently been studied. For instance, clone

adaptation following selection has been shown in cancer cells following ATG7 knockout where clones that could not use canonical autophagy upregulated NRF2 [85]. Another study in pancreatic ductal adenocarcinoma showed that autophagy inhibition upregulates macropinocytosis via NRF2 activation, indicating cancer cells still use the lysosomal pathway even after autophagy inhibition [112].

Preclinical and Clinical Targeting of Autophagy in Cancer

Pharmacologic Modulation of Autophagy

Autophagy can be directly or indirectly modulated upstream and at various steps along the autophagy pathway using available compounds (**Table 1.2**). Common inducers of autophagy are rapamycin, metformin, lithium, and verapamil [113]. Rapamycin inhibits mTORC1 which enhances autophagy since mTOR is a negative regulator of autophagy. Rapamycin does not completely inhibit mTORC1 but it can induce autophagy at lower concentrations compared to ATP-competitive inhibitors in certain cell types, making it a viable option for achieving autophagy enhancement in the clinic [114]. Metformin, an antidiabetic agent, upregulates AMPK which induces ULK1 phosphorylation, leading to an active autophagic state [113]. Lithium, a mood-stabilizing drug, induces autophagy in a mTOR independent manner. It is suggested that it reduces mitochondrial uptake of Ca^{2+} released by the IP_3 receptor which causes a slight mitochondrial respiration defect and enhanced AMPK activation [115]. Verapamil was found through a large-scale drug screen to be a mTOR independent autophagy inducer of autophagy that has protective effects in models for Huntington's disease [116]. It lowers intracytosolic Ca^{2+} levels, inducing autophagy [113].

Autophagy inhibitors include chloroquine (CQ) and its derivative hydroxychloroquine (HCQ), DC661 which is a novel dimeric CQ, bafilomycin A1, spautin-1, wortmannin, and 3-methyladenine (3-MA) [117]. CQ, HCQ, Lys05, and DC661 are late-stage autophagy inhibitors. They are lysosomotropic agents that stop the fusion of autophagosomes to lysosomes [117]. More recently, it has been found that these drugs target palmitoyl-protein thioesterase (PPT1) on lysosomes, causing deacidification of the lysosome and inhibition of autophagy [118]. HCQ and Lys05 were able to inhibit PPT1 activity, but only DC661 maintained activity in the acidic environment, making it a promising autophagy inhibitor less prone to pH changes in tumors [118]. Bafilomycin A1 inhibits lysosomal hydrolases by blocking lysosomal proton transport; this blockage causes de-acidification of lysosomes since bafilomycin A1 does not allow the vacuolar-type H+-ATPases to couple with proton transport with ATP hydrolysis to maintain the acidic microenvironment [117]. Spautin-1 inhibits VPS34 by promoting the degradation of VPS34 complexes. This is achieved by its ability to inhibit the ubiquitin-specific peptidases USP10 and USP13, which are enzymes that deubiquitinate Beclin-1. When Beclin-1 is ubiquitinated, proteasomal degradation is activated instead of autophagic degradation [117]. Wortmannin and 3-MA are both PI3K inhibitors [117]. Wortmannin exerts effects on VPS34 while inhibiting PI3K via irreversible binding [119]. 3-MA targets VPS34 but also inhibits PI3K. It does not have high potency and needs to be used at high concentrations to prevent autophagy which also causes off-target effects [117]. More recent, targeted autophagy inhibitors are SBI-0206965, SAR405, NSC185058, and verteporfin [120]. SBI-0206965 is a small molecule inhibitor of ULK1 and has been shown to synergize with rapamycin to achieve autophagy inhibition and cell death [121]. SAR405

is a VPS34 inhibitor and its use affects vesicle trafficking between late endosomes and lysosomes, resulting in lysosomal function impairment [120]. NSC185058 is an ATG4 inhibitor, causing inhibition of LC3 lipidation and autophagy both *in vitro* and *in vivo* [122]. Verteporfin inhibits early-stage autophagy by not allowing autophagosome formation and does not cause autophagosome accumulation. It is not a potent single agent but has shown to be efficacious in dual treatment with gemcitabine and therefore may be a viable autophagy inhibitor in pancreatic ductal adenocarcinoma when combined with gemcitabine [123].

Table 1.2. Compounds used to modulate autophagy.

Compound	Inducer or Inhibitor	Function
Rapamycin	Inducer	Inhibits mTORC1
Metformin	Inducer	Upregulates AMPK which promotes ULK1 phosphorylation
Lithium	Inducer	Decreases IP3 levels
Verapamil	Inducer	Decreases intracytosolic Ca^{2+} levels
Chloroquine (CQ)/ Hydroxychloroquine (HCQ)	Inhibitor	Inhibits autophagosome-lysosome fusion
Lys05	Inhibitor	Inhibits autophagosome-lysosome fusion
DC661	Inhibitor	Inhibits autophagosome-lysosome fusion

Bafilomycin A1	Inhibitor	Blocks lysosomal proton transport which inhibits lysosomal hydrolases
Spautin-1	Inhibitor	VPS34 inhibitor
Wortmannin	Inhibitor	PI3K inhibitor
3-methyladenine (3-MA)	Inhibitor	PI3K inhibitor
SBI-0206965	Inhibitor	ULK1 inhibitor
SAR405	Inhibitor	VPS34 inhibitor
NSC185058	Inhibitor	ATG4 inhibitor
Verteporfin	Inhibitor	Inhibits autophagosome formation

Preclinical Assessment of Autophagy Inhibition

To date, extensive preclinical studies support the idea of inhibiting autophagy to improve clinical outcomes in cancer patients. This was revealed both *in vitro* and *in vivo* in cases where chemotherapies cause cancer cells to upregulate autophagy as a survival mechanism and combining autophagy inhibition genetically or pharmacologically demonstrates anti-tumor effects.

One of the first studies that showed autophagy serves as a survival pathway in tumor cells treated with apoptosis activators was done in a mouse model of B cell lymphoma with a p53-estrogen receptor tamoxifen-induced knockin where p53 can be temporally activated *in vivo*. Treatment with CQ modestly prevented tumor growth in the absence of p53 activation and also delayed tumor growth in p53 activated (and therefore apoptosis induced) tumors. Further analysis elucidated the p53 activated tumor cells that survived induced apoptosis and subsequent autophagy inhibition by CQ or ATG5

knockdown enhanced tumor cell death, suggesting a rationale for using autophagy inhibitors in combination therapies with apoptosis inducers [124]. Following this, many other studies have documented the activation of autophagy as a cytoprotective mechanism after treatment with other cancer therapies and subsequently show that autophagy inhibition promotes tumor cell death including in colorectal cancer following treatment with 5-fluorouracil both *in vitro* and *in vivo* [125], in prostate cancer cells following treatment with proteasome inhibitors such as bortezomib [126] or treatment with TKI inhibitors [127], in glioma cells after treatment with dual PI3K-mTOR inhibitors PI-103 and NVP-BEZ235 [128], and in ovarian cancer cells following paclitaxel [129]. Interestingly, some of these types of studies show that CQ or HCQ exhibits this affect but not always genetic knockdown or autophagy inhibitors that target other steps of the autophagy pathway. For instance, in renal carcinoma cells, HCQ inhibited cell growth and promoted apoptosis but ATG7 knockdown alone did not mimic the results of HCQ, indicating there are distinctions in autophagy independent functions that may contribute to sensitivities to [130]. These types of studies led to many clinical trials targeting autophagy in multiple types of cancer.

Assessing Autophagy in the Clinic

Currently, the majority of clinical trials target autophagy inhibition instead of autophagy induction. The most common autophagy drugs used in clinical trials are CQ and HCQ since they are FDA-approved, are low cost, and have a low toxicity profile [41, 131, 132, 133]. HCQ is used more often since it is less toxic than CQ at peak concentrations [120]. There are currently over 90 cancer clinical trials (ClinicalTrials.gov) using HCQ alone or in combination with other chemotherapies, radiation, and/or

immunotherapies. These trials are assessing the safety and efficacy of repurposing HCQ in cancer patients.

Pharmacokinetics (PK) and pharmacodynamics (PD) are critical elements in drug discovery, development, and approval. PK explains what the body does to the drug by how it is absorbed, distributed, metabolized, and excreted from the body. PD is what the drug does to the body and its mechanism of action. Dose, described by PK, leads to certain exposure of the drug throughout the body which in turn elicits a response based on that drug, described by PD [134]. Since PK and the subsequent PD are important in determining drug efficacy and function *in vivo*, doing these types of studies is vital to the drug development process.

Since HCQ is the most commonly use autophagy inhibitor in the clinic, its PK and tolerability is well-described. HCQ is almost completely and rapidly absorbed in the gastrointestinal tract following oral administration with a bioavailability of approximately 0.75 [135, 136, 137]. HCQ is approximately 50% bound to plasma proteins and it extensively sequesters in tissue [135, 138, 139]. It has a high volume of distribution and a prolonged half-life of 40-50 days due to its ability to partition into red blood cells and strongly bind to heme proteins [138, 139, 140]. HCQ is metabolized into multiple active metabolites including desethylhydroxychloroquine (DHCQ), desethylchloroquine (DCQ), and bisdesethylchloroquine (BDCQ), where DHCQ is the most abundant metabolite [135, 139, 141]. HCQ is cleared equally by the kidney and the liver [139].

In one completed phase II trial (NCT01273805), patients with previously treated metastatic pancreatic cancer were treated with either 400 mg or 600 mg of HCQ twice daily. Tolerability and efficacy were similar in both cohorts. Two of the 20 patients did not

have progressive disease at two months [142]. In another completed phase I trial treating non-small cell lung cancer, the safety and tolerability of HCQ with or without erlotinib, an epidermal growth factor receptor (EGFR) tyrosine kinase inhibitor (TKI) [143], was assessed in patients that previously responded to EGFR TKIs. Out of the 19 patients in the HCQ plus erlotinib cohort, one had partial response and four had stable disease. No maximum tolerated dose (MTD) was reached for HCQ and there were no adverse side effects. Moving forward, the recommended phase II dose of HCQ was the highest tested dose of 1000 mg when given in combination with 150 mg erlotinib [144]. More recent clinical trials include a phase II in pancreatic cancer where patients were treated with either gemcitabine plus nab-paclitaxel or gemcitabine plus nab-paclitaxel plus 1,200 mg HCQ daily prior to resection [145]. Overall, there was no difference in relapse-free survival between the two cohorts but there was significant improvement in response rates in the HCQ cohort compared to the gemcitabine/nab-paclitaxel only cohort. It was noted that this study did not control for adjuvant therapy but there was a trend toward improved survival in the group that received HCQ preoperatively suggesting the addition of HCQ postoperatively may benefit patients that received it preoperatively. In another phase II trial (NCT01227135) in chronic myeloid leukemia, patients were either given standard-of-care TKI inhibitor imatinib or imatinib plus 400-800 mg HCQ daily based on dose limiting toxicity. In this trial, there was no statistical difference in success rates between the two groups but there was an increasing trend towards success in the imatinib plus HCQ group at 24 months [146].

Although PK is well-known, autophagy PD has been harder to assess, especially in the clinic. Various preclinical studies and clinical trials have assessed p62 and LC3-II

levels in peripheral blood mononuclear cells (PBMCs) and peripheral lymphocytes to correlate autophagy inhibition. In the phase II trial (NCT01273805) previously described where pancreatic cancer patients were treated with HCQ alone, one of four patients and four of nine patients assessable with blood collection in the 400 mg and 600 mg cohorts, respectively, showed increased LC3-II levels in peripheral lymphocytes, suggesting autophagy inhibition is achievable with HCQ but inconsistent across the patient population [142]. Further, a phase I study combining HCQ with vorinostat in patients with solid tumors found that PBMCs may not be appropriate for monitoring HCQ-driven correlative PD endpoints because the levels of lysosomal protease cathepsin D gene expression, which they had previously showed to be a key mediator of HCQ and HCQ plus vorinostat-induced apoptosis, were only increased in patients given a combinatorial dose higher than the MTD [147]. In the chronic myeloid leukemia clinical trial, LC3-II puncta were often undetectable in peripheral blood and *ex vivo* HCQ treatment was required to determine LC3-II expression. This trial concluded that clinically achievable doses of HCQ are unlikely to achieve sufficient trough plasma concentration to accomplish meaningful autophagy inhibition [146]. One of the more positive trials where autophagy biomarkers correlated to HCQ dose was in the phase II trial in pancreatic cancer where patients were treated with either gemcitabine plus nab-paclitaxel or gemcitabine plus nab-paclitaxel plus high dose HCQ. This trial found a statistically significant increase in cytoplasmic p62 accumulation in the resected specimens from HCQ-treated patients but no difference in LC3-II staining between the two cohorts [145]. Given the large number of clinical trials using HCQ to target cancer, it is important to understand how HCQ exposure leads to cellular responses including the inhibition of

autophagy. These trials also highlight the potential need for more potent autophagy inhibitors to achieve sufficient autophagy inhibition in patients.

Autophagy in Breast Cancer

As of the beginning of 2020, breast cancer is the most diagnosed cancer in women and the second highest type of cancer-related death, accounting for approximately 15% of all cancer deaths in women [148]. Therefore, new therapies in breast cancer are important, especially given the number of patients that develop resistance to current breast cancer therapies [149]. Targeting autophagy in breast cancer is an encouraging prospect in this heterogenous disease given evidence that inhibition of autophagy enhances tumor cell death in combination with many anticancer therapies [149].

There are three major sub-types of breast cancer: 1) luminal which are estrogen or progesterone receptor (ER or PR) positive, 2) human epidermal growth factor 2 (HER2) enriched which overexpress the Erb-B2 receptor tyrosine kinase 2 (ERBB2), and 3) triple negative which do not express ER or PR nor contain HER2 amplification [150]. The luminal sub-type can be either HER2 positive (luminal B) or not (luminal A). Approximately 70% of diagnosed breast cancers are ER or PR positive, 15-20% are HER2 positive, and 15% are triple negative [150]. Triple negative tumors are characterized by a more aggressive phenotype and are most likely to become metastatic and resistant to therapy [149]. ER positive breast cancers are typically treated with anti-estrogen therapies such as tamoxifen, a selective estrogen receptor modulator. HER2 positive breast cancer is typically treated with HER2 directed antibodies such as trastuzumab plus cytotoxic chemotherapy. Triple negative breast cancer is typically treated with chemotherapy alone.

Cytotoxic chemotherapy options include docetaxel plus cyclophosphamide, Adriamycin plus cyclophosphamide, or Adriamycin plus cyclophosphamide plus paclitaxel [150].

However, it has been found that autophagy is as a mechanism of resistance to many of these therapies. For instance, autophagy facilitates resistance to anti-estrogen therapy in ER positive breast cancer [151]. It was further shown *in vivo* that tamoxifen plus CQ slowed tumor growth significantly in ER positive, tamoxifen-resistant cells [152]. When ER positive MCF7 cells were treated with paclitaxel, autophagy was upregulated [77]. HER2 positive SKBR3 cells increased autophagy when treated with the anti-HER2 monoclonal antibody trastuzumab and subsequent autophagy inhibition or knockdown of LC3 resulted in reduced cell proliferation and sensitized cells to trastuzumab treatment [80]. Protective autophagy also promotes resistance of HER2 positive cells to lapatinib, a chemotherapy sometimes used to treat HER2 positive patients [153]. Other studies have analyzed other chemotherapies that are either used as second- or third-line treatments or that may have potential usage in breast cancer patients and have also found autophagy as a cytoprotective mechanism against these treatments. For instance, autophagy was upregulated following camptothecin treatment [154]. In triple negative breast cancer cells, endoplasmic reticulum stress aggravators combined with autophagy inhibition both in vitro and in vivo caused significant attenuation of tumors [155]. Autophagy was also found to be a mechanism of resistance in breast tumor cells following ionizing radiation [156]. This evidence indicates the potential benefit of autophagy inhibition in all types of breast cancer patients.

Interestingly, triple negative breast cancers happen to be the ones most dependent on autophagy, shown by knockdown of ATG5, ATG7, and Beclin-1 as well as

pharmacological inhibition of autophagy using CQ [43]. Other subtypes of breast cancer were able to survive despite the loss of essential autophagy genes, indicating they are not innately dependent on autophagy for survival. Consequently, triple negative breast cancers are more sensitive to autophagy inhibition [43, 157, 158]. On the other hand, HER2 positive breast cancers display low levels of basal autophagy and Beclin-1 loss is correlated with HER2 amplification [159, 160]. However, these types of breast cancer may still benefit from autophagy inhibition when it is combined with other chemotherapies.

Autophagy inhibition is currently being tested in a handful of clinical trials in breast cancer using CQ or HCQ. Results from one clinical where 500 mg CQ daily was given to patients two to six weeks prior to breast surgery showed no significant effects on breast cancer cell proliferation compared to the placebo cohort while there were issues associated with toxicity, potentially demonstrating the limitation of CQ clinically due to high inter-subject variability and possibly not targeting autophagy with CQ at the achievable doses in patients [161]. Currently, five clinical trials are recruiting or are about to start recruiting breast cancer patients for trials involving autophagy inhibition by HCQ (clinicaltrials.gov).

Autophagy in Osteosarcoma

Osteosarcoma (OSA), a rare type of bone cancer, mostly affects children, teenagers, and young adults between the ages of 10 and 30, and elderly adults. Many patients present with metastases or multifocal disease when diagnosed, and these patients have less than a 25% survival rate. The average three-year event-free survival rate in patients with good prognosis is about 75%. Survival rates have not made significant improvements in the past 30 years. Standard OSA treatment is neoadjuvant

chemotherapy and subsequent surgery which is followed up with adjuvant chemotherapy [162, 163]. Chemotherapy regimens for almost all OSA patients includes methotrexate, doxorubicin, carboplatin, and ifosfamide [164]. However, 35-45% of patients still have recurrent disease within five years of initial treatment [165, 166]. This includes patients that either initially responded to chemotherapy but then relapsed or that were unresponsive to begin with [22, 162, 163, 166, 167]. It is not known when chemotherapy resistance occurs but proposed mechanisms imply changes in signaling transduction pathways such as MAPK and PI3K, alterations of topoisomerase II, increased DNA damage repair, and chemotherapy-induced autophagy [166]. These indicate potential targets that may prevent chemoresistance or that may re-sensitize patients to the current standard OSA chemotherapies.

Recently, autophagy has been implicated as a mechanism of resistance to OSA standard of care treatment [22]. In one study, doxorubicin, cisplatin, and methotrexate induced HSP90AA1, a heat shock protein that has been found to be expressed extracellularly and involved in tumor progression and cancer cell invasion, by promoting autophagy *in vitro* and *in vivo* [168]. In human OSA cell lines, upregulation of high mobility group box 1 (HMGB1) during cisplatin, doxorubicin, and methotrexate promotes autophagy and subsequent drug resistance *in vitro* and *in vivo* [169, 170]. Human OSA cells treated with high dose cisplatin upregulated autophagy and cell proliferation was substantially decreased following combination treatment of 3-MA with cisplatin compared to those treated with cisplatin alone [171]. A few other studies in OSA have showed that combination treatment with an autophagy inhibitor can increase cell death [172, 173, 174, 175, 176, 177]. Recently, it was shown that overexpression of the oncogene COPS3

increases lung metastasis from OSA tumors and that Beclin-1, LC3-I, and LC3-II immunoprecipitated with COPS3, indicating that COPS3 overexpression induces autophagy. When autophagy was subsequently inhibited in this model, metastasis was significantly decreased [178]. Human OSA cells treated with the histone deacetylase inhibitor trichostatin A (TSA) induce autophagy as a survival mechanism and autophagy inhibition or genetic knockdown of autophagy following TSA treatment enhanced cell death [179].

Conversely, studies in OSA have demonstrated that chemotherapy treatments induce autophagy and this leads to cancer cell death. In a human OSA cell line, pelargonidin, a type of flavonoid plant product that when rich in the diet can lower risk for cancer development, induced cell death through the upregulation of autophagy [180]. Autophagy upregulation also accounted for the synergistic cytotoxicity between doxorubicin and roscovitine, a cyclin-dependent kinase inhibitor, in sarcoma cell lines including a human OSA line [181]. Human OSA cells treated with the mTOR inhibitor rapamycin had increased cell death and induced autophagy. Combination treatment of mTOR with cisplatin further enhanced cytotoxicity and stimulated autophagy [182]. Radiation therapy in combination with arsenic trioxide also induced autophagy and increased cytotoxicity in human OSA cells [183]. One study discovered that even though autophagy was upregulated in both cisplatin-sensitive and resistant OS cells, autophagy inhibition in the sensitive cells was more effective than autophagy inhibition in the resistant cells [184]. The conflicting evidence suggests that autophagy modulation in OSA is context-dependent, and caution should be taken when determining whether autophagy inhibition or enhancement is beneficial [22, 185].

Clinical data of autophagy in OSA is very limited. A recent study showed that high heat shock protein 27 (HSP27), which has correlates with chemoresistance and cytoprotective autophagy, is associated with poor response to chemotherapy and lower overall survival in OSA patients both at diagnosis and after neoadjuvant chemotherapy [186]. Further, this study showed that patients with little to no LC3-II puncta at resection following neoadjuvant chemotherapy have a poor prognosis. Therefore, the favorable risk group was HSP27-/LC3-II+ at resection; however, HSP27 and LC3-II should also be considered as independent biomarkers in OSA since there was no correlation between the presence of LC3-II puncta and total HSP27 expression. There is currently one clinical trial looking at combining HCQ with gemcitabine and paclitaxel in OSA in the clinic (NCT03598595). Overall, much more can be elucidated about how autophagy impacts OSA and OSA treatment clinically.

Autophagy in Comparative Oncology

Although the majority of clinical trials in relation to autophagy have been conducted in humans, canine companions are a valuable surrogate model for cancer trials. Dogs get naturally occurring OSA just as humans do. They have similar environmental risk factors to humans, are a more outbred population than inbred laboratory animals, have faster progression of disease compared to human malignancies that allows for more rapid collection of data, and are a good clinical model for drug testing and approval due to a lack of gold standard treatment regimens and lower research costs [187, 188]. Further, when canine cancers are compared to human cancers, many times they are indistinguishable from one another. For instance, genome wide studies have shown that the dog OSA profile is indistinguishable from the human pediatric osteosarcoma profile,

and that dog OSA is more akin to human OSA than any other human cancer to human OSA [187]. This is important because it means the dog can be used to study human OSA since it is one of the most common cancers in dogs but rare in humans.

Autophagy in canine cancer has been less extensively studied compared to autophagy in human cancer. However, trends of both cytoprotective and cytotoxic autophagy exist. One study looking at multidrug analyses in canine soft tissue sarcomas used microinjections of multiple drugs to determine patient-specific tumor responses and found a subset of doxorubicin resistant tumors in which subsequent treatment of the preclinical autophagy inhibitor PS-1001 enhanced antitumor activity, and increased macrophage infiltration [189]. Another study of canine OSA cells determined that the autophagy inhibitor spautin-1 either alone or combined with doxorubicin treatment enhanced cell killing [190]. On the other hand, canine cancer cell lines treated with cannabidiol (CBD) had increased autophagy that presumably led to apoptotic cell death, indicating that CBD in the cell lines induced cytotoxic autophagy [191]. Another recent study found that canine squamous cell carcinomas activate autophagy prior to cell death following treatment with the survivin inhibitor YM155 and this toxic effect was diminished when autophagy was inhibited with CQ [192].

Clinically, even less is known about autophagy in canine cancer. One study analyzed Beclin-1 expression in 70 cases of canine mammary tumors and found that low cytoplasmic Beclin-1 expression was a poor prognostic factor for overall survival, indicating that loss of Beclin-1 is associated with aggressive clinicopathologic features [193]. Another retrospective study in canine mammary tumors found that lower p62 levels results in high grade carcinomas while high p62 levels were found in normal tissue and

adenomas [194]. Both of these studies suggest low autophagy levels results in more aggressive tumors. On the contrary, there has been one phase I/II clinical trial in dogs with lymphoma analyzing autophagy inhibition. Dogs with lymphoma have similar pathogenesis and response to treatment as human lymphoma patients. Patients received between 5 mg/kg up to 12.5 mg/kg HCQ daily plus 25 mg/m^2 doxorubicin. There was an increase in autophagic vesicles after HCQ treatment and a slight but not significant increase in LC3-II in patients that received HCQ. Nine of the twelve dogs achieved remission and the combination dosing provided superior overall response rates and progression-free intervals compared to dogs only receiving doxorubicin alone [195]. Overall, more studies would help elucidate the fate of cancer in response to autophagy inhibition or enhancement in canine cancer.

Summary

Autophagy plays important and context-dependent roles in many types of cancer and is therefore a promising target in cancer patients [55, 60]. However, it is important to understand which patients will benefit from autophagy manipulation and when this manipulation is beneficial. The following chapters explore some of this complexity and attempt to clarify a few aspects of autophagy inhibition as it relates to HCQ dosing in breast cancer as well as explore autophagy dependency in OSA. First, since HCQ is being used in many clinical trials but the PD is difficult to evaluate, PK/PD was assessed *in vivo* in non-tumor bearing mice to establish exposure observed in the clinic and determine if that exposure leads to consistent autophagy inhibition. PD including cell death, cell cycle, and autophagic flux following clinically achievable HCQ treatment was

also assessed *in vitro* in both 2D cell culture and 3D tumor organoids and *in vivo* in tumor-bearing mice to demonstrate that *in vitro* studies are a surrogate for what is observed *in vivo*. Secondly, autophagy dependency was determined by gene knockouts in canine OSA. Clones deficient in autophagy from OSA cell lines that were differentially dependent on autophagy were then explored. All of these findings highlight the variable roles autophagy plays in patients even with the same type of cancer and the need to determine which patients will benefit the most from autophagy inhibition clinically.

References

1. Yang Z, Klionsky DJ. Eaten alive: a history of macroautophagy. Nat Cell Biol. 2010 Sep;12(9):814-22. doi: 10.1038/ncb0910-814. PubMed PMID: 20811353; PubMed Central PMCID: PMCPMC3616322.

2. De Duve C, Wattiaux R. Functions of lysosomes. Annu Rev Physiol. 1966;28:435-92. doi: 10.1146/annurev.ph.28.030166.002251. PubMed PMID: 5322983.

3. Ravikumar B, Sarkar S, Davies JE, et al. Regulation of mammalian autophagy in physiology and pathophysiology. Physiol Rev. 2010 Oct;90(4):1383-435. doi: 10.1152/physrev.00030.2009. PubMed PMID: 20959619.

4. Mizushima N, Levine B, Cuervo AM, et al. Autophagy fights disease through cellular self-digestion. Nature. 2008 Feb 28;451(7182):1069-75. doi: 10.1038/nature06639. PubMed PMID: 18305538; PubMed Central PMCID: PMCPMC2670399.

5. Mizushima N, Yoshimori T, Ohsumi Y. The role of Atg proteins in autophagosome formation. Annu Rev Cell Dev Biol. 2011;27:107-32. doi: 10.1146/annurev-cellbio-092910-154005. PubMed PMID: 21801009.

6. Arias E, Cuervo AM. Chaperone-mediated autophagy in protein quality control. Curr Opin Cell Biol. 2011 Apr;23(2):184-9. doi: 10.1016/j.ceb.2010.10.009. PubMed PMID: 21094035; PubMed Central PMCID: PMCPMC3078170.

7. Cheng Y, Ren X, Hait WN, et al. Therapeutic targeting of autophagy in disease: biology and pharmacology. Pharmacol Rev. 2013;65(4):1162-97. doi: 10.1124/pr.112.007120. PubMed PMID: 23943849; PubMed Central PMCID: PMCPMC3799234.

8. Kondo Y, Kanzawa T, Sawaya R, et al. The role of autophagy in cancer development and response to therapy. Nat Rev Cancer. 2005 Sep;5(9):726-34. doi: 10.1038/nrc1692. PubMed PMID: 16148885.

9. Lecker SH, Goldberg AL, Mitch WE. Protein degradation by the ubiquitin-proteasome pathway in normal and disease states. J Am Soc Nephrol. 2006 Jul;17(7):1807-19. doi: 10.1681/ASN.2006010083. PubMed PMID: 16738015.

10. Pankiv S, Clausen TH, Lamark T, et al. p62/SQSTM1 binds directly to Atg8/LC3 to facilitate degradation of ubiquitinated protein aggregates by autophagy. J Biol Chem. 2007 Aug 17;282(33):24131-45. doi: 10.1074/jbc.M702824200. PubMed PMID: 17580304.

11. Chalhoub N, Baker SJ. PTEN and the PI3-kinase pathway in cancer. Annu Rev Pathol. 2009;4:127-50. doi: 10.1146/annurev.pathol.4.110807.092311. PubMed PMID: 18767981; PubMed Central PMCID: PMCPMC2710138.

12. Capra M, Nuciforo PG, Confalonieri S, et al. Frequent alterations in the expression of serine/threonine kinases in human cancers. Cancer Res. 2006 Aug 15;66(16):8147-54. doi: 10.1158/0008-5472.CAN-05-3489. PubMed PMID: 16912193.

13. Lomonosova E, Chinnadurai G. BH3-only proteins in apoptosis and beyond: an overview. Oncogene. 2008 Dec;27 Suppl 1:S2-19. doi: 10.1038/onc.2009.39. PubMed PMID: 19641503; PubMed Central PMCID: PMCPMC2928556.

14. Simonsen A, Tooze SA. Coordination of membrane events during autophagy by multiple class III PI3-kinase complexes. J Cell Biol. 2009 Sep 21;186(6):773-82. doi: 10.1083/jcb.200907014. PubMed PMID: 19797076; PubMed Central PMCID: PMCPMC2753151.

15. Molejon MI, Ropolo A, Re AL, et al. The VMP1-Beclin 1 interaction regulates autophagy induction. Sci Rep. 2013;3:1055. doi: 10.1038/srep01055. PubMed PMID: 23316280; PubMed Central PMCID: PMCPMC3542764.

16. Bernard A, Klionsky DJ. Toward an understanding of autophagosome-lysosome fusion: The unsuspected role of ATG14. Autophagy. 2015 Apr 3;11(4):583-4. doi: 10.1080/15548627.2015.1029220. PubMed PMID: 25920502; PubMed Central PMCID: PMCPMC4502729.

17. Duffy A, Le J, Sausville E, et al. Autophagy modulation: a target for cancer treatment development. Cancer Chemother Pharmacol. 2015 Mar;75(3):439-47. doi: 10.1007/s00280-014-2637-z. PubMed PMID: 25422156.

18. Yang ZJ, Chee CE, Huang S, et al. The role of autophagy in cancer: therapeutic implications. Mol Cancer Ther. 2011 Sep;10(9):1533-41. doi: 10.1158/1535-7163.MCT-11-0047. PubMed PMID: 21878654; PubMed Central PMCID: PMCPMC3170456.

19. Heras-Sandoval D, Perez-Rojas JM, Hernandez-Damian J, et al. The role of PI3K/AKT/mTOR pathway in the modulation of autophagy and the clearance of protein aggregates in neurodegeneration. Cell Signal. 2014 Dec;26(12):2694-701. doi: 10.1016/j.cellsig.2014.08.019. PubMed PMID: 25173700.

20. Pages G, Guerin S, Grall D, et al. Defective Thymocyte Maturation in p44 MAP Kinase (Erk 1) Knockout Mice. Science. 1999;286(5443):1374-1377.

21. Pearson G, Robinson F, Beers Gibson T, et al. Mitogen-Activated Protein (MAP) Kinase Pathways: Regulation and Physiological Functions*. Endocrine Reviews. 2001;22(2):153-183. doi: 10.1210/edrv.22.2.0428.

22. O'Farrill JS, Gordon N. Autophagy in Osteosarcoma. In: Kleinerman MD, Eugenie S, editors. Current Advances in Osteosarcoma: Springer International Publishing; 2014.

23. Manning BD, Toker A. AKT/PKB Signaling: Navigating the Network. Cell. 2017 Apr 20;169(3):381-405. doi: 10.1016/j.cell.2017.04.001. PubMed PMID: 28431241; PubMed Central PMCID: PMCPMC5546324.

24. Shaw RJ, Cantley LC. Ras, PI(3)K and mTOR signalling controls tumour cell growth. Nature. 2006 May 25;441(7092):424-30. doi: 10.1038/nature04869. PubMed PMID: 16724053.

25. Shaw RJ. LKB1 and AMP-activated protein kinase control of mTOR signalling and growth. Acta Physiol (Oxf). 2009 May;196(1):65-80. doi: 10.1111/j.1748-1716.2009.01972.x. PubMed PMID: 19245654; PubMed Central PMCID: PMCPMC2760308.

26. Inoki K, Li Y, Zhu T, et al. TSC2 is phosphorylated and inhibited by Akt and suppresses mTOR signalling. Nat Cell Biol. 2002 Sep;4(9):648-57. doi: 10.1038/ncb839. PubMed PMID: 12172553.

27. Sarkar S, Ravikumar B, Floto RA, et al. Rapamycin and mTOR-independent autophagy inducers ameliorate toxicity of polyglutamine-expanded huntingtin and related proteinopathies. Cell Death Differ. 2009 Jan;16(1):46-56. doi: 10.1038/cdd.2008.110. PubMed PMID: 18636076.

28. Doherty J, Baehrecke EH. Life, death and autophagy. Nat Cell Biol. 2018 Oct;20(10):1110-1117. doi: 10.1038/s41556-018-0201-5. PubMed PMID: 30224761.

29. Denton D, Kumar S. Autophagy-dependent cell death. Cell Death Differ. 2019 Mar;26(4):605-616. doi: 10.1038/s41418-018-0252-y. PubMed PMID: 30568239; PubMed Central PMCID: PMCPMC6460387.

30. Byun JY, Yoon CH, An S, et al. The Rac1/MKK7/JNK pathway signals upregulation of Atg5 and subsequent autophagic cell death in response to oncogenic Ras. Carcinogenesis. 2009 Nov;30(11):1880-8. doi: 10.1093/carcin/bgp235. PubMed PMID: 19783847.

31. Elgendy M, Sheridan C, Brumatti G, et al. Oncogenic Ras-induced expression of Noxa and Beclin-1 promotes autophagic cell death and limits clonogenic survival. Mol Cell. 2011 Apr 8;42(1):23-35. doi: 10.1016/j.molcel.2011.02.009. PubMed PMID: 21353614.

32. Chen Y, McMillan-Ward E, Kong J, et al. Oxidative stress induces autophagic cell death independent of apoptosis in transformed and cancer cells. Cell Death Differ. 2008 Jan;15(1):171-82. doi: 10.1038/sj.cdd.4402233. PubMed PMID: 17917680.

33. Booth LA, Tavallai S, Hamed HA, et al. The role of cell signalling in the crosstalk between autophagy and apoptosis. Cell Signal. 2014 Mar;26(3):549-55. doi: 10.1016/j.cellsig.2013.11.028. PubMed PMID: 24308968; PubMed Central PMCID: PMCPMC4054685.

34. Yousefi S, Perozzo R, Schmid I, et al. Calpain-mediated cleavage of Atg5 switches autophagy to apoptosis. Nat Cell Biol. 2006 Oct;8(10):1124-32. doi: 10.1038/ncb1482. PubMed PMID: 16998475.

35. Rubinstein AD, Eisenstein M, Ber Y, et al. The autophagy protein Atg12 associates with antiapoptotic Bcl-2 family members to promote mitochondrial apoptosis. Mol Cell. 2011 Dec 9;44(5):698-709. doi: 10.1016/j.molcel.2011.10.014. PubMed PMID: 22152474.

36. Levine B, Yuan J. Autophagy in cell death: an innocent convict? J Clin Invest. 2005 Oct;115(10):2679-88. doi: 10.1172/JCI26390. PubMed PMID: 16200202; PubMed Central PMCID: PMCPMC1236698.

37. Wei Y, Pattingre S, Sinha S, et al. JNK1-mediated phosphorylation of Bcl-2 regulates starvation-induced autophagy. Mol Cell. 2008 Jun 20;30(6):678-88. doi: 10.1016/j.molcel.2008.06.001. PubMed PMID: 18570871; PubMed Central PMCID: PMCPMC2478643.

38. Tang D, Kang R, Livesey KM, et al. Endogenous HMGB1 regulates autophagy. J Cell Biol. 2010 Sep 6;190(5):881-92. doi: 10.1083/jcb.200911078. PubMed PMID: 20819940; PubMed Central PMCID: PMCPMC2935581.

39. Germain M, Nguyen AP, Le Grand JN, et al. MCL-1 is a stress sensor that regulates autophagy in a developmentally regulated manner. EMBO J. 2011 Jan 19;30(2):395-407. doi: 10.1038/emboj.2010.327. PubMed PMID: 21139567; PubMed Central PMCID: PMCPMC3025469.

40. Young MM, Takahashi Y, Khan O, et al. Autophagosomal membrane serves as platform for intracellular death-inducing signaling complex (iDISC)-mediated caspase-8 activation and apoptosis. J Biol Chem. 2012 Apr 6;287(15):12455-68. doi: 10.1074/jbc.M111.309104. PubMed PMID: 22362782; PubMed Central PMCID: PMCPMC3320995.

41. Thorburn A, Thamm DH, Gustafson DL. Autophagy and cancer therapy. Mol Pharmacol. 2014 Jun;85(6):830-8. doi: 10.1124/mol.114.091850. PubMed PMID: 24574520; PubMed Central PMCID: PMCPMC4014668.

42. White E, Mehnert JM, Chan CS. Autophagy, Metabolism, and Cancer. Clin Cancer Res. 2015 Nov 15;21(22):5037-46. doi: 10.1158/1078-0432.CCR-15-0490. PubMed PMID: 26567363; PubMed Central PMCID: PMCPMC4646728.

43. Maycotte P, Gearheart CM, Barnard R, et al. STAT3-mediated autophagy dependence identifies subtypes of breast cancer where autophagy inhibition can be efficacious. Cancer Res. 2014 May 1;74(9):2579-90. doi: 10.1158/0008-5472.CAN-13-3470. PubMed PMID: 24590058; PubMed Central PMCID: PMCPMC4008672.

44. Singh SS, Vats S, Chia AY, et al. Dual role of autophagy in hallmarks of cancer. Oncogene. 2018 Mar;37(9):1142-1158. doi: 10.1038/s41388-017-0046-6. PubMed PMID: 29255248.

45. Hanahan D, Weinberg RA. Hallmarks of cancer: the next generation. Cell. 2011 Mar 4;144(5):646-74. doi: 10.1016/j.cell.2011.02.013. PubMed PMID: 21376230.

46. Kimmelman AC. The dynamic nature of autophagy in cancer. Genes Dev. 2011 Oct 1;25(19):1999-2010. doi: 10.1101/gad.17558811. PubMed PMID: 21979913; PubMed Central PMCID: PMCPMC3197199.

47. Li X, He S, Ma B. Autophagy and autophagy-related proteins in cancer. Mol Cancer. 2020 Jan 22;19(1):12. doi: 10.1186/s12943-020-1138-4. PubMed PMID: 31969156; PubMed Central PMCID: PMCPMC6975070.

48. Mathew R, Karp CM, Beaudoin B, et al. Autophagy suppresses tumorigenesis through elimination of p62. Cell. 2009 Jun 12;137(6):1062-75. doi: 10.1016/j.cell.2009.03.048. PubMed PMID: 19524509; PubMed Central PMCID: PMCPMC2802318.

49. Moscat J, Diaz-Meco MT, Wooten MW. Signal integration and diversification through the p62 scaffold protein. Trends Biochem Sci. 2007 Feb;32(2):95-100. doi: 10.1016/j.tibs.2006.12.002. PubMed PMID: 17174552.

50. Rodriguez OC, Choudhury S, Kolukula V, et al. Dietary downregulation of mutant p53 levels via glucose restriction: mechanisms and implications for tumor therapy. Cell Cycle. 2012 Dec 1;11(23):4436-46. doi: 10.4161/cc.22778. PubMed PMID: 23151455; PubMed Central PMCID: PMCPMC3552926.

51. Qu X. Promotion of tumorigenesis by heterozygous disruption of the beclin 1 autophagy gene. Journal of Clinical Investigation. 2003;112(12):1809-1820. doi: 10.1172/jci200320039.

52. Liang XH, Jackson S, Seaman M, et al. Induction of autophagy and inhibition of tumorigenesis by beclin 1. Nature. 1999;402(6762).

53. Aita VM, Liang XH, Murty VVVS, et al. Cloning and genomic organization of beclin 1, a candidate tumor suppressor gene on chromosome 17q21. Genomics. 1999;59:59-65.

54. Ding ZB, Shi YH, Zhou J, et al. Association of autophagy defect with a malignant phenotype and poor prognosis of hepatocellular carcinoma. Cancer Res. 2008 Nov 15;68(22):9167-75. doi: 10.1158/0008-5472.CAN-08-1573. PubMed PMID: 19010888.

55. Onorati AV, Dyczynski M, Ojha R, et al. Targeting autophagy in cancer. Cancer. 2018 Aug;124(16):3307-3318. doi: 10.1002/cncr.31335. PubMed PMID: 29671878; PubMed Central PMCID: PMCPMC6108917.

56. An CH, Kim MS, Yoo NJ, et al. Mutational and expressional analyses of ATG5, an autophagy-related gene, in gastrointestinal cancers. Pathol Res Pract. 2011 Jul 15;207(7):433-7. doi: 10.1016/j.prp.2011.05.002. PubMed PMID: 21664058.

57. Kang MR, Kim MS, Oh JE, et al. Frameshift mutations of autophagy-related genes ATG2B, ATG5, ATG9B and ATG12 in gastric and colorectal cancers with microsatellite instability. J Pathol. 2009 Apr;217(5):702-6. doi: 10.1002/path.2509. PubMed PMID: 19197948.

58. White E, Karp C, Strohecker AM, et al. Role of autophagy in suppression of inflammation and cancer. Curr Opin Cell Biol. 2010 Apr;22(2):212-7. doi: 10.1016/j.ceb.2009.12.008. PubMed PMID: 20056400; PubMed Central PMCID: PMCPMC2857707.

59. Zhong Z, Sanchez-Lopez E, Karin M. Autophagy, Inflammation, and Immunity: A Troika Governing Cancer and Its Treatment. Cell. 2016 Jul 14;166(2):288-298. doi: 10.1016/j.cell.2016.05.051. PubMed PMID: 27419869; PubMed Central PMCID: PMCPMC4947210.

60. Kocaturk NM, Akkoc Y, Kig C, et al. Autophagy as a molecular target for cancer treatment. Eur J Pharm Sci. 2019 Jun 15;134:116-137. doi: 10.1016/j.ejps.2019.04.011. PubMed PMID: 30981885.

61. Degenhardt K, Mathew R, Beaudoin B, et al. Autophagy promotes tumor cell survival and restricts necrosis, inflammation, and tumorigenesis. Cancer Cell. 2006 Jul;10(1):51-64. doi: 10.1016/j.ccr.2006.06.001. PubMed PMID: 16843265; PubMed Central PMCID: PMCPMC2857533.

62. Vaupel P, Mayer A. Hypoxia in cancer: significance and impact on clinical outcome. Cancer Metastasis Rev. 2007 Jun;26(2):225-39. doi: 10.1007/s10555-007-9055-1. PubMed PMID: 17440684.

63. Majmundar AJ, Wong WJ, Simon MC. Hypoxia-inducible factors and the response to hypoxic stress. Mol Cell. 2010 Oct 22;40(2):294-309. doi: 10.1016/j.molcel.2010.09.022. PubMed PMID: 20965423; PubMed Central PMCID: PMCPMC3143508.

64. Chourasia AH, Tracy K, Frankenberger C, et al. Mitophagy defects arising from BNip3 loss promote mammary tumor progression to metastasis. EMBO Rep. 2015 Sep;16(9):1145-63. doi: 10.15252/embr.201540759. PubMed PMID: 26232272; PubMed Central PMCID: PMCPMC4576983.

65. Takamura A, Komatsu M, Hara T, et al. Autophagy-deficient mice develop multiple liver tumors. Genes Dev. 2011 Apr 15;25(8):795-800. doi: 10.1101/gad.2016211. PubMed PMID: 21498569; PubMed Central PMCID: PMCPMC3078705.

66. Singla M, Bhattacharyya S. Autophagy as a potential therapeutic target during epithelial to mesenchymal transition in renal cell carcinoma: An in vitro study. Biomed Pharmacother. 2017 Oct;94:332-340. doi: 10.1016/j.biopha.2017.07.070. PubMed PMID: 28772211.

67. Sharifi MN, Mowers EE, Drake LE, et al. Autophagy Promotes Focal Adhesion Disassembly and Cell Motility of Metastatic Tumor Cells through the Direct Interaction of Paxillin with LC3. Cell Rep. 2016 May 24;15(8):1660-72. doi: 10.1016/j.celrep.2016.04.065. PubMed PMID: 27184837; PubMed Central PMCID: PMCPMC4880529.

68. Catalano M, D'Alessandro G, Lepore F, et al. Autophagy induction impairs migration and invasion by reversing EMT in glioblastoma cells. Mol Oncol. 2015 Oct;9(8):1612-25. doi: 10.1016/j.molonc.2015.04.016. PubMed PMID: 26022108; PubMed Central PMCID: PMCPMC5528793.

69. Peng YF, Shi YH, Shen YH, et al. Promoting colonization in metastatic HCC cells by modulation of autophagy. PLoS One. 2013;8(9):e74407. doi: 10.1371/journal.pone.0074407. PubMed PMID: 24058558; PubMed Central PMCID: PMCPMC3772859.

70. Macintosh RL, Timpson P, Thorburn J, et al. Inhibition of autophagy impairs tumor cell invasion in an organotypic model. Cell Cycle. 2012 May 15;11(10):2022-9. doi: 10.4161/cc.20424. PubMed PMID: 22580450; PubMed Central PMCID: PMCPMC3359125.

71. Sosa MS, Bragado P, Aguirre-Ghiso JA. Mechanisms of disseminated cancer cell dormancy: an awakening field. Nat Rev Cancer. 2014 Sep;14(9):611-22. doi: 10.1038/nrc3793. PubMed PMID: 25118602; PubMed Central PMCID: PMCPMC4230700.

72. Vera-Ramirez L, Vodnala SK, Nini R, et al. Autophagy promotes the survival of dormant breast cancer cells and metastatic tumour recurrence. Nat Commun. 2018 May 22;9(1):1944. doi: 10.1038/s41467-018-04070-6. PubMed PMID: 29789598; PubMed Central PMCID: PMCPMC5964069.

73. Lu Z, Luo RZ, Lu Y, et al. The tumor suppressor gene ARHI regulates autophagy and tumor dormancy in human ovarian cancer cells. J Clin Invest. 2008 Dec;118(12):3917-29. doi: 10.1172/JCI35512. PubMed PMID: 19033662; PubMed Central PMCID: PMCPMC2582930.

74. Wu CZ, Zheng JJ, Bai YH, et al. HMGB1/RAGE axis mediates the apoptosis, invasion, autophagy, and angiogenesis of the renal cell carcinoma. Onco Targets Ther. 2018;11:4501-4510. doi: 10.2147/OTT.S167197. PubMed PMID: 30122942; PubMed Central PMCID: PMCPMC6078191.

75. Yang A, Herter-Sprie G, Zhang H, et al. Autophagy Sustains Pancreatic Cancer Growth through Both Cell-Autonomous and Nonautonomous Mechanisms. Cancer Discov. 2018 Mar;8(3):276-287. doi: 10.1158/2159-8290.CD-17-0952. PubMed PMID: 29317452; PubMed Central PMCID: PMCPMC5835190.

76. Sousa CM, Biancur DE, Wang X, et al. Pancreatic stellate cells support tumour metabolism through autophagic alanine secretion. Nature. 2016 Aug 25;536(7617):479-83. doi: 10.1038/nature19084. PubMed PMID: 27509858; PubMed Central PMCID: PMCPMC5228623.

77. Ajabnoor GM, Crook T, Coley HM. Paclitaxel resistance is associated with switch from apoptotic to autophagic cell death in MCF-7 breast cancer cells. Cell Death Dis. 2012 Jan 26;3:e260. doi: 10.1038/cddis.2011.139. PubMed PMID: 22278287; PubMed Central PMCID: PMCPMC3270273.

78. Qadir MA, Kwok B, Dragowska WH, et al. Macroautophagy inhibition sensitizes tamoxifen-resistant breast cancer cells and enhances mitochondrial depolarization. Breast Cancer Res Treat. 2008 Dec;112(3):389-403. doi: 10.1007/s10549-007-9873-4. PubMed PMID: 18172760.

79. Sun WL, Chen J, Wang YP, et al. Autophagy protects breast cancer cells from epirubicin-induced apoptosis and facilitates epirubicin-resistance development. Autophagy. 2011 Sep;7(9):1035-44. doi: 10.4161/auto.7.9.16521. PubMed PMID: 21646864.

80. Vazquez-Martin A, Oliveras-Ferraros C, Menendez JA. Autophagy facilitates the development of breast cancer resistance to the anti-HER2 monoclonal antibody trastuzumab. PLoS One. 2009 Jul 16;4(7):e6251. doi: 10.1371/journal.pone.0006251. PubMed PMID: 19606230; PubMed Central PMCID: PMCPMC2708925.

81. Shuhua W, Chenbo S, Yangyang L, et al. Autophagy-related genes Raptor, Rictor, and Beclin1 expression and relationship with multidrug resistance in colorectal carcinoma. Hum Pathol. 2015 Nov;46(11):1752-9. doi: 10.1016/j.humpath.2015.07.016. PubMed PMID: 26363527.

82. Ge J, Chen Z, Huang J, et al. Upregulation of autophagy-related gene-5 (ATG-5) is associated with chemoresistance in human gastric cancer. PLoS One. 2014;9(10):e110293. doi: 10.1371/journal.pone.0110293. PubMed PMID: 25329677; PubMed Central PMCID: PMCPMC4201506.

83. Levy JMM, Towers CG, Thorburn A. Targeting autophagy in cancer. Nat Rev Cancer. 2017 Sep;17(9):528-542. doi: 10.1038/nrc.2017.53. PubMed PMID: 28751651; PubMed Central PMCID: PMCPMC5975367.

84. New M, Van Acker T, Sakamaki JI, et al. MDH1 and MPP7 Regulate Autophagy in Pancreatic Ductal Adenocarcinoma. Cancer Res. 2019 Apr 15;79(8):1884-1898. doi: 10.1158/0008-5472.CAN-18-2553. PubMed PMID: 30765601; PubMed Central PMCID: PMCPMC6522344.

85. Towers CG, Fitzwalter BE, Regan D, et al. Cancer Cells Upregulate NRF2 Signaling to Adapt to Autophagy Inhibition. Dev Cell. 2019 Sep 23;50(6):690-703 e6. doi: 10.1016/j.devcel.2019.07.010. PubMed PMID: 31378590; PubMed Central PMCID: PMCPMC7233142.

86. Levy JM, Thompson JC, Griesinger AM, et al. Autophagy inhibition improves chemosensitivity in BRAF(V600E) brain tumors. Cancer Discov. 2014 Jul;4(7):773-80. doi: 10.1158/2159-8290.CD-14-0049. PubMed PMID: 24823863; PubMed Central PMCID: PMCPMC4090283.

87. Amaravadi RK, Kimmelman AC, Debnath J. Targeting Autophagy in Cancer: Recent Advances and Future Directions. Cancer Discov. 2019 Sep;9(9):1167-1181. doi: 10.1158/2159-8290.CD-19-0292. PubMed PMID: 31434711; PubMed Central PMCID: PMCPMC7306856.

88. Prior IA, Hood FE, Hartley JL. The Frequency of Ras Mutations in Cancer. Cancer Res. 2020 Jul 15;80(14):2969-2974. doi: 10.1158/0008-5472.CAN-19-3682. PubMed PMID: 32209560; PubMed Central PMCID: PMCPMC7367715.

89. Karsli-Uzunbas G, Guo JY, Price S, et al. Autophagy is required for glucose homeostasis and lung tumor maintenance. Cancer Discov. 2014 Aug;4(8):914-27. doi: 10.1158/2159-8290.CD-14-0363. PubMed PMID: 24875857; PubMed Central PMCID: PMCPMC4125614.

90. Guo JY, Chen HY, Mathew R, et al. Activated Ras requires autophagy to maintain oxidative metabolism and tumorigenesis. Genes Dev. 2011 Mar 1;25(5):460-70. doi: 10.1101/gad.2016311. PubMed PMID: 21317241; PubMed Central PMCID: PMCPMC3049287.

91. Kim MJ, Woo SJ, Yoon CH, et al. Involvement of autophagy in oncogenic K-Ras-induced malignant cell transformation. J Biol Chem. 2011 Apr 15;286(15):12924-32. doi: 10.1074/jbc.M110.138958. PubMed PMID: 21300795; PubMed Central PMCID: PMCPMC3075639.

92. Kinsey CG, Camolotto SA, Boespflug AM, et al. Protective autophagy elicited by RAF-->MEK-->ERK inhibition suggests a treatment strategy for RAS-driven cancers. Nat Med. 2019 Apr;25(4):620-627. doi: 10.1038/s41591-019-0367-9. PubMed PMID: 30833748; PubMed Central PMCID: PMCPMC6452642.

93. Lee CS, Lee LC, Yuan TL, et al. MAP kinase and autophagy pathways cooperate to maintain RAS mutant cancer cell survival. Proc Natl Acad Sci U S A. 2019 Mar 5;116(10):4508-4517. doi: 10.1073/pnas.1817494116. PubMed PMID: 30709910; PubMed Central PMCID: PMCPMC6410784.

94. Ma XH, Piao SF, Dey S, et al. Targeting ER stress-induced autophagy overcomes BRAF inhibitor resistance in melanoma. J Clin Invest. 2014 Mar;124(3):1406-17. doi: 10.1172/JCI70454. PubMed PMID: 24569374; PubMed Central PMCID: PMCPMC3934165.

95. Xie X, Koh JY, Price S, et al. Atg7 Overcomes Senescence and Promotes Growth of BrafV600E-Driven Melanoma. Cancer Discov. 2015 Apr;5(4):410-23. doi: 10.1158/2159-8290.CD-14-1473. PubMed PMID: 25673642; PubMed Central PMCID: PMCPMC4390491.

96. Mulcahy Levy JM, Zahedi S, Griesinger AM, et al. Autophagy inhibition overcomes multiple mechanisms of resistance to BRAF inhibition in brain tumors.

Elife. 2017 Jan 17;6. doi: 10.7554/eLife.19671. PubMed PMID: 28094001; PubMed Central PMCID: PMCPMC5241115.

97. Liu EY, Ryan KM. Autophagy and cancer--issues we need to digest. J Cell Sci. 2012 May 15;125(Pt 10):2349-58. doi: 10.1242/jcs.093708. PubMed PMID: 22641689.

98. Morselli E, Tasdemir E, Maiuri MC, et al. Mutant p53 protein localized in the cytoplasm inhibits autophagy. Cell Cycle. 2008 Oct;7(19):3056-61. doi: 10.4161/cc.7.19.6751. PubMed PMID: 18818522.

99. Herrero-Martin G, Hoyer-Hansen M, Fumaroia C, et al. TAK1 activates AMPK-dependent cytoprotective autophagy in TRAIL-treated epithelial cells. The EMBO Journal. 2009;28(6):677-685. doi: 10.1038/.

100. Cordani M, Oppici E, Dando I, et al. Mutant p53 proteins counteract autophagic mechanism sensitizing cancer cells to mTOR inhibition. Mol Oncol. 2016 Aug;10(7):1008-29. doi: 10.1016/j.molonc.2016.04.001. PubMed PMID: 27118659; PubMed Central PMCID: PMCPMC5423176.

101. Zhou G, Wang J, Zhao M, et al. Gain-of-function mutant p53 promotes cell growth and cancer cell metabolism via inhibition of AMPK activation. Mol Cell. 2014 Jun 19;54(6):960-74. doi: 10.1016/j.molcel.2014.04.024. PubMed PMID: 24857548; PubMed Central PMCID: PMCPMC4067806.

102. Agarwal S, Bell CM, Taylor SM, et al. p53 Deletion or Hotspot Mutations Enhance mTORC1 Activity by Altering Lysosomal Dynamics of TSC2 and Rheb. Mol Cancer Res. 2016 Jan;14(1):66-77. doi: 10.1158/1541-7786.MCR-15-0159. PubMed PMID: 26385560; PubMed Central PMCID: PMCPMC4715954.

103. Kenzelmann Broz D, Attardi LD. TRP53 activates a global autophagy program to promote tumor suppression. Autophagy. 2013 Sep;9(9):1440-2. doi: 10.4161/auto.25833. PubMed PMID: 23899499; PubMed Central PMCID: PMCPMC4026029.

104. Morselli E, Shen S, Ruckenstuhl C, et al. p53 inhibits autophagy by interacting with the human ortholog of yeast Atg17, RB1CC1/FIP200. Cell Cycle. 2011 Aug 15;10(16):2763-9. doi: 10.4161/cc.10.16.16868. PubMed PMID: 21775823.

105. Saini H, Hakeem I, Mukherjee S, et al. Autophagy Regulated by Gain of Function Mutant p53 Enhances Proteasomal Inhibitor-Mediated Cell Death through Induction of ROS and ERK in Lung Cancer Cells. J Oncol. 2019;2019:6164807. doi: 10.1155/2019/6164807. PubMed PMID: 30723502; PubMed Central PMCID: PMCPMC6339715.

106. Schofield HK, Zeller J, Espinoza C, et al. Mutant p53R270H drives altered metabolism and increased invasion in pancreatic ductal adenocarcinoma. JCI Insight. 2018 Jan 25;3(2). doi: 10.1172/jci.insight.97422. PubMed PMID: 29367463; PubMed Central PMCID: PMCPMC5821189.

107. Yang A, Rajeshkumar NV, Wang X, et al. Autophagy is critical for pancreatic tumor growth and progression in tumors with p53 alterations. Cancer Discov. 2014 Aug;4(8):905-13. doi: 10.1158/2159-8290.CD-14-0362. PubMed PMID: 24875860; PubMed Central PMCID: PMCPMC4125497.

108. Mo S, Dai W, Xiang W, et al. Prognostic and predictive value of an autophagy-related signature for early relapse in stages I-III colon cancer. Carcinogenesis. 2019 Jul 20;40(7):861-870. doi: 10.1093/carcin/bgz031. PubMed PMID: 30933267.

109. Zhou Z, Mo S, Dai W, et al. Development and Validation of an Autophagy Score Signature for the Prediction of Post-operative Survival in Colorectal Cancer. Front Oncol. 2019;9:878. doi: 10.3389/fonc.2019.00878. PubMed PMID: 31552190; PubMed Central PMCID: PMCPMC6746211.

110. Piao S, Ojha R, Rebecca VW, et al. ALDH1A1 and HLTF modulate the activity of lysosomal autophagy inhibitors in cancer cells. Autophagy. 2017;13(12):2056-2071. doi: 10.1080/15548627.2017.1377377. PubMed PMID: 28981387; PubMed Central PMCID: PMCPMC5788553.

111. Eng CH, Wang Z, Tkach D, et al. Macroautophagy is dispensable for growth of KRAS mutant tumors and chloroquine efficacy. Proc Natl Acad Sci U S A. 2016 Jan 5;113(1):182-7. doi: 10.1073/pnas.1515617113. PubMed PMID: 26677873; PubMed Central PMCID: PMCPMC4711870.

112. Su H, Yang F, Fu R, et al. Cancer cells escape autophagy inhibition via NRF2-induced macropinocytosis. Cancer Cell. 2021 May 10;39(5):678-693 e11. doi: 10.1016/j.ccell.2021.02.016. PubMed PMID: 33740421; PubMed Central PMCID: PMCPMC8119368.

113. Rubinsztein DC, Codogno P, Levine B. Autophagy modulation as a potential therapeutic target for diverse diseases. Nat Rev Drug Discov. 2012 Sep;11(9):709-30. doi: 10.1038/nrd3802. PubMed PMID: 22935804; PubMed Central PMCID: PMCPMC3518431.

114. Nyfeler B, Bergman P, Triantafellow E, et al. Relieving autophagy and 4EBP1 from rapamycin resistance. Mol Cell Biol. 2011 Jul;31(14):2867-76. doi: 10.1128/MCB.05430-11. PubMed PMID: 21576371; PubMed Central PMCID: PMCPMC3133392.

115. Cardenas C, Miller RA, Smith I, et al. Essential regulation of cell bioenergetics by constitutive InsP3 receptor Ca2+ transfer to mitochondria. Cell. 2010 Jul 23;142(2):270-83. doi: 10.1016/j.cell.2010.06.007. PubMed PMID: 20655468; PubMed Central PMCID: PMCPMC2911450.

116. Williams A, Sarkar S, Cuddon P, et al. Novel targets for Huntington's disease in an mTOR-independent autophagy pathway. Nat Chem Biol. 2008 May;4(5):295-305. doi: 10.1038/nchembio.79. PubMed PMID: 18391949; PubMed Central PMCID: PMCPMC2635566.

117. Pasquier B. Autophagy inhibitors. Cell Mol Life Sci. 2016 Mar;73(5):985-1001. doi: 10.1007/s00018-015-2104-y. PubMed PMID: 26658914.

118. Rebecca VW, Nicastri MC, Fennelly C, et al. PPT1 Promotes Tumor Growth and Is the Molecular Target of Chloroquine Derivatives in Cancer. Cancer Discov. 2019 Feb;9(2):220-229. doi: 10.1158/2159-8290.CD-18-0706. PubMed PMID: 30442709; PubMed Central PMCID: PMCPMC6368875.

119. Powis G, Bonjouklian R, Berggren MM, et al. Wortmannin, a Potent and Selective Inhibitor of Phosphatidylinositol-3kinase. Cancer Research. 1994;54:2419-2423.

120. Chude CI, Amaravadi RK. Targeting Autophagy in Cancer: Update on Clinical Trials and Novel Inhibitors. Int J Mol Sci. 2017 Jun 16;18(6). doi: 10.3390/ijms18061279. PubMed PMID: 28621712; PubMed Central PMCID: PMCPMC5486101.

121. Egan DF, Chun MG, Vamos M, et al. Small Molecule Inhibition of the Autophagy Kinase ULK1 and Identification of ULK1 Substrates. Mol Cell. 2015 Jul 16;59(2):285-97. doi: 10.1016/j.molcel.2015.05.031. PubMed PMID: 26118643; PubMed Central PMCID: PMCPMC4530630.

122. Akin D, Wang SK, Habibzadegah-Tari P, et al. A novel ATG4B antagonist inhibits autophagy and has a negative impact on osteosarcoma tumors. Autophagy. 2014;10(11):2021-35. doi: 10.4161/auto.32229. PubMed PMID: 25483883; PubMed Central PMCID: PMCPMC4502682.

123. Donohue E, Thomas A, Maurer N, et al. The autophagy inhibitor verteporfin moderately enhances the antitumor activity of gemcitabine in a pancreatic ductal adenocarcinoma model. J Cancer. 2013;4(7):585-96. doi: 10.7150/jca.7030. PubMed PMID: 24069069; PubMed Central PMCID: PMCPMC3781989.

124. Amaravadi RK, Yu D, Lum JJ, et al. Autophagy inhibition enhances therapy-induced apoptosis in a Myc-induced model of lymphoma. J Clin Invest. 2007 Feb;117(2):326-36. doi: 10.1172/JCI28833. PubMed PMID: 17235397; PubMed Central PMCID: PMCPMC1765515.

125. Li J, Hou N, Faried A, et al. Inhibition of autophagy augments 5-fluorouracil chemotherapy in human colon cancer in vitro and in vivo model. Eur J Cancer. 2010 Jul;46(10):1900-9. doi: 10.1016/j.ejca.2010.02.021. PubMed PMID: 20231086.

126. Zhu K, Dunner K, Jr., McConkey DJ. Proteasome inhibitors activate autophagy as a cytoprotective response in human prostate cancer cells. Oncogene. 2010 Jan 21;29(3):451-62. doi: 10.1038/onc.2009.343. PubMed PMID: 19881538; PubMed Central PMCID: PMCPMC2809784.

127. Wu Z, Chang PC, Yang JC, et al. Autophagy Blockade Sensitizes Prostate Cancer Cells towards Src Family Kinase Inhibitors. Genes Cancer. 2010 Jan;1(1):40-9. doi: 10.1177/1947601909358324. PubMed PMID: 20811583; PubMed Central PMCID: PMCPMC2930266.

128. Fan QW, Cheng C, Hackett C, et al. Akt and Autophagy Cooperate to Promote Survival of Drug-Resistant Glioma. Science Signaling. 2010;3(147). doi: 10.1126/scisignal.2001017.

129. Zhang SF, Wang XY, Fu ZQ, et al. TXNDC17 promotes paclitaxel resistance via inducing autophagy in ovarian cancer. Autophagy. 2015;11(2):225-38. doi: 10.1080/15548627.2014.998931. PubMed PMID: 25607466; PubMed Central PMCID: PMCPMC4502659.

130. Lee HO, Mustafa A, Hudes GR, et al. Hydroxychloroquine Destabilizes Phospho-S6 in Human Renal Carcinoma Cells. PLoS One. 2015;10(7):e0131464. doi:

10.1371/journal.pone.0131464. PubMed PMID: 26134285; PubMed Central PMCID: PMCPMC4489871.

131. Cheong H. Integrating autophagy and metabolism in cancer. Arch Pharm Res. 2015 Mar;38(3):358-71. doi: 10.1007/s12272-015-0562-2. PubMed PMID: 25614051.

132. Ruiz-Irastorza G, Ramos-Casals M, Brito-Zeron P, et al. Clinical efficacy and side effects of antimalarials in systemic lupus erythematosus: a systematic review. Ann Rheum Dis. 2010 Jan;69(1):20-8. doi: 10.1136/ard.2008.101766. PubMed PMID: 19103632.

133. Manic G, Obrist F, Kroemer G, et al. Chloroquine and hydroxychloroquine for cancer therapy. Mol Cell Oncol. 2014;1(1):e29911. doi: 10.4161/mco.29911. PubMed PMID: 27308318; PubMed Central PMCID: PMCPMC4905171.

134. Pacey S, Workman P, Sarker D. Pharmacokinetics and Pharmacodynamics in Drug Development. In: Schwab M, editor. Encyclopedia of Cancer: Springer Berlin Heidelberg; 2011. p. 2845-2848.

135. Lim HS, Im JS, Cho JY, et al. Pharmacokinetics of hydroxychloroquine and its clinical implications in chemoprophylaxis against malaria caused by Plasmodium vivax. Antimicrob Agents Chemother. 2009 Apr;53(4):1468-75. doi: 10.1128/AAC.00339-08. PubMed PMID: 19188392; PubMed Central PMCID: PMCPMC2663072.

136. Estes ML, Ewing-Wilson D, Chou SM, et al. Chloroquine neuromyotoxicity. Clinical and pathologic perspective. Am J Med. 1987 Mar;82(3):447-55. PubMed PMID: 3826099.

137. Carmichael SJ, Charles B, Tett SE. Population pharmacokinetics of hydroxychloroquine in patients with rheumatoid arthritis. Ther Drug Monit. 2003 Dec;25(6):671-81. PubMed PMID: 14639053.

138. Tett SE. Clincal Pharamcokinetics of Slow-Acting Antirheumatic Drugs. Clin Pharmacokinet. 1993;25(5):392-407.

139. Ducharme J, Farinotti R. Clinical pharmacokinetics and metabolism of chloroquine. Focus on recent advancements. Clin Pharmacokinet. 1996

Oct;31(4):257-74. doi: 10.2165/00003088-199631040-00003. PubMed PMID: 8896943.

140. Furst DE. Pharmacokinetics of hydroxychloroquine and chloroquine during treatment of rheumatic diseases. Lupus. 1996 Jun;5 Suppl 1:S11-5. PubMed PMID: 8803904.

141. Cardoso CD, Bonato PS. Enantioselective metabolism of hydroxychloroquine employing rats and mice hepatic microsomes. Brazilian Journal of Pharmaceutical Sciences. 2009 Oct-Dec;45(4):659-667. PubMed PMID: WOS:000277065000007; English.

142. Wolpin BM, Rubinson DA, Wang X, et al. Phase II and pharmacodynamic study of autophagy inhibition using hydroxychloroquine in patients with metastatic pancreatic adenocarcinoma. Oncologist. 2014 Jun;19(6):637-8. doi: 10.1634/theoncologist.2014-0086. PubMed PMID: 24821822; PubMed Central PMCID: PMCPMC4041680.

143. Boehrer S, Ades L, Braun T, et al. Erlotinib exhibits antineoplastic off-target effects in AML and MDS: a preclinical study. Blood. 2008 Feb 15;111(4):2170-80. doi: 10.1182/blood-2007-07-100362. PubMed PMID: 17925489.

144. Goldberg SB, Supko JG, Neal JW, et al. A phase I study of erlotinib and hydroxychloroquine in advanced non-small-cell lung cancer. J Thorac Oncol. 2012 Oct;7(10):1602-8. doi: 10.1097/JTO.0b013e318262de4a. PubMed PMID: 22878749; PubMed Central PMCID: PMCPMC3791327.

145. Zeh HJ, Bahary N, Boone BA, et al. A Randomized Phase II Preoperative Study of Autophagy Inhibition with High-Dose Hydroxychloroquine and Gemcitabine/Nab-Paclitaxel in Pancreatic Cancer Patients. Clin Cancer Res. 2020 Jul 1;26(13):3126-3134. doi: 10.1158/1078-0432.CCR-19-4042. PubMed PMID: 32156749; PubMed Central PMCID: PMCPMC8086597.

146. Horne GA, Stobo J, Kelly C, et al. A randomised phase II trial of hydroxychloroquine and imatinib versus imatinib alone for patients with chronic myeloid leukaemia in major cytogenetic response with residual disease. Leukemia. 2020 Jul;34(7):1775-1786. doi: 10.1038/s41375-019-0700-9. PubMed PMID: 31925317; PubMed Central PMCID: PMCPMC7224085.

147. Mahalingam D, Mita M, Sarantopoulos J, et al. Combined autophagy and HDAC inhibition: a phase I safety, tolerability, pharmacokinetic, and pharmacodynamic

analysis of hydroxychloroquine in combination with the HDAC inhibitor vorinostat in patients with advanced solid tumors. Autophagy. 2014 Aug;10(8):1403-14. doi: 10.4161/auto.29231. PubMed PMID: 24991835; PubMed Central PMCID: PMCPMC4203517.

148. Siegel RL, Miller KD, Jemal A. Cancer statistics, 2020. CA Cancer J Clin. 2020 Jan;70(1):7-30. doi: 10.3322/caac.21590. PubMed PMID: 31912902.

149. Cocco S, Leone A, Piezzo M, et al. Targeting Autophagy in Breast Cancer. Int J Mol Sci. 2020 Oct 22;21(21). doi: 10.3390/ijms21217836. PubMed PMID: 33105796; PubMed Central PMCID: PMCPMC7660056.

150. Waks AG, Winer EP. Breast Cancer Treatment: A Review. JAMA. 2019 Jan 22;321(3):288-300. doi: 10.1001/jama.2018.19323. PubMed PMID: 30667505.

151. Schoenlein PV, Periyasamy-Thandavan S, Samaddar JS, et al. Autophagy facilitates the progression of ERalpha-positive breast cancer cells to antiestrogen resistance. Autophagy. 2009 Apr;5(3):400-3. doi: 10.4161/auto.5.3.7784. PubMed PMID: 19221464.

152. Cook KL, Warri A, Soto-Pantoja DR, et al. Hydroxychloroquine inhibits autophagy to potentiate antiestrogen responsiveness in ER+ breast cancer. Clin Cancer Res. 2014 Jun 15;20(12):3222-32. doi: 10.1158/1078-0432.CCR-13-3227. PubMed PMID: 24928945; PubMed Central PMCID: PMCPMC4073207.

153. Chen S, Zhu X, Qiao H, et al. Protective autophagy promotes the resistance of HER2-positive breast cancer cells to lapatinib. TUMOR BIOL. 2015;37:2321-2331. doi: 10.1007/s13277-015-3800-9.

154. Abedin MJ, Wang D, McDonnell MA, et al. Autophagy delays apoptotic death in breast cancer cells following DNA damage. Cell Death Differ. 2007 Mar;14(3):500-10. doi: 10.1038/sj.cdd.4402039. PubMed PMID: 16990848.

155. Thomas S, Sharma N, Golden EB, et al. Preferential killing of triple-negative breast cancer cells in vitro and in vivo when pharmacological aggravators of endoplasmic reticulum stress are combined with autophagy inhibitors. Cancer Lett. 2012 Dec 1;325(1):63-71. doi: 10.1016/j.canlet.2012.05.030. PubMed PMID: 22664238.

156. Chaachouay H, Ohneseit P, Toulany M, et al. Autophagy contributes to resistance of tumor cells to ionizing radiation. Radiother Oncol. 2011 Jun;99(3):287-92. doi: 10.1016/j.radonc.2011.06.002. PubMed PMID: 21722986.

157. Hamurcu Z, Delibasi N, Gecene S, et al. Targeting LC3 and Beclin-1 autophagy genes suppresses proliferation, survival, migration and invasion by inhibition of Cyclin-D1 and uPAR/Integrin beta1/ Src signaling in triple negative breast cancer cells. J Cancer Res Clin Oncol. 2018 Mar;144(3):415-430. doi: 10.1007/s00432-017-2557-5. PubMed PMID: 29288363.

158. Claude-Taupin A, Fonderflick L, Gauthier T, et al. ATG9A Is Overexpressed in Triple Negative Breast Cancer and Its In Vitro Extinction Leads to the Inhibition of Pro-Cancer Phenotypes. Cells. 2018 Dec 6;7(12). doi: 10.3390/cells7120248. PubMed PMID: 30563263; PubMed Central PMCID: PMCPMC6316331.

159. Negri T, Tarantino E, Orsenigo M, et al. Chromosome band 17q21 in breast cancer: significant association between beclin 1 loss and HER2/NEU amplification. Genes Chromosomes Cancer. 2010 Oct;49(10):901-9. doi: 10.1002/gcc.20798. PubMed PMID: 20589936.

160. Lozy F, Cai-McRae X, Teplova I, et al. ERBB2 overexpression suppresses stress-induced autophagy and renders ERBB2-induced mammary tumorigenesis independent of monoallelic Becn1 loss. Autophagy. 2014 Apr;10(4):662-76. doi: 10.4161/auto.27867. PubMed PMID: 24492513; PubMed Central PMCID: PMCPMC4091153.

161. Arnaout A, Robertson SJ, Pond GR, et al. A randomized, double-blind, window of opportunity trial evaluating the effects of chloroquine in breast cancer patients. Breast Cancer Res Treat. 2019 Nov;178(2):327-335. doi: 10.1007/s10549-019-05381-y. PubMed PMID: 31392517.

162. Lamplot JD, Denduluri S, Qin J, et al. The Current and Future Therapies for Human Osteosarcoma. Curr Cancer Ther Rev. 2013 Feb;9(1):55-77. doi: 10.2174/1573394711309010006. PubMed PMID: 26834515; PubMed Central PMCID: PMCPMC4730918.

163. Moore DD, Luu HH. Osteosarcoma. In: Peabody TD, Attar S, editors. Orthopaedic Oncology: Primary and Metastatic Tumors of the Skeletal System: Springer International Publishing; 2014. p. 65-92.

164. Misaghi A, Goldin A, Awad M, et al. Osteosarcoma: a comprehensive review. SICOT J. 2018;4:12. doi: 10.1051/sicotj/2017028. PubMed PMID: 29629690; PubMed Central PMCID: PMCPMC5890448.

165. Gelderblom H, Jinks RC, Sydes M, et al. Survival after recurrent osteosarcoma: data from 3 European Osteosarcoma Intergroup (EOI) randomized controlled trials. Eur J Cancer. 2011 Apr;47(6):895-902. doi: 10.1016/j.ejca.2010.11.036. PubMed PMID: 21216138.

166. Luetke A, Meyers PA, Lewis I, et al. Osteosarcoma treatment - where do we stand? A state of the art review. Cancer Treat Rev. 2014 May;40(4):523-32. doi: 10.1016/j.ctrv.2013.11.006. PubMed PMID: 24345772.

167. Taran SJ, Taran R, Malipatil NB. Pediatric Osteosarcoma: An Updated Review. Indian J Med Paediatr Oncol. 2017 Jan-Mar;38(1):33-43. doi: 10.4103/0971-5851.203513. PubMed PMID: 28469335; PubMed Central PMCID: PMCPMC5398104.

168. Xiao X, Wang W, Li Y, et al. HSP90AA1-mediated autophagy promotes drug resistance in osteosarcoma. J Exp Clin Cancer Res. 2018 Aug 28;37(1):201. doi: 10.1186/s13046-018-0880-6. PubMed PMID: 30153855; PubMed Central PMCID: PMCPMC6114771.

169. Huang J, Liu K, Yu Y, et al. Targeting HMGB1-mediated autophagy as a novel therapeutic strategy for osteosarcoma. Autophagy. 2012 Feb 1;8(2):275-7. doi: 10.4161/auto.8.2.18940. PubMed PMID: 22301993; PubMed Central PMCID: PMCPMC3336081.

170. Huang J, Ni J, Liu K, et al. HMGB1 promotes drug resistance in osteosarcoma. Cancer Res. 2012 Jan 1;72(1):230-8. doi: 10.1158/0008-5472.CAN-11-2001. PubMed PMID: 22102692.

171. Zhang Z, Shao Z, Xiong L, et al. Expression of Beclin1 in osteosarcoma and the effects of down-regulation of autophagy on the chemotherapeutic sensitivity. J Huazhong Univ Sci Technolog Med Sci. 2009 Dec;29(6):737-40. doi: 10.1007/s11596-009-0613-3. PubMed PMID: 20037818.

172. Kim HJ, Lee SG, Kim YJ, et al. Cytoprotective role of autophagy during paclitaxel-induced apoptosis in Saos-2 osteosarcoma cells. Int J Oncol. 2013 Jun;42(6):1985-92. doi: 10.3892/ijo.2013.1884. PubMed PMID: 23563171.

173. Zhao D, Yuan H, Yi F, et al. Autophagy prevents doxorubicininduced apoptosis in osteosarcoma. Mol Med Rep. 2014 May;9(5):1975-81. doi: 10.3892/mmr.2014.2055. PubMed PMID: 24639013.

174. Guo Y, Huang C, Li G, et al. Paxilitaxel induces apoptosis accompanied by protective autophagy in osteosarcoma cells through hypoxia-inducible factor-1alpha pathway. Mol Med Rep. 2015 Sep;12(3):3681-3687. doi: 10.3892/mmr.2015.3860. PubMed PMID: 26017247.

175. Zhou P, Li Y, Li B, et al. Autophagy inhibition enhances celecoxib-induced apoptosis in osteosarcoma. Cell Cycle. 2018;17(8):997-1006. doi: 10.1080/15384101.2018.1467677. PubMed PMID: 29884091; PubMed Central PMCID: PMCPMC6103699.

176. Miao X-D, Cao L, Zhang Q, et al. Effect of PI3K-mediated autophagy in human osteosarcoma MG63 cells on sensitivity to chemotherapy with cisplatin. Asian Pacific Journal of Tropical Medicine. 2015;8(9):731-738. doi: 10.1016/j.apjtm.2015.07.024.

177. Liu K, Ren T, Huang Y, et al. Apatinib promotes autophagy and apoptosis through VEGFR2/STAT3/BCL-2 signaling in osteosarcoma. Cell Death Dis. 2017 Aug 24;8(8):e3015. doi: 10.1038/cddis.2017.422. PubMed PMID: 28837148; PubMed Central PMCID: PMCPMC5596600.

178. Zhang F, Yan T, Guo W, et al. Novel oncogene COPS3 interacts with Beclin1 and Raf-1 to regulate metastasis of osteosarcoma through autophagy. J Exp Clin Cancer Res. 2018 Jul 3;37(1):135. doi: 10.1186/s13046-018-0791-6. PubMed PMID: 29970115; PubMed Central PMCID: PMCPMC6029018.

179. Bai Y, Chen Y, Chen X, et al. Trichostatin A activates FOXO1 and induces autophagy in osteosarcoma. Arch Med Sci. 2019 Jan;15(1):204-213. doi: 10.5114/aoms.2018.73860. PubMed PMID: 30697272; PubMed Central PMCID: PMCPMC6348367.

180. Chen Y, Wang S, Geng B, et al. Pelargonidin induces antitumor effects in human osteosarcoma cells via autophagy induction, loss of mitochondrial membrane potential, G2/M cell cycle arrest and downregulation of PI3K/AKT signalling pathway. JBUON. 2018;23(3):735-740.

181. Lambert LA, Qiao N, Hunt KK, et al. Autophagy: a novel mechanism of synergistic cytotoxicity between doxorubicin and roscovitine in a sarcoma model.

Cancer Res. 2008 Oct 1;68(19):7966-74. doi: 10.1158/0008-5472.CAN-08-1333. PubMed PMID: 18829554; PubMed Central PMCID: PMCPMC2561224.

182. Xie ZG, Xie Y, Dong QR. Inhibition of the mammalian target of rapamycin leads to autophagy activation and cell death of MG63 osteosarcoma cells. Oncol Lett. 2013 Nov;6(5):1465-1469. doi: 10.3892/ol.2013.1531. PubMed PMID: 24179542; PubMed Central PMCID: PMCPMC3813609.

183. Chiu HW, Lin W, Ho SY, et al. Synergistic effects of arsenic trioxide and radiation in osteosarcoma cells through the induction of both autophagy and apoptosis. Radiat Res. 2011 May;175(5):547-60. doi: 10.1667/RR2380.1. PubMed PMID: 21388295.

184. Mukherjee S, Dash S, Lohitesh K, et al. The dynamic role of autophagy and MAPK signaling in determining cell fate under cisplatin stress in osteosarcoma cells. PLoS One. 2017;12(6):e0179203. doi: 10.1371/journal.pone.0179203. PubMed PMID: 28598976; PubMed Central PMCID: PMCPMC5466322.

185. He H, Ni J, Huang J. Molecular mechanisms of chemoresistance in osteosarcoma (Review). Oncol Lett. 2014 May;7(5):1352-1362. doi: 10.3892/ol.2014.1935. PubMed PMID: 24765137; PubMed Central PMCID: PMCPMC3997672.

186. Livingston JA, Wang WL, Tsai JW, et al. Analysis of HSP27 and the Autophagy Marker LC3B(+) Puncta Following Preoperative Chemotherapy Identifies High-Risk Osteosarcoma Patients. Mol Cancer Ther. 2018 Jun;17(6):1315-1323. doi: 10.1158/1535-7163.MCT-17-0901. PubMed PMID: 29592877; PubMed Central PMCID: PMCPMC5984702.

187. Varshney J, Scott MC, Largaespada DA, et al. Understanding the Osteosarcoma Pathobiology: A Comparative Oncology Approach. Vet Sci. 2016 Jan 18;3(1). doi: 10.3390/vetsci3010003. PubMed PMID: 29056713; PubMed Central PMCID: PMCPMC5644613.

188. Mueller F, Fuchs B, Kaser-Hotz B. Comparative Biology of Human and Canine Osteosarcoma. Anticancer Research. 2007;27(1A):155-164. doi: 10.3390/vetsci3010003.

189. Frazier JP, Bertout JA, Kerwin WS, et al. Multidrug Analyses in Patients Distinguish Efficacious Cancer Agents Based on Both Tumor Cell Killing and Immunomodulation. Cancer Res. 2017 Jun 1;77(11):2869-2880. doi:

10.1158/0008-5472.CAN-17-0084. PubMed PMID: 28364003; PubMed Central PMCID: PMCPMC5546104.

190. Schott CR, Ludwig L, Mutsaers AJ, et al. The autophagy inhibitor spautin-1, either alone or combined with doxorubicin, decreases cell survival and colony formation in canine appendicular osteosarcoma cells. PLoS One. 2018;13(10):e0206427. doi: 10.1371/journal.pone.0206427. PubMed PMID: 30372478; PubMed Central PMCID: PMCPMC6205606.

191. Henry JG, Shoemaker G, Prieto JM, et al. The effect of cannabidiol on canine neoplastic cell proliferation and mitogen-activated protein kinase activation during autophagy and apoptosis. Vet Comp Oncol. 2021 Jun;19(2):253-265. doi: 10.1111/vco.12669. PubMed PMID: 33247539.

192. Miyamoto R, Tani H, Ikeda T, et al. Commitment toward cell death by activation of autophagy with survivin inhibitor YM155 in two canine squamous cell carcinoma cell lines with high expression of survivin. Res Vet Sci. 2021 Mar;135:412-415. doi: 10.1016/j.rvsc.2020.10.025. PubMed PMID: 33160684.

193. Liu JL, Chang KC, Lo CC, et al. Expression of autophagy-related protein beclin-1 in malignant canine mammary tumors. BMC Veterinary Research. 2013;9(75). doi: 10.1186/1746-6148-9-75.

194. Mariotti F, Magi GE, Gavazza A, et al. p62/SQSTM1 expression in canine mammary tumours: Evolutionary notes. Vet Comp Oncol. 2019 Dec;17(4):570-577. doi: 10.1111/vco.12523. PubMed PMID: 31332942.

195. Barnard RA, Wittenburg LA, Amaravadi RK, et al. Phase I clinical trial and pharmacodynamic evaluation of combination hydroxychloroquine and doxorubicin treatment in pet dogs treated for spontaneously occurring lymphoma. Autophagy. 2014 Aug;10(8):1415-25. doi: 10.4161/auto.29165. PubMed PMID: 24991836; PubMed Central PMCID: PMCPMC4203518.

Chapter Two

PK/PD Assessment of HCQ in Breast Cancer

Summary

Hydroxychloroquine (HCQ) is being tested in a number of human clinical trials to determine the role of autophagy in response to standard anticancer therapies. However, HCQ pharmacodynamic responses are difficult to assess in patients and preclinical studies in mouse models are equivocal with regard to HCQ exposure and inhibition of autophagy. Here, pharmacokinetic (PK) assessment of HCQ in non-tumor bearing mice established 60 mg/kg as the human equivalent dose of HCQ in mice. Autophagy inhibition, cell proliferation, and cell death were assessed in 2D cell culture and 3D tumor organoids in breast cancer. Mice challenged with breast cancer xenografts were then treated with 60 mg/kg HCQ and subsequent PK and pharmacodynamic (PD) responses were assessed. Although autophagic flux was significantly inhibited in cells irrespective of autophagy dependency status, autophagy dependent tumors had decreased cell proliferation and increased cell death at earlier time points compared to autophagy independent tumors. Understanding HCQ PK and PD in mice as well as the corresponding correlation to cell culture models allows for a comparison to human PK as reported in recent trials and as such the subsequent PD associated with autophagy inhibition in tissues.

Introduction/Motivation

Macroautophagy ("autophagy") is a normal cellular process in which cell components are taken up by vesicles called autophagosomes that fuse with lysosomes where the components are degraded and recycled. Autophagy is induced by metabolic stress and in cells undergoing remodeling or differentiation [1, 2]. It plays important roles in many diseases including cancer by enhancing survival and therapy resistance [3]. Hydroxychloroquine (HCQ) is a lipophilic weak base that prevents lysosomal acidification by sequestering in lysosomes and raising their pH, which in turn blocks the fusion of autophagosomes to lysosomes [4]. HCQ is commonly used as an autophagy inhibitor in cancer clinical trials because it is already FDA approved, has a low toxicity profile, and is inexpensive [5, 6, 7, 8].

HCQ pharmacokinetic (PK) parameters have been well characterized in humans. Following oral administration, HCQ is almost completely and rapidly absorbed in the gastrointestinal tract and is about 75% bioavailable [9, 10, 11]. Approximately 50% of HCQ is bound to plasma proteins and extensively sequesters in tissue [9, 12, 13]. It partitions into red blood cells and binds strongly to heme proteins, leading to a high volume of distribution and a prolonged half-life of 40-50 days [12, 13, 14]. HCQ is dealkylated in the liver by cytochrome P450 enzymes into active metabolites including desethylhydroxychloroquine (DHCQ) [9, 13, 15]. HCQ clearance is divided nearly equally between hepatic and renal mechanisms [13].

While HCQ PK is well described in humans, the pharmacodynamics (PD) associated with HCQ exposure is difficult to assess. There are over 90 cancer clinical

trials (ClinicalTrials.gov) that currently or have previously investigated the effects of HCQ alone and in combination with chemo-, immuno-, and/or radiation therapies. Trials use between 200 and 1200 mg of HCQ daily but the number of patients with partial or stable responses is variable [16, 17, 18, 19]. Further, when assessing patients for LC3-II or p62 accumulation as markers for autophagy inhibition, studies have found that autophagy inhibition is achievable with HCQ but inconsistent across patient populations [16, 19, 20]. Monitoring HCQ-driven correlative PD endpoints also has not been successful at doses less than the maximum tolerated dose [21]. Given the large number of clinical trials using HCQ to target cancer, it is important to understand how HCQ exposure modulates cellular responses.

Mice are a widely used pre-clinical cancer research model system and have been used in numerous autophagy-modulation studies [22, 23, 24, 25, 26]. However, many human tumors do not grow in immunodeficient mouse models which makes it impossible to study certain cancers using this model. For instance, triple negative breast cancers grow in immunodeficient mouse models, but most luminal estrogen receptor positive and human epidermal growth factor receptor 2 positive breast xenografts cannot grow [27, 28]. However, there are reports of growing these subtypes in three-dimensional cell culture as organoids [29, 30] which is important since organoids have been shown to more closely mimic *in vivo* responses compared to 2D cell culture [31, 32]. In addition, tumor organoids can accurately recapitulate *in vivo* drug responses, simplify experiments, and save time and money [31, 33, 34].

Although HCQ is used clinically as an autophagy inhibitor to prevent cancer cell survival and therapy resistance, the efficacy of HCQ is not known in humans and has not

been established in mouse models. Here, the human equivalent dose (HED) of HCQ reflected in human clinical trial data was determined in non-tumor bearing mice and the response to autophagy inhibition was assessed. Cell proliferation, death, and autophagic flux following HCQ were then evaluated in breast cancer *in vitro*. Mice with human breast xenografts were treated with the HED to characterize pharmacodynamic responses *in vivo*. Understanding HCQ PK and PD allows for comparison to human PK reported in recent trials and subsequently the PD associated with autophagy inhibition.

Materials and Methods

Mouse treatments

Protocols for the mouse studies were approved by the Institutional Animal Care and Use Committee at Colorado State University. Six- to eight-week-old non tumor-bearing female BALB/c mice (Charles River NCI, Frederick, MD) were treated with a single intraperitoneal dose (IP) of 20, 40, or 80 mg/kg HCQ (Sigma-Aldrich, H0915). Tissues and whole blood were collected at 3, 6, 12, 24, 48 and 72 hours. For tumor-bearing mice, MDA-MB-231 and MDA-MB-468 breast cancer cell lines were implanted in the third mammary fat pads of 6- to 8-week-old female athymic nude mice (Charles River NCI, Frederick, MD). MCF7 breast cancer cells were implanted in the third mammary fat pads of 6- to 8-week-old ovariectomized female athymic nude mice (Charles River NCI, Wilmington, MA) and supplemented with 0.18 mg 17β-estradiol 60 day slow release tablets (Innovative Research of America, SE-121). Tumors were grown to between 150 and 400 mm^3 then treated with a single IP dose of 60 mg/kg HCQ or once daily with a 60

mg/kg HCQ IP dose for one week. Tissues, tumors, and whole blood were collected at 3, 6, 12, 24, 48, and 72 hours following the single dose or 24 hours following the last daily dose.

Drug Measurements

Levels of HCQ and DHCQ in whole blood and tissues were determined via a validated liquid chromatography-tandem mass spectrometry (LC-MS/MS) assay. Briefly, tissues and tumors were prepared in milli-Q and homogenized using a large tissue homogenizer or a sonic dismembranator on ice with several pulses. HCQ standards were prepared in milli-Q and DHCQ standards were prepared from a 1 mg/mL stock in DMSO then diluted in 50/50 acetonitrile/milli-Q. Standards and samples were vortexed and centrifuged prior to analysis. Samples were analyzed on a C18 5 µm, 4.6 x 150 mm column in a Shimadzu HPLC system coupled to a 3200 Q-TRAP triple quadrupole mass spectrometer (Applied Biosystems) using chloroquine as an internal standard. Non-compartmental analysis (NCA) measured exposure, as determined by area under the drug concentration versus time curve ($AUC_{0\text{-}inf}$), to both HCQ and DHCQ.

Western blot analysis

Tissues and tumors were flash frozen in lysis buffer (1% Triton X-100, 150 mM NaCl, 10 mM Tris pH 7.5, 100 mM Na-orthovanadate [Alexis Biochemicals, 400-032-G025], 34.8 µg/mL PMSF [Fluka Biochemica, 78830], and 1x protease inhibitor cocktail [Roche, 11836153001]). Samples were homogenized for 20 s and sonicated with three 3 second bursts on ice then centrifuged at 14,000 rpm for 10 min at 4°C. Supernatant was

collected and protein concentration was determined using the Pierce BCA Protein Assay Kit (Thermo Scientific, 23225). Twenty μg of protein was resolved on a 4-20% SDS-polyacrylamide gel (Bio Rad, 4568095) and transferred onto PVDF membranes (Bio Rad, 1704272). Membranes were blocked in 2.5% nonfat dry milk in tris-buffered saline/Tween 80 (TBST) (10 mM Tris pH 7.5, 100 mM NaCl, and 0.1% Tween 80 [Fisher Chemicals, BP338-500]) for 1 hour at room temperature. Blots were probed with polyclonal anti-LC3B antibody (Novus Biologicals, NB100-2220) at 1:1,000, monoclonal anti-α-tubulin antibody (Sigma-Aldrich, T5168) at 1:5,000, monoclonal anti-p62/SQSTM1 antibody (Novus Biologicals, H00008878-M01) at 1:1,000, or monoclonal anti-GAPDH antibody (Novus Biologicals, NB300-221) at 1:1,000 in blocking solution overnight at 4°C. Blots were washed three times in TBST then incubated at room temperature for 1 hour with HRP conjugated secondary antibodies anti-rabbit-HRP (Pierce, 31460) at 1:2000 or anti-mouse-HRP (Pierce, 31430) at 1:2,000 for p62, 1:5,000 for α-tubulin, or 1:10,000 for GAPDH in blocking solution. Alpha-tubulin or total protein were used as housekeeping controls. Blots were washed three times with TBST. Immunodetection was carried out using SuperSignal West Dura (Thermo Scientific, 34075) and imaged in a ChemiDoc XRS+ (Bio Rad, Hercules, CA) using Image Labs version 3.0 software. Densitometry quantification of LC3 and p62 levels was performed by NIH ImageJ software (http://rsb.info.nih.gov/nih-image/) or by Image Labs total protein normalization.

Immunofluorescence analysis

Tumor samples were put into 5% PLP solution for 24 hours at 4°C then placed in 30% sucrose solution for 24 hours at 4°C. Samples were fixed in 4% paraformaldehyde

then placed in OCT and cryosectioned at 5 μm. Sample slides were rehydrated in PBS plus 0.05% Tween 20 (PBST) then washed with 0.1 M glycine/PBS to reduce tissue autofluorescence. Non-specific binding was blocked with 5% donkey serum in immunofluorescence (IF) buffer (0.2% Triton X-100, 0.1% BSA, 0.05% Tween 20, PBS) for 30 min at room temperature. Sections were probed for primary anti-Ki67 (Cell Signaling Technology, 9027) diluted 1:400, primary anti-cleaved caspase-3 (Cell Signaling Technology, 9664) diluted 1:200, or rabbit IgG isotype control (Cell Signaling Technology, 3900) diluted to same the concentration as other primary antibodies in IF buffer for 1 hour at room temperature. Slides were washed 3 times in PBST then incubated with Cy3 secondary antibody (Jackson ImmunoResearch, 711-165-152 lot #142318) diluted 1:200 in IF buffer for 30 min at room temperature. Three washes were performed then slides were counterstained with filtered DAPI working solution (Thermo Scientific, 62248) diluted 1:500 in PBS for 15 min at room temperature. Slides were cover-slipped with ProLong Diamond Antifade Mountant (Invitrogen, P36961) and imaged using an Olympus IX83 confocal microscope and Hamamatsu digital camera.

Cell culture

Cell lines were validated mycoplasma free and maintained at 37°C and 5% CO_2 in DMEM (Corning, 10-017-CV) buffered with 10 mM HEPES (Fisher Scientific, BP-299-100) and supplemented with 10% FBS (Peak Serum, PS-FB3), 1% penicillin-streptomycin (Corning, 30-002-CI), and 1% sodium pyruvate (Corning, 25-000-CI). MCF7 media was also supplemented with 10 μg/mL insulin (Fisher Scientific, 12585014). Cells were used for no more than 20 passages.

Organoid culture

To form organoids, cells were grown on Cultrex 3D Culture Matrix RGF Basement Membrane Extract (BME) (R&D Systems, 344501001). Briefly, 100 μL/cm^2 BME was plated and allowed to solidify at 37°C for a minimum of 30 min before plating cells. Cells were grown for 2 days on BME before drugging.

Drug sensitivity, cell death, and autophagic flux live cell imaging assays

For 2D HCQ drug sensitivity, cell death, and autophagic flux assays, 3,000 cells were plated per well in a 96-well plate a few hours before drugging. NucLight red-labeled cells were used for drug sensitivity and cell death assays and cells transduced with LC3-mCherry-GFP were used for autophagic flux assays. For HCQ sensitivity assays, cells were treated with HCQ concentrations ranging from 0 to 40 μM HCQ. For the apoptosis assays, cells were plated in buffered MEM (Corning, 10-010-CV) 5 hours before drugging with 10 μM HCQ (equal dosing) and either 8 μM (MDA-MB-231 and MDA-MB-468) or 15 μM (MCF7) HCQ (equal toxicity) combined with 5 μM caspase 3/7 green fluorescent dye (Essen BioScience, 4440). For cytotoxicity assays, cells were plated in buffered MEM 5 hours before drugging with 10 μM HCQ and either 8 μM (MDA-MB-231 and MDA-MB-468) or 15 μM (MCF7) HCQ combined with 100 nM YOYO green fluorescent dye (Invitrogen, Y3601). For autophagic flux assays, cells were plated in buffered DMEM 5 hours before drugging with 10 μM HCQ and either 8 μM (MDA-MB-231 and MDA-MB-468) or 15 μM (MCF7) HCQ. Plates were imaged once every 24 hr on an IncuCyte Zoom

(Essen BioScience). All organoid cultures were performed the same way except 5,000 cells/well were plated on 100 μL/cm^2 BME two days prior to drugging.

Cell cycle

300,000 cells/well were plated in 6-well plates the day before drugging with HCQ. Cells grew for 48 hr following drugging then were trypsinized, spun down, washed once with PBS, then fixed with 70% ethanol and stored at -20°C for up to two weeks. Cells were stained with FxCycle PI/RNase (Life Technologies, F10797) at a concentration of 2 million cells/mL then analyzed on a Gallios flow cytometer (Beckman Coulter). Flow results were analyzed via FlowJo.

Cell proliferation via EdU

For 2D cell culture experiments, 750,000 cells/plate were plated in 60 mm dishes the day before drugging with HCQ. Once drugged with HCQ, cells grew for 48 hr. One hr (MCF7 and MDA-MB-231) or two hr (MDA-MB-468) before 48 hr time point, cells were treated with 10 μM EdU. Cells were trypsinized, spun down, washed once with cold PBS, then fixed in ice cold 70% ethanol. Fixed cells were stored at 4°C for a minimum of two days. Cells were re-hydrated in PBS for 1 hr then stained using the Click-iT EdU flow cytometry Alexa Fluor 647 kit (Invitrogen, C10424) by permeabilizing and staining cells. Cells were washed an extra time with PBS just before putting at final concentration of 1 million cells/mL in PBS. 100 μg/mL RNase A (Thermo Scientific, FEREN0531) and 1 μL of a 1:4 dilution from stock Sytox Blue (Thermo Scientific, S34857) was added per 1 million cells. Cells incubated overnight before flow on a Gallios flow cytometer.

For tumor organoid experiments, 100 μL/cm^2 BME was plated then 30 min later, 750,000 cells were plated. Tumor organoids were allowed to establish for two days before treatment with HCQ. Once drugged with HCQ, cells grew for 48 hr. Four hr before 48 hr time point, cells were treated with 10 μM EdU. Cells were isolated from BME using cell harvesting buffer (R&D Systems, 3448020CH) protocol. Briefly, cells were washed 3 times with PBS, cell harvesting buffer was added to the plate on ice, pipetted up and down, moved to a 15 mL conical, topped with cell harvesting buffer, and shaken on a plate shaker at 650 RPM for 30 min at 4°C. Conical tubes were centrifuged, supernatant was removed, and cells were washed once more with cell harvesting buffer. To break up organoids, cells were incubated with trypsin at room temp for 10 min then fixed with 4% PFA for 15 min. Cells were permeabilized and stained following the Click-iT EdU flow cytometry Alexa Fluor 647. Cells were washed an extra time with PBS then incubated with 100 μg/mL RNase A and 1 μL of a 1:4 dilution from stock Sytox Blue per 1 million cells for a minimum of 30 min before analyzing on a Gallios flow cytometer. All results were analyzed via FlowJo.

Autophagic flux flow cytometry

Cells transduced with a LC3-mCherry-GFP reporter were used. Cells were plated at 325,000 cells/well in a 6-well plate for 24 hr, 200,000 cells/dish in a 60 mm dish for 96 hr, or 50,000 (MDA-MB-231) or 100,000 (MCF7, MDA-MB-468) cells/plate for 144 hr in a 60 mm dish, allowed a day to attach and grow, then drugged with HCQ. For use in flow cytometry analysis, control cells were treated with 10 nM bafilomycin A1 (Fisher Scientific, AAJ67193XF) 24 hr prior to the endpoint to completely inhibit autophagy. Cells were

trypsinized, washed once with cold PBS, and resuspended in PBS, keeping cold and on ice. Samples were flowed on an Aurora 4 laser (Cytek Biosciences) flow cytometer then data analyzed via FlowJo. To determine the percent of cells using autophagy, the bafilomycin-treated control cells were gated so that 5-10% of cells were positive in an angled, diagonal area to the upper left of the events on a mCherry versus GFP plot. This gate was pasted directly onto all other samples for the same cell line from the same replicate.

Live/Dead staining

700,000 cells/plate for 48 hr, 200,000 cells/plate for 96 hr, or 50,000 cells/plate for 144 hr were plated in 60 mm dishes the day before drugging with HCQ. Cells were grown for given time frame then trypsinized, spun down, and washed once with cold PBS. Cells were re-suspended in PBS at a concentration of 1 million cells/mL then 1 μL of a 1:4 dilution from stock Sytox Blue was added. Cells were incubated for 15 min at room temperature then kept on ice until ready to flow and analyzed on a Gallios flow cytometer as soon as possible. Results were analyzed via FlowJo.

Statistical analysis

Statistical analysis was performed using Graphpad Prism. Two-way ANOVA using multiple comparisons with Dunnett correction between controls and drug-treated cells or unpaired two-tailed t-tests between controls and HCQ-treated mice were used to determine statistical significance with *$p \leq 0.05$, **$p \leq 0.01$, ***$p \leq 0.001$, or ****$p \leq 0.0001$. All error bars are standard deviation.

Results

HCQ exposure is dose dependent *in vivo*

HCQ and DHCQ levels were measured in whole blood, liver, gut, kidney, and brain following a single IP dose of 20, 40, or 80 mg/kg HCQ (**Figure 2.1**). Drug levels were dose dependent and concentrations of HCQ and DHCQ decreased over time. Highest concentrations were observed in the liver. In whole blood, there were still detectable levels of HCQ and DHCQ at 72 hours following all doses. HCQ levels were undetectable in liver after 24 hours, but DHCQ levels were detectable at relevant concentrations up to 72 hours. Concentrations of HCQ and DHCQ in the gut were similar over the entire 72 hours, with slightly more DHCQ than HCQ present at all doses 24 hr and later. Kidney drug levels were similar to gut and showed the same trends with higher DHCQ levels following 12 hr. HCQ can cross the blood brain barrier [35] and therefore can be detected in the brain. The concentrations of HCQ and DHCQ in the brain were approximately ten-fold less than whole blood, liver, kidney, and gut, suggesting that HCQ and DHCQ enter the central nervous system to a lesser degree than other tissues.

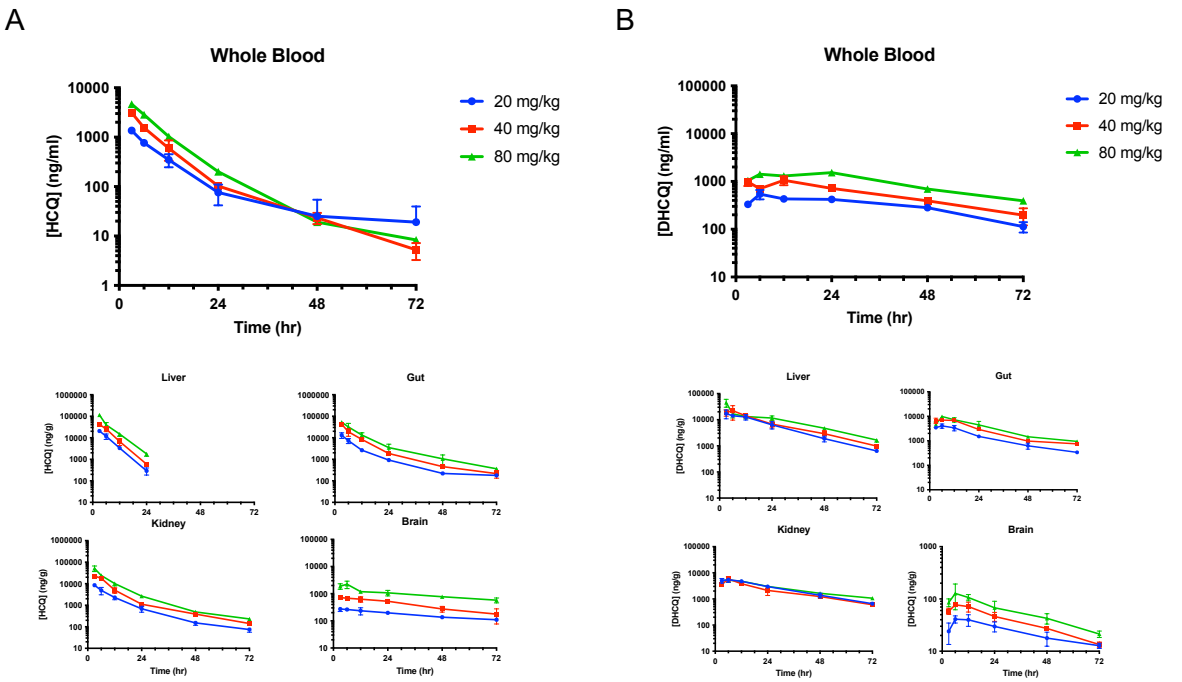

Figure 2.4 HCQ and DHCQ PK in whole blood and tissues. Whole blood, liver, gut, kidney, and brain HCQ (**A**) and DHCQ (**B**) levels from mice treated with 20, 40, or 80 mg/kg HCQ for 3, 6, 12, 24, 48, or 72 hr.

HCQ PK parameters calculated using noncompartmental analysis (**Table 2.1** and **Table 2.2**) show that maximal concentration (C_{max}) in whole blood, liver, gut, kidney, and brain increased in a dose dependent manner. Time to maximal concentration (T_{max}) occurred at 3 hours in whole blood, liver, gut, kidney, and brain at all doses except for brain at 80 mg/kg where T_{max} occurred at 6 hours. Half-lives for whole blood, liver, gut, kidney, and brain were approximately 14.5 hours, 3.5 hours, 17.5 hours, 15 hours, and 48 hours, respectively, regardless of dose. The area under the drug concentration versus time curve ($AUC_{0\text{-}inf}$) increased as dose increased in all tissues, showing exposure of HCQ is dose dependent. DHCQ PK parameters in whole blood (**Table 2.3**) and tissues (**Table 2.4**) had similar trends as HCQ. C_{max} and $AUC_{0\text{-}inf}$ increased in a dose-dependent manner. DHCQ T_{max} occurred mostly between 5 and 9 hours in all tissue. DHCQ half-

lives are all slightly longer than HCQ for all tissues except brain where DHCQ is more rapidly eliminated from the brain.

Table 2.1. Pharmacokinetic parameters of HCQ from whole blood in mice.

Dose (mg/kg)	C_{max} (µg/mL)	T_{max} (hr)	Half-Life (hr)	$AUC_{0\text{-}inf}$ (hr*µg/mL)	CL (mL/hr)	MRT (hr)	VDss (mL)	VDz (mL)
20	1.4	3	21.8	13.7	1476	16.2	23961	51296
40	3.1	3	11.2	24.3	1649	9.0	14796	26629
80	4.7	3	10.5	40.4	1981	8.8	17506	29932

Table 2.2. Pharmacokinetic parameters of HCQ in tissues in mice.

	Dose (mg/kg)	C_{max} (µg/mL)	T_{max} (hr)	Half-Life (hr)	$AUC_{0\text{-}inf}$ (hr*µg/mL)
Liver	20	20.6	3	3.4	147.9
	40	41.7	3	3.4	307.4
	80	114.7	3	4.2	684.9
Gut	20	13.1	3	20.4	125.6
	40	42.8	3	15.8	341.7
	80	53.0	3	16.0	522.2
Kidney	20	8.5	3	15.1	86.7
	40	22.5	3	16.2	228.6
	80	51.4	3	13.8	420.9
Brain	20	0.272	3	57.2	21.2
	40	0.717	3	32.5	37.4
	80	2.22	6	53.6	115.7

Table 2.3. Pharmacokinetic parameters of DHCQ from whole blood in mice.

Dose (mg/kg)	C_{max} (µg/mL)	T_{max} (hr)	Half-Life (hr)	$AUC_{0\text{-}inf}$ (hr*µg/mL)	CL (mL/hr)	MRT (hr)	VDss (mL)	VDz (mL)
20	0.543	8	25.6	27.3	736	41.1	30267	26846
40	1.2	9	26.1	48.3	838	39.4	32992	31175
80	1.53	18	24.6	84.1	952	41.5	39471	33715

Table 2.4. Pharmacokinetic parameters of DHCQ in tissues in mice.

	Dose (mg/kg)	C_{max} (µg/mL)	T_{max} (hr)	Half-Life (hr)	$AUC_{0\text{-}inf}$ (hr*µg/mL)
Liver	20	18.7	6	14.7	410.6
	40	23.0	5	17.6	511.7
	80	45.3	3	17.8	716.3
Gut	20	4.2	5	22.5	116.4
	40	7.8	7	24.9	224.2
	80	9.8	6	23.7	283.7
Kidney	20	5.7	8	22.4	198.1
	40	5.8	6	28.6	170.6
	80	5.6	5	32.4	238.2
Brain	20	0.041	6	36.2	2.4
	40	0.077	6	25.8	3.3
	80	0.127	6	26.9	5.1

To relate HCQ to DHCQ PK, a two-compartment semi-physiologic model was assembled in Matlab (version 2021a) with instantaneous absorption (**Figure 2.2 A**) using a system of three ordinary differential equations to describe how HCQ is metabolized to DHCQ and how HCQ moves from the liver to other compartments:

(1) $\frac{dm_{blood}}{dt} = Q_{liv}(C_{v,liv} - C_a) + Q_{rb}(C_{v,rb} - C_a) + V_{blood}\frac{V_{max,kid}}{K_{m,kid}}$

(2) $\frac{dm_{liv}}{dt} = Q_{liv}(C_a - C_{v,liv}) - V_{liv}\frac{C_{liv}*V_{max,liv}}{K_{m,liv}+C_{liv}}$

(3) $\frac{dm_{rb}}{dt} = Q_{rb}(C_a - C_{v,liv})$

Where, d_m is the amount of HCQ in the compartment, Q is the flow rate of the respective compartment, C_v is the concentration of HCQ leaving the respective compartment, C_a is the concentration of HCQ in arterial blood, V is the volume of the respective compartment, and V_{max} and K_m are metabolism constants for conversion of HCQ to DHCQ or kidney elimination constants. The parameter values used are represented in **Table 2.5**. The model was somewhat able to predict HCQ concentrations over time (**Figure 2.2 B**). However, more work needs to be done to more closely predict HCQ and DHCQ concentrations over time since all blood levels predicted are high at the early time points. Further, assessing the error in PK parameters and then performing Markov Chain Monte Carlo (MCMC) analysis to refine estimates of the parameters to predict which time points are most important for data collection can be done.

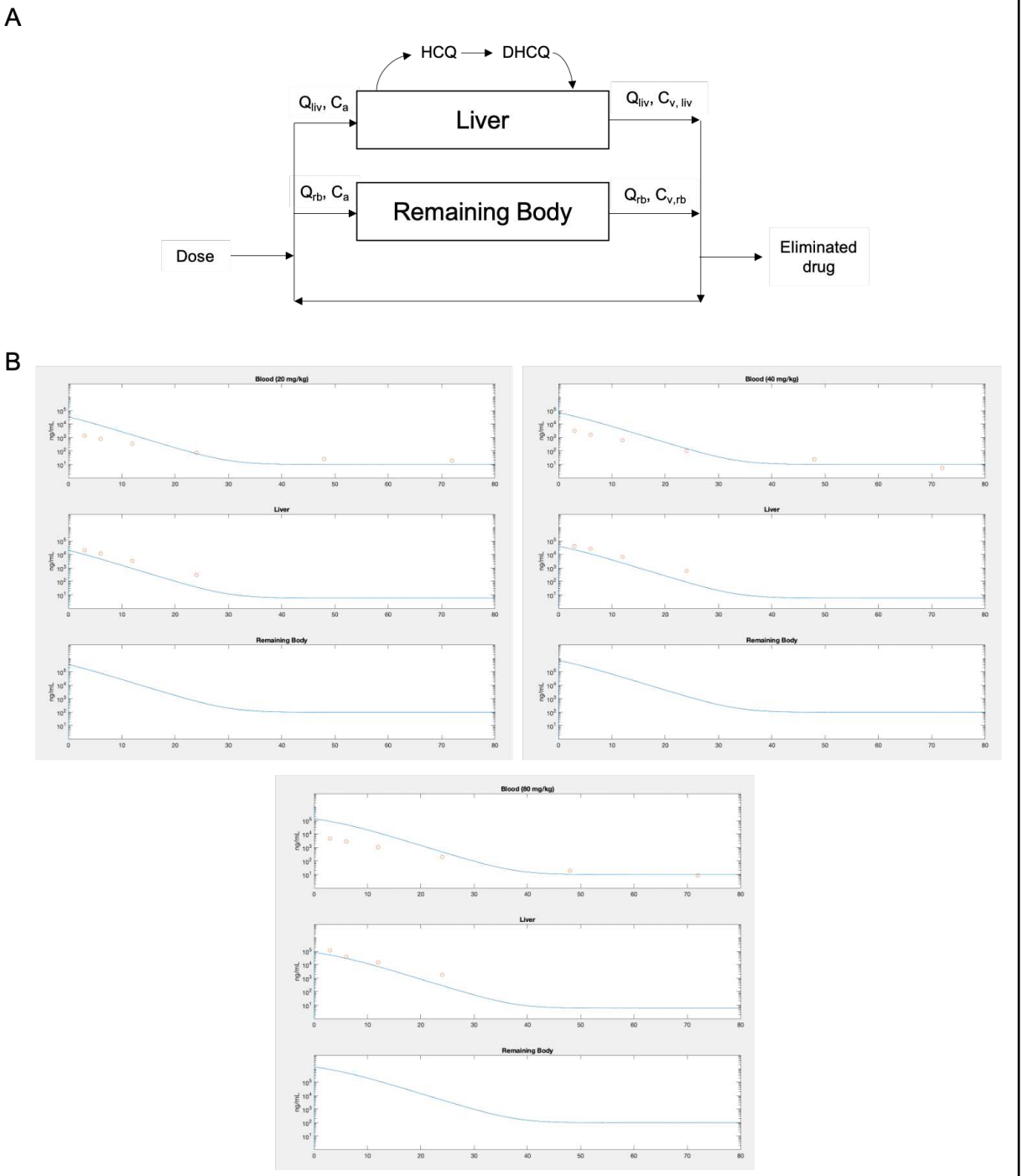

Figure 2.2 Two-compartment semi-physiologic model of HCQ and DHCQ. Two compartment PK model diagram (**A**). Predicted versus actual concentrations of HCQ in whole blood, liver, and the remaining body (**B**).

Table 2.5. Parameters for a two-compartment semi-physiologic model of HCQ in mice.

Parameter	**Mouse**
Body weight	0.02 kg
$V_{max,\ liv}$	1171 μM/hr
$K_{m,\ liv}$	357 μM
$V_{max,\ kid}$	32500 μM/hr
$K_{m,\ kid}$	1000 μM
Cardiac Output Fractions	
Liver	0.161
Kidney	0.175
Remaining body	0.664
Body Weight Fractions	
Liver	0.055
Blood	0.049
Remaining body	0.896

To determine equivalent dose exposure for HCQ in mice compared to humans, area under drug concentration versus time curves in whole blood from both mice and humans were directly compared since these AUC's represent exposure in each species. The human equivalent dose (HED) of steady state HCQ concentration was calculated by using the average human patient AUC over 24-hour dosing time period estimated at steady state in humans given an oral 600 mg dose [36] and comparing this to the AUC_{0-}

$_{24\ hr}$ corrected with an accumulation factor in mice found in this study. The HED in mice is 60 mg/kg in whole blood with a standard deviation of 20 mg/kg (**Figure 2.3**), suggesting most doses used for *in vivo* mouse studies are within the limits of exposure achievable in humans.

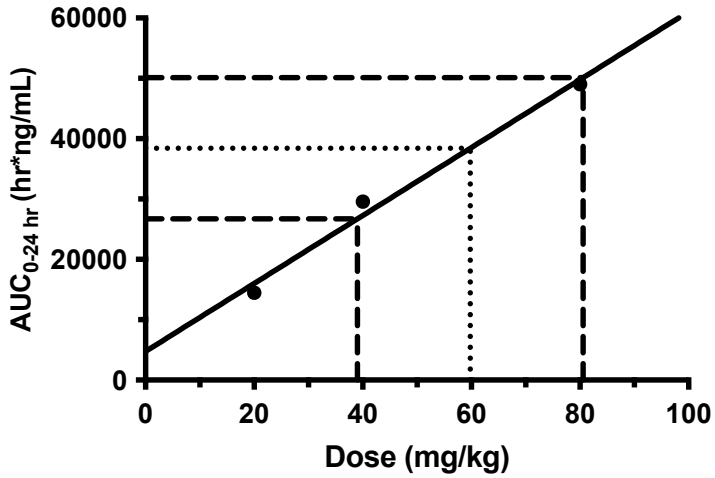

Figure 2.3 Human equivalent HCQ dose in mice. Mouse HCQ AUC (single data points) was compared to clinical trial human HCQ AUC data to find that the HD in mice is 60 mg/kg +/- 20 mg/kg. The dotted line represents the mean human HCQ AUC and the dashed lines represent human AUC standard deviation. Human data taken from Rosenfeld et al [36].

Autophagy inhibition is variable in tissues

Pharmacodynamic response was assessed by western blot analysis of LC3 and p62 in the liver, kidney, gut, and brain at various time points (**Figure 2.4**). Autophagy inhibition in the liver was observed at later time points, most noticeably at 48 hr based on the LC3-II/tubulin ratio. Since liver autophagy was inhibited most at later time points, only 24 hr, 48 hr, and 72 hr time points were assessed in the gut, kidney, and brain. The gut and the kidney showed no autophagy inhibition by either LC3 or p62 levels. Brain

autophagy inhibition was evident in a few mice at 24 and 48 hr but was not dose related. There was no difference in p62 expression in controls compared to HCQ-treated mice in liver or kidney. Effects of HCQ and/or DHCQ on LC3-II expression over time measured by western blot in the liver demonstrate counterclockwise hysteresis, showing it takes time for HCQ and DHCQ to build up before an effect is observed (**Figure 2.5**). There is not much difference between the curves when comparing LC3-II levels to either whole blood or liver HCQ concentrations, indicating that HCQ whole blood concentrations can be used as a surrogate for autophagy effects. Further, DHCQ has a similar effect as HCQ on LC3-II levels. When HCQ and DHCQ concentrations are added together to determine total active drug, the hysteresis curves are still counterclockwise and similar to HCQ or DHCQ alone, indicating that although DHCQ is active, it does not significantly change how quickly autophagy is affected and also requires a buildup to achieve an effect.

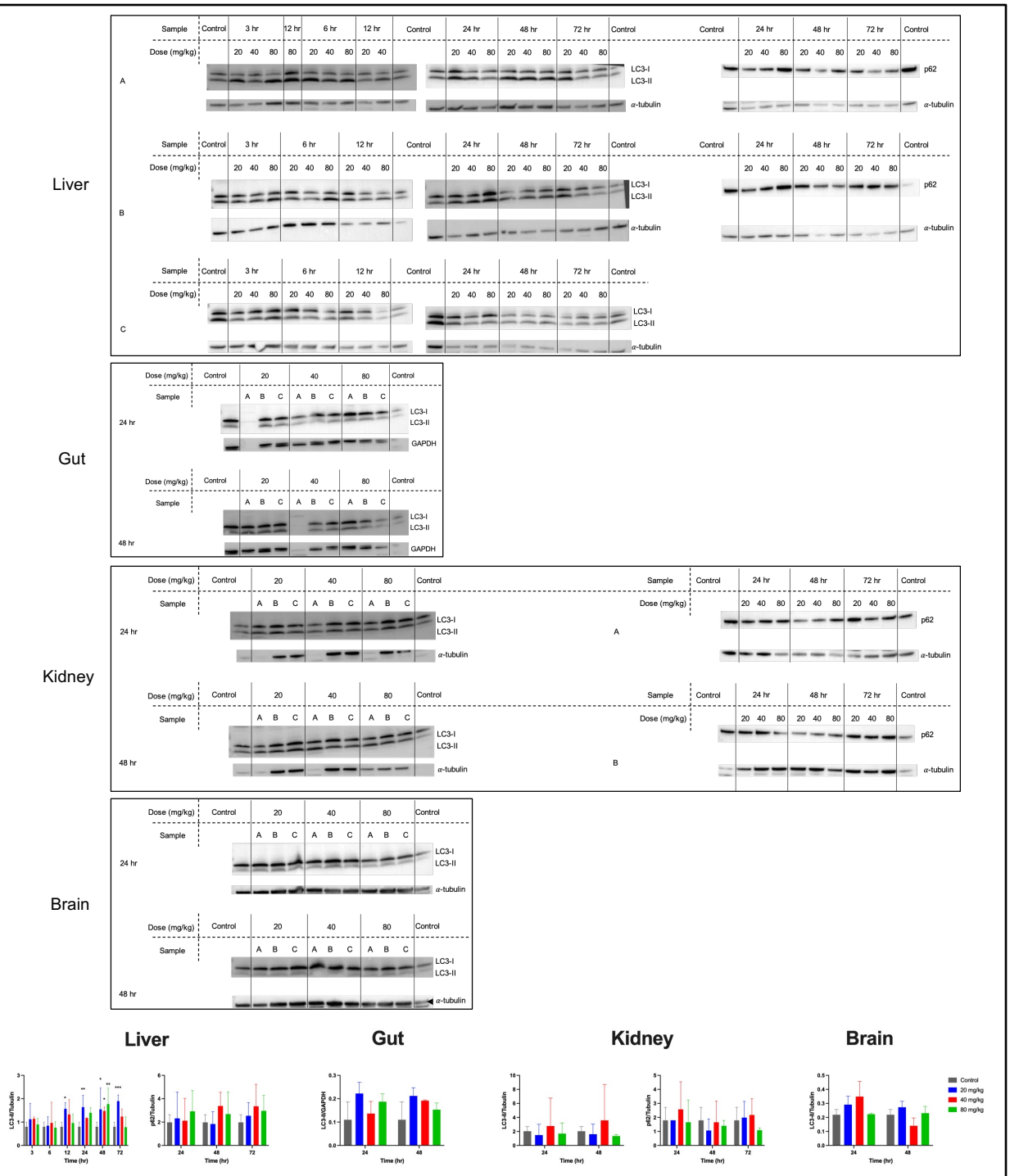

Figure 2.4 Western blots of LC3 and p62 in mice treated with 20, 40, or 80 mg/kg HCQ. LC3 and p62 western blot quantification of liver, gut, kidney, and brain. LC3 protein was analyzed as LC3-II/tubulin or LC3-II/GAPDH ratios. Significance is represented compared to control.

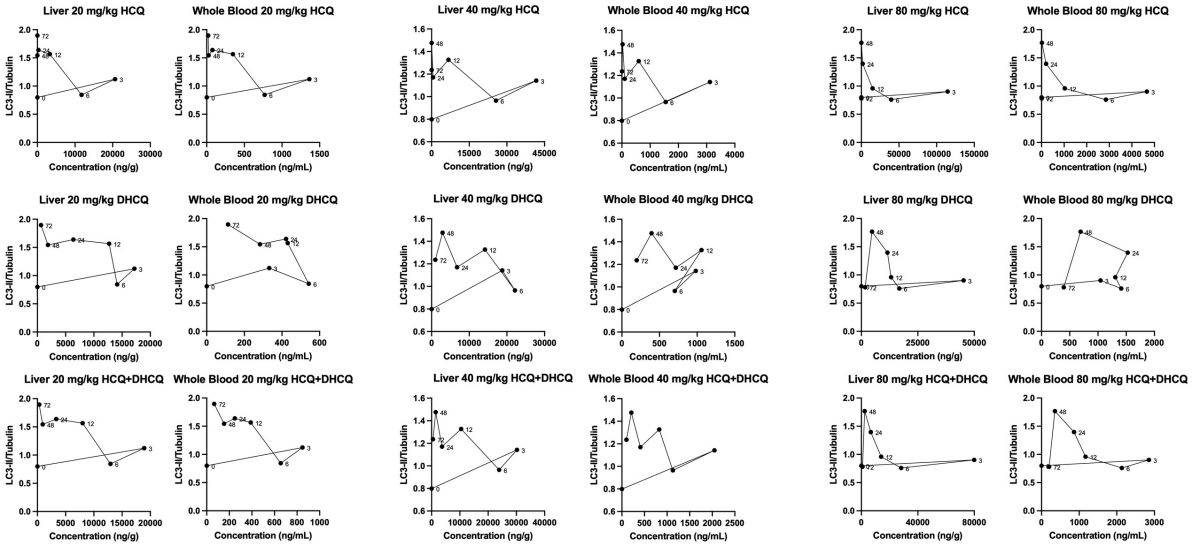

Figure 2.5 Hysteresis curves showing relationship between liver LC3-II levels in liver and concentration of HCQ and/or DHCQ found in liver or whole blood. LC3-II ratios quantified from western blots were compared to the amount of HCQ and/or DHCQ detected in liver or whole blood at those time points.

HCQ exhibits anti-proliferative effects and decreases autophagic flux but does not induce significant cell death in *in vitro* 2D culture

In vitro two-dimensional cell culture experiments were performed to validate standard cell culture methods as a sufficient pharmacodynamic model comparable to in vivo results and to assess how HCQ is affecting cell growth, death, and long-term autophagy in breast cancer. To investigate differences in HCQ uptake and response between breast cancers with different sensitivities to autophagy inhibition determined via shRNA knockdowns and responses to chloroquine *in vitro* and when grown as tumor xenografts [37], MDA-MB-468 (triple negative basal), MDA-MB-231 (triple negative claudin-low), and MCF7 (luminal) cells, listed from most autophagy sensitive to least autophagy sensitive, were treated with increasing doses of HCQ in buffered DMEM for up to 120 hr. Cells are more affected by lower doses of HCQ at later time points (**Figure**

2.6). The median dose at which half of cells were affected (Dm) at 96 hr was calculated. As expected, autophagy independent MCF7 had the highest Dm of 14.6 ± 2.9 μM, while autophagy dependent MDA-MB-231 and MDA-MB-468 Dm's were lower at 7.8 ± 3.9 μM and 7.9 ± 2.6 μM, respectively (**Figure 2.6**).

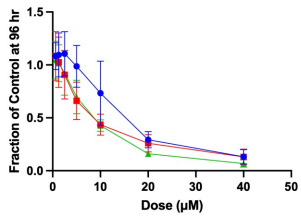

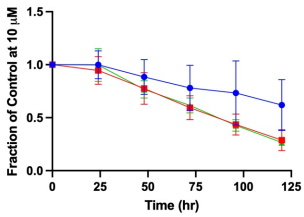

	Dm Mean (μM)	Standard Deviation
MCF7	14.6	2.9
MDA-MB-231	7.8	3.5
MDA-MB-468	7.9	2.6

Figure 2.6 Cell growth in 2D *in vitro* cell culture following HCQ treatment. HCQ screen in breast cancer lines in buffered media from 0.625 to 40 μM HCQ. Dm is calculated at 96 hr.

Since cancer patients are generally treated with 200 mg to 400 mg HCQ, the maximal concentration of HCQ achievable in patients is between 10 μM and 20 μM based on dosing an average size patient. Therefore, cells were treated with either 10 μM (equal dosing) or their Dm value (equal toxicity, 8 μM for MDA-MB-231 and MDA-MB-468 and 15 μM for MCF7) for the following experiments. To determine if the cells were dying via apoptosis, cells were treated with HCQ for 144 hr with a Caspase 3/7 fluorescent dye and monitored in a live cell imaging system. There were no differences in Caspase 3/7 signal between control and HCQ-treated cells in any cell line (**Figure 2.7 A**), indicating that either cell growth is inhibited or that cells are dying by another cell death pathway. To assess whether HCQ causes death in a caspase 3/7 independent manner, cell death was measured in a live cell imaging system using the cytotoxicity agent YOYO, a fluorescent dye that is cell membrane impermeable and binds free DNA in solution as an indicator of cell death (**Figure 2.7 B**). No difference between control and HCQ-treated cell death was

detected. However, when cells were stained with a live/dead stain and analyzed via flow cytometry after 48 hr, 96 hr, or 144 hr of HCQ treatment, modest cell death that was time and dose dependent was observed in the autophagy dependent cells (**Figure 2.7 C**). Overall, this indicates that cell death is not the major cellular pharmacodynamic response to HCQ in 2D culture.

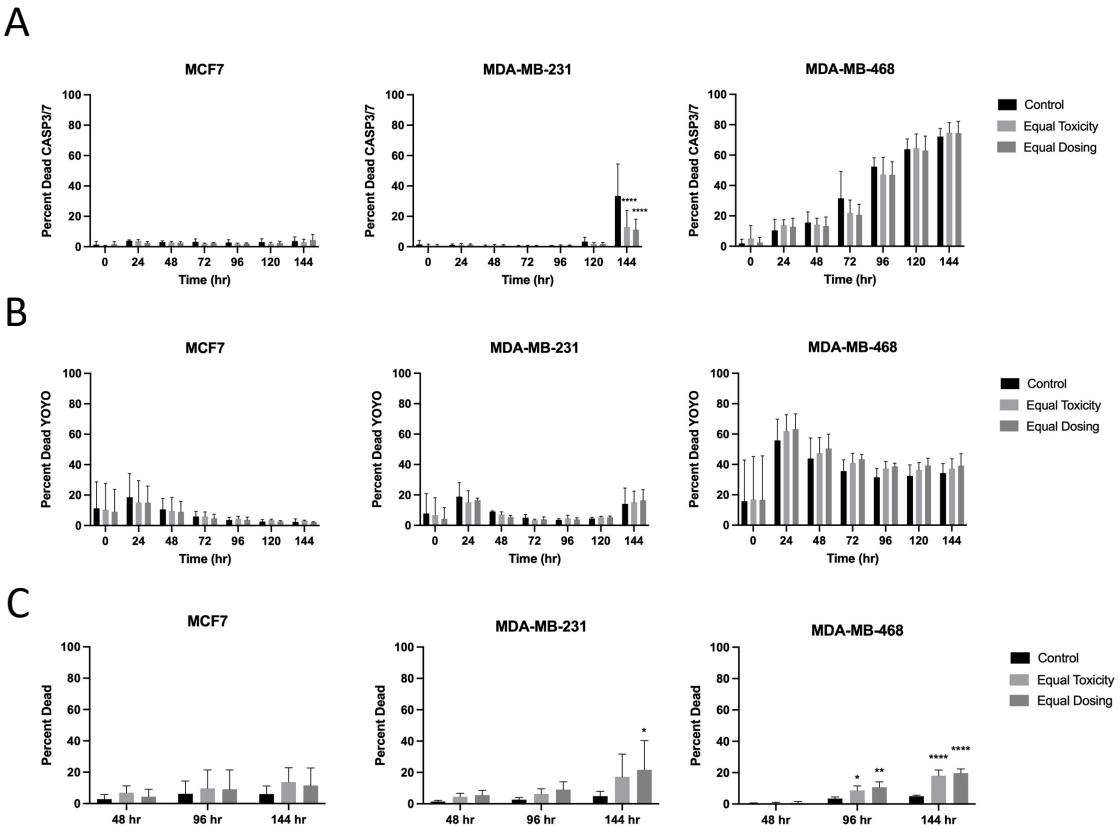

Figure 2.7 Cell death in 2D *in vitro* cell culture following HCQ treatment. Cell death measuring apoptosis via Caspase 3/7 in the IncuCyte (A), measuring cell death that is not necessarily apoptosis-dependnet using YOYO in the IncuCyte(B), or measuring cell death using Sytox Blue staining via flow cytometry (C).

To discern whether cells were growth inhibited, cell cycle assays were performed following HCQ dosing for 48 hr. Cell cycle analysis showed that when HCQ concentration is high enough, an increase in G1 and a decrease in G2/M and S is observed (**Figure 2.8**

A). MCF7 cells treated with 10 μM (less than the Dm) have similar percentages of cells to control in these phases compared to 15 μM. In contrast, MDA-MB-231 and MDA-MB-468 cells experienced a decrease in G2/M and an increase in G0/G1 at all HCQ doses used (their Dm and higher). These results were further supported by cell cycle analysis via EdU incorporation. After HCQ treatment for 48 hr, there were more MDA-MB-231 and MDA-MB-468 cells in G1 and less cells in S and G2/M phases of the cell cycle when treated with both HCQ concentrations but MCF7 cells treated with 10 μM were not different from their control counterparts as the MCF7 cells treated with 15 μM were (**Figure 2.8 B**). Changes in cell cycle were most enhanced in MDA-MB-468, indicating that HCQ more greatly affects cells that are inherently autophagy dependent.

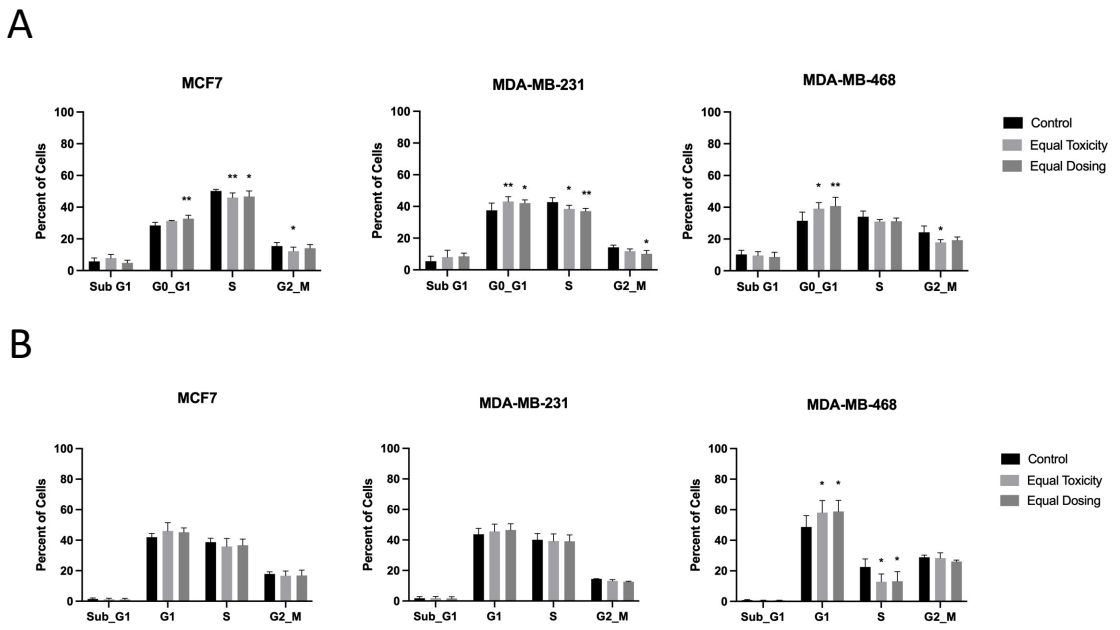

Figure 2.8 Cell cycle analysis in 2D *in vitro* cell culture following HCQ treatment. Cell cycle measured by PI/RNAse staining (A) and cell cycle analysis via EdU incorporation (B) via flow cytometry.

Autophagic flux following HCQ treatment was assessed by flow cytometry using cells transduced with a LC3-mCherry-GFP reporter. This reporter works by tagging autophagosomes. GFP gets quenched in acidic environments. Therefore, when an autophagosome fuses with a lysosome, GFP signal decreases and indicates autophagic flux is occurring. Autophagy was inhibited significantly in the MCF7 cells following as little as 24 hr but autophagy inhibition was not significant in the MDA-MB-231 and MDA-MB-468 until 144 hr or 96 hr, respectively (**Figure 2.9 A**). Results were similar using a live cell imaging system (**Figure 2.9 B**). This indicates that HCQ has prolonged PD affects that may not be observed at short time points.

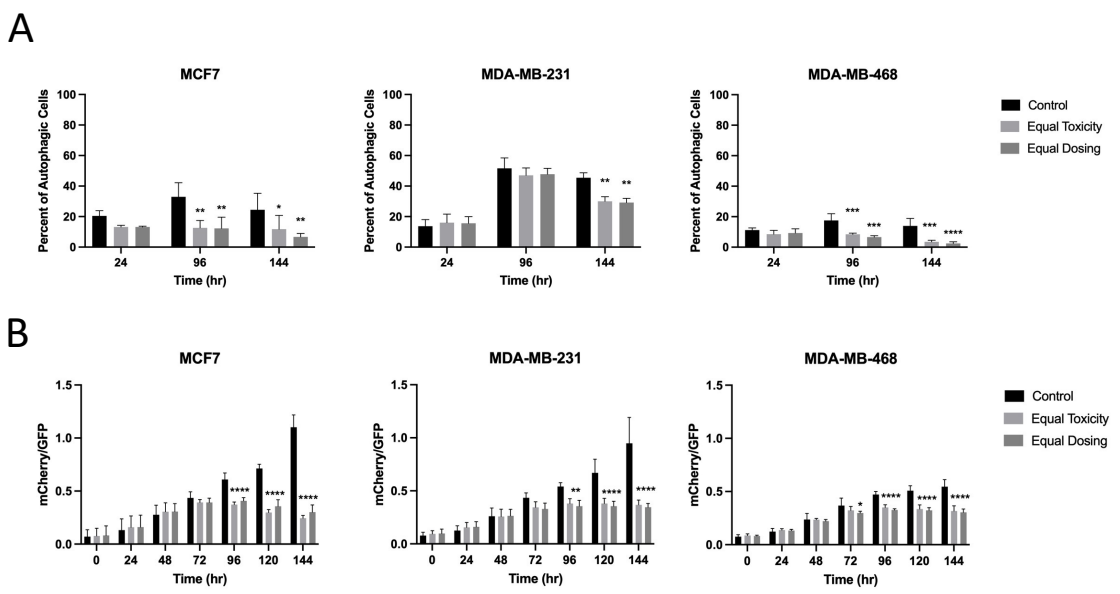

Figure 2.9 Autophagic flux in 2D *in vitro* cell culture following HCQ treatment. Autophagic flux measured by using cells with a LC3-mCherry-GFP construct via flow cytometry (A) and in the IncuCyte (B).

HCQ induces cell death and decreases autophagic flux in tumor organoids

Cells were grown on a basement membrane matrix to obtain three-dimensional tumor organoids to better recapitulate *in vivo* tumors. Caspase 3/7-dependent cell death was assessed by live cell imaging in the IncuCyte. There was significant caspase 3/7 cell death in MCF7 at 96 hr but by 144 hr, the difference between control and HCQ-treated organoids was no longer significant. No significant caspase 3/7 cell death was observed in MDA-MB-468 organoids but there was caspase 3/7 dependent cell death in MDA-MB-231 organoids treated with HCQ 96 hr and later (**Figure 2.10 A**). Cytotoxicity measured by YOYO staining showed significant cell death in MDA-MB-231 and MDA-MB-468 organoids at time points as early as 72 hr following HCQ treatment but not significantly in MCF7 organoids at equal dosing until 120 hr (**Figure 2.10 B**), indicating that HCQ causes more cell death in autophagy dependent tumors than autophagy independent tumors.

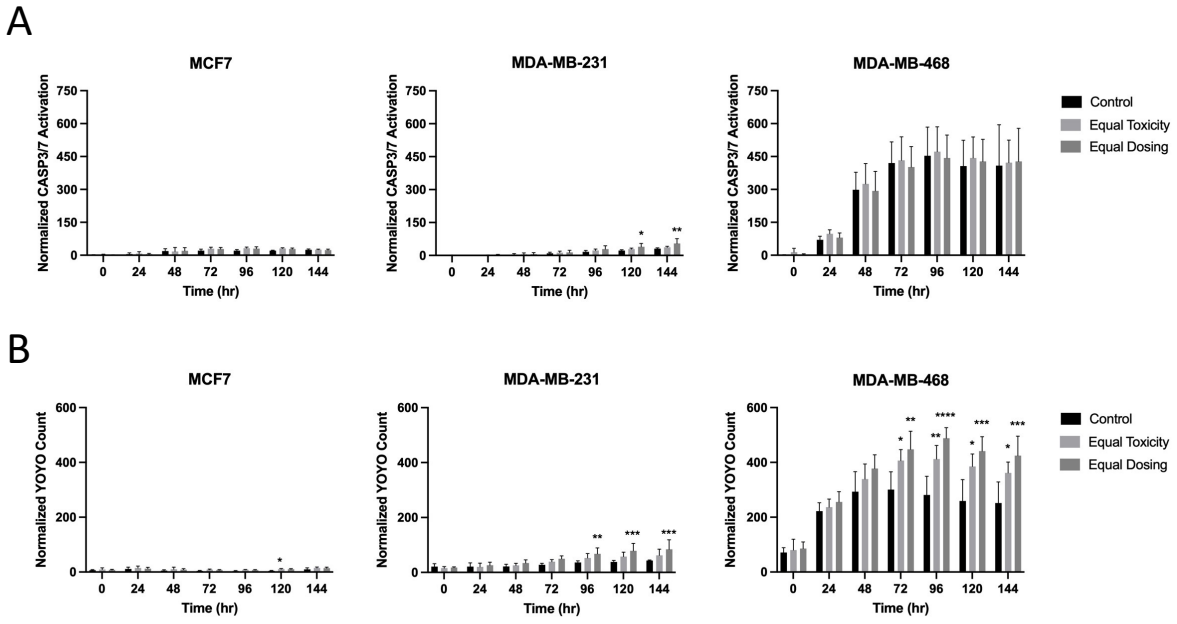

Figure 2.10 Cell death in tumor organoids following HCQ treatment. Cell death measuring apoptosis via Caspase 3/7 in the IncuCyte (A) or measuring cell death that is not necessarily apoptosis-dependent using YoYo in the IncuCyte (B).

Cell cycle analysis was assessed in tumor organoids via EdU incorporation (**Figure 2.11**). Results were similar to 2D culture; there was no difference in HCQ-treated MCF7 cells compared to controls but MDA-MB-231 and MDA-MB-468 cells both had significantly less cells in S phase at both HCQ concentrations used. Consistent with the 2D results, MDA-MB-468 cells also had a significant increase in G1 cells following HCQ treatment.

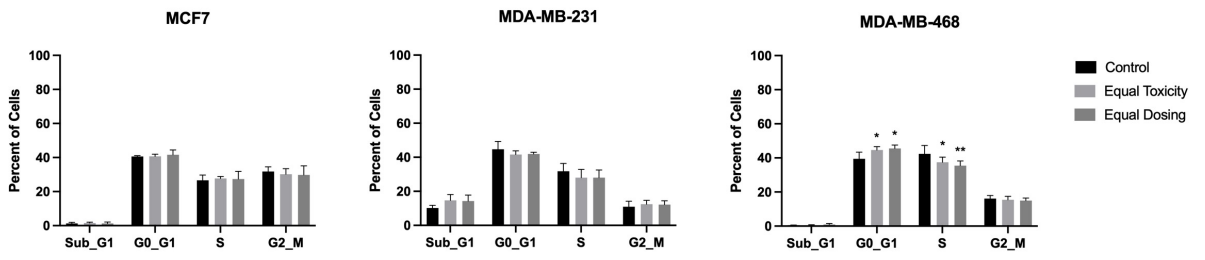

Figure 2.11 Cell cycle analysis in tumor organoids following HCQ treatment. Cell cycle measured by EdU incorporation via flow cytometry.

To assess autophagic flux, organoids transduced with a LC3-mCherry-GFP construct were imaged in the IncuCyte over 6 days. Similar to the 2D cell culture results, autophagy was inhibited significantly between control and HCQ-treated organoids at later time points (**Figure 2.12**). MCF7 and MDA-MB-468 organoid autophagic flux inhibition was sustained and enhanced by 144 hr. MDA-MB-231 organoid autophagic flux inhibition following HCQ was less marked compared to control which was consistent with the 2D cell culture results.

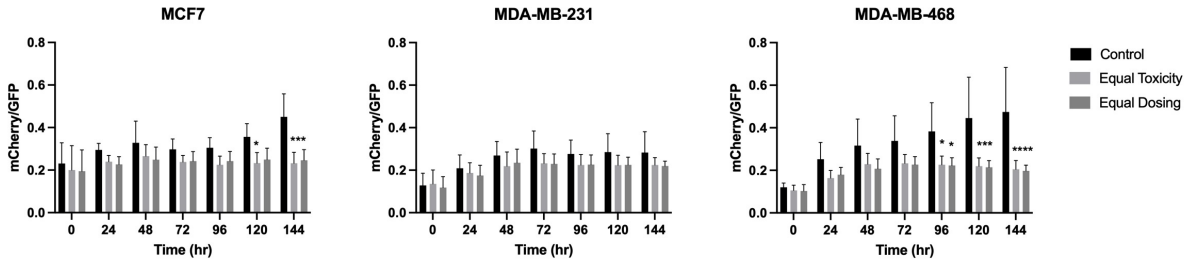

Figure 2.12 Autophagic flux in tumor organoids following HCQ treatment. Autophagic flux measured by red to the green ratio in the IncuCyte.

Autophagy dependent tumors take up more HCQ *in vivo*

To assess how HCQ affects autophagy dependent and independent tumors *in vivo*, MCF7, MDA-MB-231, or MDA-MB-468 cells were implanted into mice and once the tumors were at least 100 mm^3, the mice were treated with either 60 mg/kg HCQ once or daily for one week to analyze steady state levels.

Whole blood HCQ and DHCQ amounts were similar in both MDA-MB-231 and MCF7 cohorts while both tumor HCQ and DHCQ amounts were higher in MDA-MB-231 compared to MCF7. MDA-MB-468 HCQ and DHCQ amounts were also similar to MDA-MB-231 (**Figure 2.13 A**). Tumor levels of HCQ and DHCQ were higher in MDA-MB-231 and MDA-MB-468 compared to MCF7 at steady state (**Figure 2.13 B**), indicating that more HCQ and DHCQ is distributed into autophagy sensitive tumors. In the steady state cohort, whole blood levels were similar for HCQ and DHCQ in MDA-MB-231 and MCF7 but the MDA-MB-231 cohort had higher tumor HCQ and DHCQ levels compared to the MCF7 cohort (**Figure 2.13 C**). When the steady state tumor group was compared to the 24 hr single dose tumors in each tumor type, HCQ and DHCQ levels were significantly higher in tumors in the steady state group compared to the single dose groups (**Figure**

2.13 C), indicating that HCQ and DHCQ move into the tumor after 24 hr and tumor and blood saturation is not achieved by 24 hr. When analyzing DHCQ:HCQ ratios found in tumors, MDA-MB-231 and MDA-MB-468 had higher ratios compared to MCF7 (**Figure 2.13 D**), indicating that more DHCQ was formed compared to HCQ in the autophagy dependent tumors.

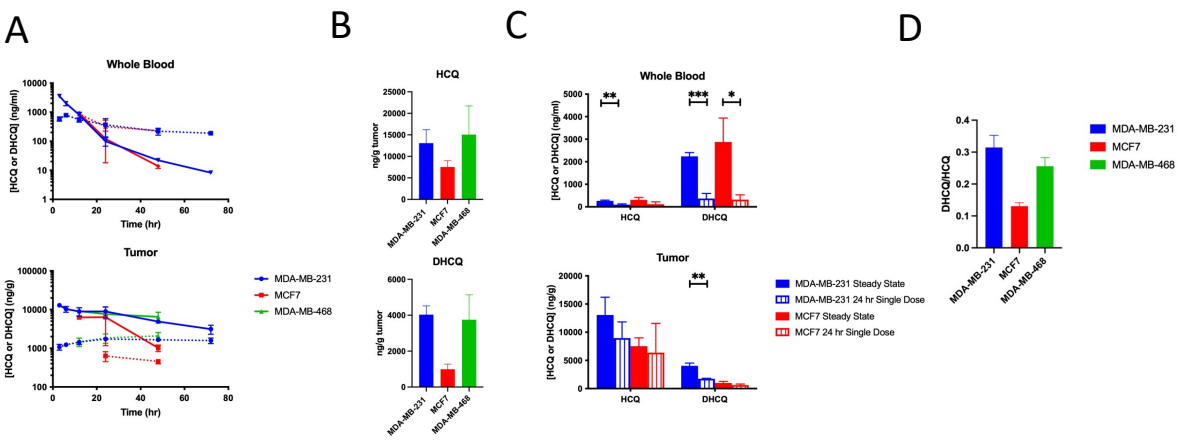

Figure 2.13 HCQ and DHCQ PK in breast tumor-bearing mice following 60 mg/kg HCQ. Exposure of HCQ and DHCQ in whole blood and tumor. Solid lines represent HCQ and dotted lines represent DHCQ (A). Tumor levels of HCQ and DHCQ at steady state (B). Whole blood and tumor HCQ and DHCQ amounts detected in steady state dosed mice compared to 24 hr single dose mice (C). DHCQ:HCQ ratios in tumors (D).

Autophagic responses were not different but proliferation was less in autophagy dependent tumors *in vivo*

Pharmacodynamic response was evaluated via western blot analysis of LC3 and p62 in the MDA-MB-231, MCF7, and MDA-MB-468 cohorts. There were no major differences between control and treated mice at 24 hr, 48 hr, or steady state doses although p62 levels trended higher in treated MDA-MB-468 tumors at 24 hr (**Figure 2.14**). LC3-II densitometry area normalized to total protein were highest at 12 hr, 24 hr, and

following steady state dosing in MDA-MB-231 tumors but these results were variable depending on the mouse (**Figure 2.15**). Tumor cell proliferation was measured via immunofluorescence staining of Ki67 in the MDA-MB-231 and MCF7 control and steady state cohorts. MDA-MB-231 tumors had significantly less Ki67 staining following HCQ treatment while there was no difference in cell proliferation in the MCF7 tumors after HCQ treatment (**Figure 2.16**). These results are consistent with the cell cycle results in 2D culture (**Figure 2.8**) and tumor organoids (**Figure 2.11**) because the cells that are more sensitive to autophagy inhibition (MDA-MB-231 and MDA-MB-468) have less proliferative cells at lower HCQ concentrations compared to those that are not (MCF7). Apoptotic cell death via immunofluorescence staining of cleaved caspase-3 was also performed but no tumors expressed cleaved caspase-3 (results not shown).

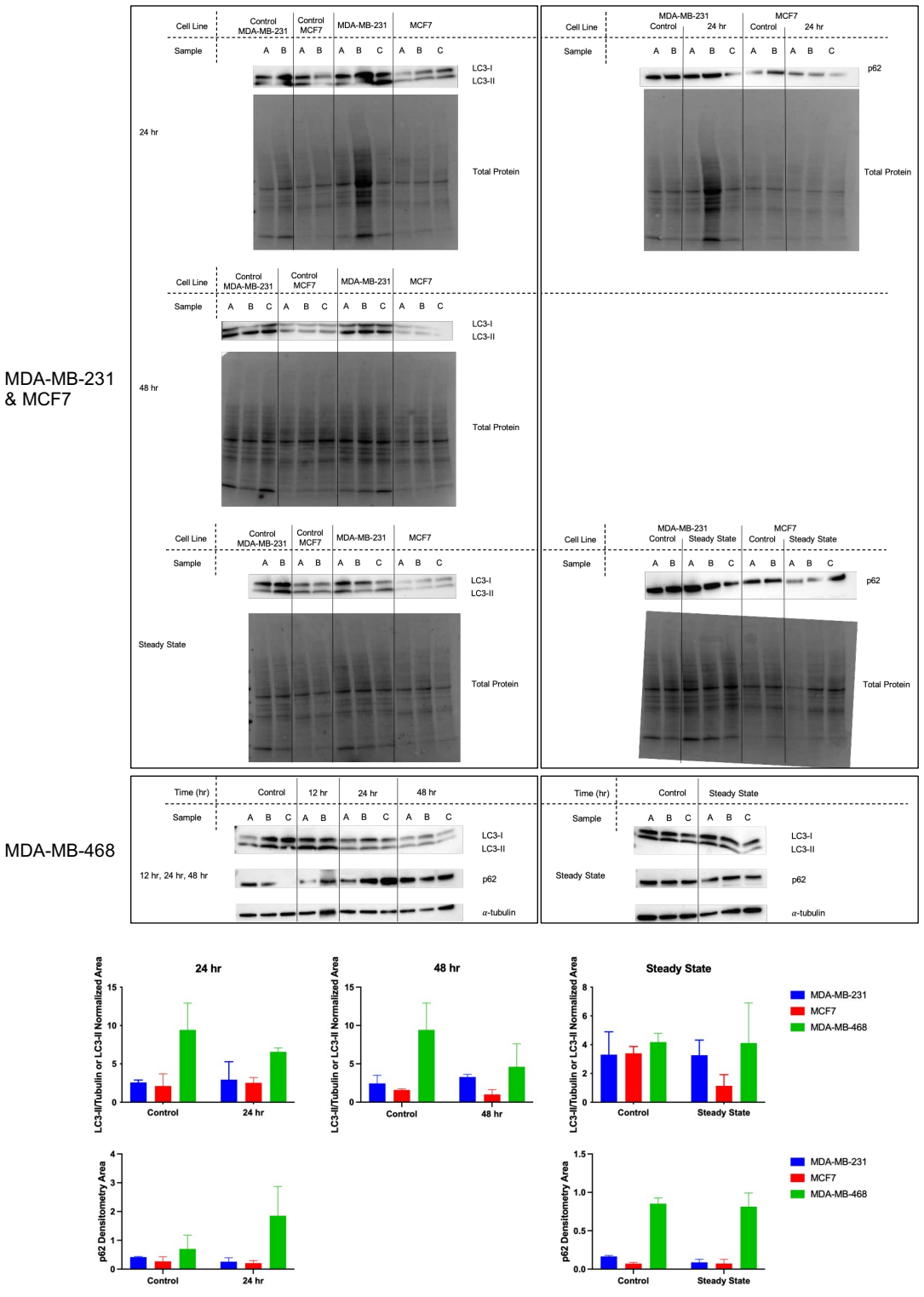

Figure 2.14 LC3 and p62 expression in breast tumors in mice following 60 mg/kg HCQ. Western blots and quantification of LC3-II and p62 normalized to total protein or tubulin in breast tumors following 24 hr, 48 hr, or steady state dosing of HCQ in mice.

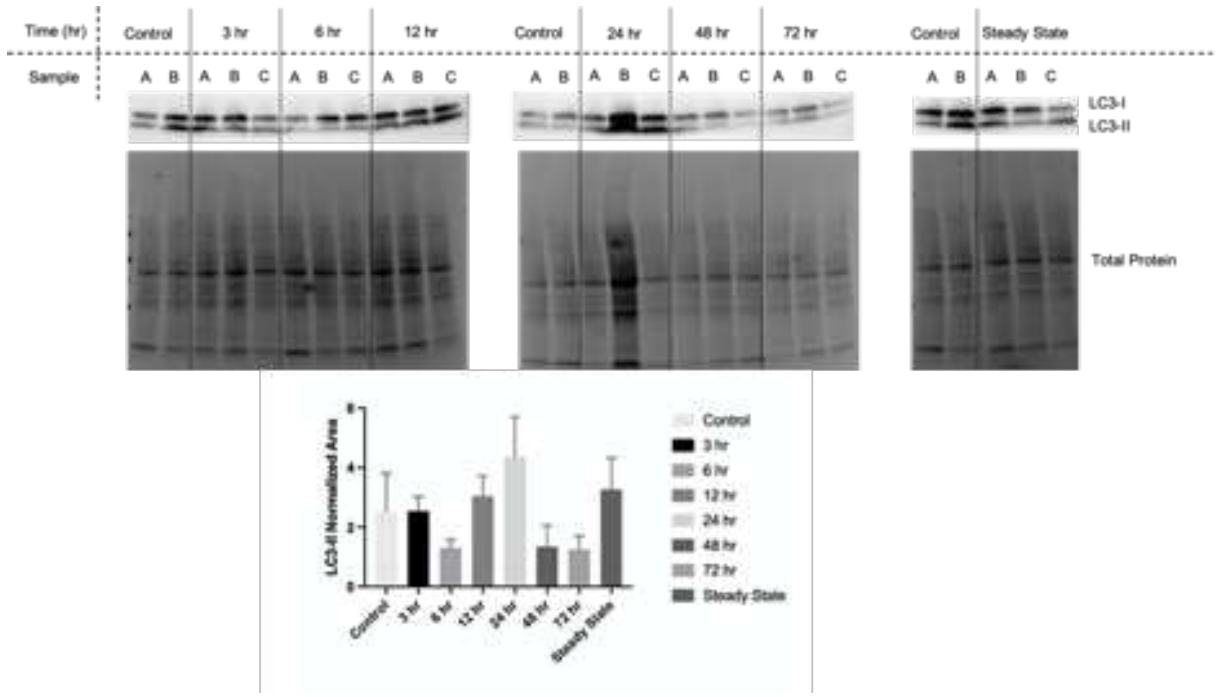

Figure 2.15 LC3 expression over time in MDA-MB-231 tumor bearing mice treated with 60 mg/kg HCQ. Western blot and quantification of LC3-II densitometry normalized to total area over 72 hr or at steady state.

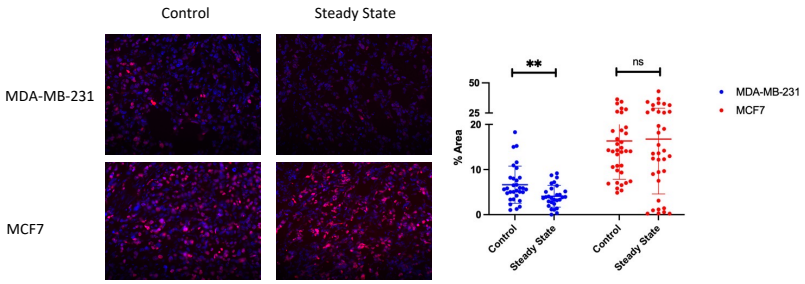

Figure 2.16 Ki67 staining in tumors following HCQ treatment. Immunofluorescent analysis of Ki67 in MDA-MB-231 and MCF7 control and steady state tumors. Blue=DAPI and red=Ki67. Quantification based on 6 or more separate fields of view on each tumor slice.

Discussion

Autophagy, a lysosomal degradation process that recycles damaged proteins, organelles, and other cellular components, has been linked to enhanced cancer cell survival and chemotherapy resistance. HCQ, an already FDA-approved drug, has been repurposed as an anticancer agent that inhibits autophagy. Although it is currently being used in over 90 clinical trials alone or in combination with other cancer treatments, the pharmacodynamic response associated with drug dosages used in the clinic is not clear. Further, pre-clinical studies in mice use varying doses of HCQ but there is currently no rationale behind those doses or the affect the associated drug exposures on autophagy inhibition *in vivo*.

This study showed that HCQ and DHCQ, the major active metabolite, levels are dose dependent in whole blood and multiple tissues *in vivo* (**Figure 2.1**). Autophagy inhibition was achieved at all doses in liver and gut at multiple time points (**Figure 2.4**). Although some autophagy inhibition was observed at the various doses in multiple tissues, there was high variability in detected autophagy inhibition between different mice. Variability and non-significant differences in autophagy inhibition is also evident in the clinic [16, 21, 38] and the results in this study show that this is difficult to control from patient to patient based on dose alone suggesting HCQ doses may need to be tailored based on their individual PD response. It further implies that autophagy inhibition may not be reliably achievable using HCQ and that more potent autophagy inhibitors such as DC661 should be considered. This work also clarified that 60 mg/kg ± 20 mg/kg HCQ is the human equivalent dose to give mice in pre-clinical studies and validates the clinical

relevance for studies that choose HCQ doses within this range (**Figure 2.3**). Calculating the HED in this way highlights the importance of normalizing pre-clinical and clinical drug exposure because mouse model efficacy is predictive of clinical response when drug concentrations in mice are appropriately corrected for therapeutic exposure [39, 40].

Mice with breast tumors treated with the HED of 60 mg/kg HCQ had similar whole blood HCQ and DHCQ levels but varying tumor levels with more HCQ and DHCQ detected in the autophagy dependent MDA-MB-231 and MDA-MB-468 tumors compared to the autophagy independent MCF7 tumors [37] (**Figure 2.13**), suggesting that autophagy dependent tumors sequester more HCQ over time. This could be due to an increase in lysosomes in autophagy dependent tumors compared to autophagy independent tumors [41]. There are important implications of this when considering dual treatment with HCQ and other drugs, especially chemotherapies that sequester in lysosomes. It could be advantageous to treat patients with HCQ prior to these drugs since HCQ also sequesters in the lysosome and could make these drugs more potent, as seen in a phase I clinical trial in dogs with lymphoma [38]. Although there is a lot of information available on HCQ effects in cancer, it is important to consider DHCQ as well since it is present at relevant concentrations and correlates to liver autophagy inhibition (**Figure 2.5**). Further, the data here suggests that DHCQ:HCQ ratios may be predictive of patient efficacy based on the autophagy dependency of the tumor (Figure 2.12); this ratio has also been implicated in patient response to HCQ treatment in a couple other studies [42, 43]. Similar to HCQ, DHCQ has a long half-life of approximately 160 hr in people [42]. However, DHCQ is not produced in cell culture experiments because there are no cytochrome P450 enzymes. Since *in vitro* studies do not take into account DHCQ but it

is an active metabolite that has the same action as HCQ, drug concentrations used *in vitro* likely do not reflect the full efficacy HCQ and subsequent DHCQ will have on PD and this should be taken into consideration when choosing HCQ doses *in vitro*. This is evidenced by comparing HCQ exposure *in vitro* to *in vivo* exposure, where 20 μM HCQ dosing in cell culture correlates best with the autophagy dependent tumors while there is no correlation between MCF7 and *in vitro* exposure (**Figure 2.17**). Further, adding in the relevant DHCQ exposure actually means that a higher concentration of HCQ can be used in cell culture to achieve the same exposure observed *in vivo* (**Figure 2.17**). This also highlights the importance of calculating maximum achievable clinically relevant doses for cell culture experiments.

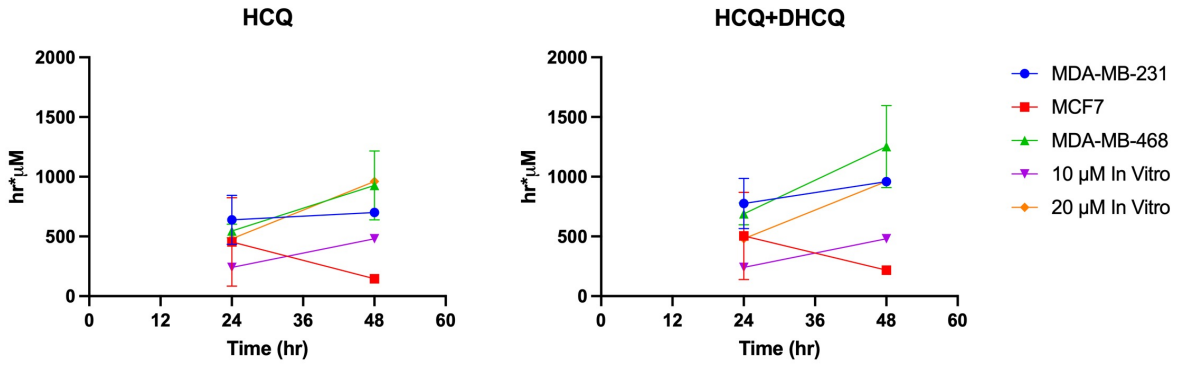

Figure 2.17 *In vitro* to *in vivo* HCQ exposure comparison. HCQ PK exposure *in vitro* compared to *in vivo*. For the breast tumors, exposure is based on AUC of concentration versus time curves. The 10 and 20 μM *in vitro* AUC is based on the theoretical exposure cells will experience based on those doses for the given time (e.g., 10 μM * 24 hr = 240 hr* μM).

Autophagy inhibition measured by western blot *in vivo* was less conclusive in all tumor types which is consistent with the non-tumor bearing mice and autophagy inhibition measured in the clinic. However, autophagy inhibition was observed *in vitro* at clinically relevant concentrations. Inhibition was most enhanced at later time points indicating that

HCQ does not decrease autophagic flux rapidly (**Figures 2.9 and 2.12**) even though HCQ uptake is observed at early time points in the tumors. This is also consistent with observing decreased cell growth compared to control following HCQ treatment at later time points (**Figure 2.6**). Further, the MDA-MB-231 cell line showed high basal autophagy even when treated with HCQ, implying that HCQ is inhibiting autophagy but not as well as other autophagy inhibitors would since this assay was based on autophagy inhibition via bafilomycin A1. Both autophagy dependent and independent cell lines had significant decreases in autophagic flux indicating autophagy is still inhibited by HCQ irrespective of dependency on autophagy. This is not in line with one study that found the basal breast cancer line SUM190 to be the most sensitive to HCQ induced autophagy inhibition *in vitro* but that could be because it only analyzed short time points [44]. Taken together, autophagy inhibition was variable *in vivo* but observed *in vitro*, suggesting that other autophagy PD measures may be necessary to better understand how HCQ is causing autophagy inhibition *in vivo* and in the clinic.

Although autophagy inhibition was inconsistent across tumor types and between controlled and treated mice, cell proliferation was consistently affected in the autophagy sensitive MDA-MB-231 and MDA-MB-468 tumors treated with HCQ alone but not in autophagy independent MCF7 tumors (**Figures 2.8, 2.11, 2.16**) indicating that autophagy dependent tumors are more affected by single agent HCQ. Further, cell proliferation was more affected in autophagy dependent tumors at lower doses of HCQ compared to MCF7 (**Figures 2.8 and 2.11**), suggesting that the MCF7 tumors *in vivo* did not have high enough HCQ levels to cause a decrease in cell proliferation that was observed in the MDA-MB-231. The ability of HCQ to inhibit cell proliferation alone varies in tumor types.

For instance, a study in mice with melanoma tumors showed that 65 mg/kg of HCQ alone did not cause decreased Ki67 but combination treatment with the mTOR inhibitor CCI-770 did cause significant decrease in Ki67 tumor expression [45]. A clinical trial also found no significant decrease in Ki67 in breast cancer patients treated with 500 mg CQ after 14 days and concluded that the cancer cells were potentially using autophagy as a cytoprotective mechanism because they were not stressed enough without the treatment of another anti-cancer therapy and therefore HCQ did not induce anti-proliferative effects [46]. These studies and the one presented here suggest that CQ and HCQ alone may not provide enough anti-proliferative effects in many cancer patients but that HCQ alone is anti-proliferative if the tumor is inherently dependent enough on autophagy. Even though HCQ did decrease cell proliferation in the autophagy dependent tumors, more potent autophagy inhibitors may produce more robust results and have less variability in achieving autophagy inhibition as a single agent compared to HCQ.

Clinically relevant HCQ concentrations were used in this study to determine if HCQ causes cancer cell death. Based on the *in vivo* and *in vitro* apoptosis and cell death assays, breast cancer cells treated with HCQ alone at the concentrations used here do not appear to die via caspase 3/7-dependent apoptosis but do undergo some cell death in 2D and organoids (**Figures 2.7 and 2.10**) and this cell death is enhanced in the autophagy dependent tumors at the later time points. Another study also observed no caspase 3-dependent cell death in head and neck squamous cell carcinoma cell lines when treated with 20 μM HCQ alone [47]. Other studies have shown that HCQ alone can induce caspase 3-dependent cell death in gastric cancer [48] and bladder cancer [49] at HCQ concentrations of 14 μM and 20 μM respectively, indicating that HCQ alone will only

induce this kind of cell death at clinically achievable concentrations in certain cancer types. However, when clinically relevant HCQ doses are combined with other treatments, HCQ enhances apoptotic cell death in other cancer types such as head and neck squamous cell carcinoma [47], melanoma [45], and gastric cancer [48], demonstrating that even though low enough doses of HCQ alone does not cause caspase 3/7-dependent apoptosis in certain cancer types, in combination with other therapies it does induce caspase 3/7-dependent apoptosis. Although combination therapies were not tested in this study, the results of these other studies suggest that combining HCQ with other treatments may enhance cell death in breast cancer.

Overall, this study shows that 2D cell culture, 3D tumor organoids, and *in vivo* studies produce similar results and *in vitro* studies can be used as surrogates to recapitulate *in vivo* tumor responses. Tumor autophagy dependency is important in the evocation of cellular responses including autophagy inhibition, cell proliferation, and cell death. Further, in certain contexts, HCQ may not be an adequate drug as a single agent depending on the clinical objective. DHCQ is also an active metabolite whose effects needs to be considered in *in vitro* experiments since it is not produced but would add to toxicity if it were present. Lastly, better biomarkers to measure autophagy inhibition in the clinic are necessary to understand how the PD relates to the PK of autophagy inhibitors.

References

1. De Duve C, Wattiaux R. Functions of lysosomes. Annu Rev Physiol. 1966;28:435-92. doi: 10.1146/annurev.ph.28.030166.002251. PubMed PMID: 5322983.

2. Yang Z, Klionsky DJ. Eaten alive: a history of macroautophagy. Nat Cell Biol. 2010 Sep;12(9):814-22. doi: 10.1038/ncb0910-814. PubMed PMID: 20811353; PubMed Central PMCID: PMCPMC3616322.

3. Duffy A, Le J, Sausville E, et al. Autophagy modulation: a target for cancer treatment development. Cancer Chemother Pharmacol. 2015 Mar;75(3):439-47. doi: 10.1007/s00280-014-2637-z. PubMed PMID: 25422156.

4. Mauthe M, Orhon I, Rocchi C, et al. Chloroquine inhibits autophagic flux by decreasing autophagosome-lysosome fusion. Autophagy. 2018;14(8):1435-1455. doi: 10.1080/15548627.2018.1474314. PubMed PMID: 29940786; PubMed Central PMCID: PMCPMC6103682.

5. Cheong H. Integrating autophagy and metabolism in cancer. Arch Pharm Res. 2015 Mar;38(3):358-71. doi: 10.1007/s12272-015-0562-2. PubMed PMID: 25614051.

6. Thorburn A, Thamm DH, Gustafson DL. Autophagy and cancer therapy. Mol Pharmacol. 2014 Jun;85(6):830-8. doi: 10.1124/mol.114.091850. PubMed PMID: 24574520; PubMed Central PMCID: PMCPMC4014668.

7. Ruiz-Irastorza G, Ramos-Casals M, Brito-Zeron P, et al. Clinical efficacy and side effects of antimalarials in systemic lupus erythematosus: a systematic review. Ann Rheum Dis. 2010 Jan;69(1):20-8. doi: 10.1136/ard.2008.101766. PubMed PMID: 19103632.

8. Manic G, Obrist F, Kroemer G, et al. Chloroquine and hydroxychloroquine for cancer therapy. Mol Cell Oncol. 2014;1(1):e29911. doi: 10.4161/mco.29911. PubMed PMID: 27308318; PubMed Central PMCID: PMCPMC4905171.

9. Lim HS, Im JS, Cho JY, et al. Pharmacokinetics of hydroxychloroquine and its clinical implications in chemoprophylaxis against malaria caused by Plasmodium vivax. Antimicrob Agents Chemother. 2009 Apr;53(4):1468-75. doi:

10.1128/AAC.00339-08. PubMed PMID: 19188392; PubMed Central PMCID: PMCPMC2663072.

10. Estes ML, Ewing-Wilson D, Chou SM, et al. Chloroquine neuromyotoxicity. Clinical and pathologic perspective. Am J Med. 1987 Mar;82(3):447-55. PubMed PMID: 3826099.

11. Carmichael SJ, Charles B, Tett SE. Population pharmacokinetics of hydroxychloroquine in patients with rheumatoid arthritis. Ther Drug Monit. 2003 Dec;25(6):671-81. PubMed PMID: 14639053.

12. Tett SE. Clincal Pharamcokinetics of Slow-Acting Antirheumatic Drugs. Clin Pharmacokinet. 1993;25(5):392-407.

13. Ducharme J, Farinotti R. Clinical pharmacokinetics and metabolism of chloroquine. Focus on recent advancements. Clin Pharmacokinet. 1996 Oct;31(4):257-74. doi: 10.2165/00003088-199631040-00003. PubMed PMID: 8896943.

14. Furst DE. Pharmacokinetics of hydroxychloroquine and chloroquine during treatment of rheumatic diseases. Lupus. 1996 Jun;5 Suppl 1:S11-5. PubMed PMID: 8803904.

15. Cardoso CD, Bonato PS. Enantioselective metabolism of hydroxychloroquine employing rats and mice hepatic microsomes. Brazilian Journal of Pharmaceutical Sciences. 2009 Oct-Dec;45(4):659-667. PubMed PMID: WOS:000277065000007; English.

16. Wolpin BM, Rubinson DA, Wang X, et al. Phase II and pharmacodynamic study of autophagy inhibition using hydroxychloroquine in patients with metastatic pancreatic adenocarcinoma. Oncologist. 2014 Jun;19(6):637-8. doi: 10.1634/theoncologist.2014-0086. PubMed PMID: 24821822; PubMed Central PMCID: PMCPMC4041680.

17. Boehrer S, Ades L, Braun T, et al. Erlotinib exhibits antineoplastic off-target effects in AML and MDS: a preclinical study. Blood. 2008 Feb 15;111(4):2170-80. doi: 10.1182/blood-2007-07-100362. PubMed PMID: 17925489.

18. Goldberg SB, Supko JG, Neal JW, et al. A phase I study of erlotinib and hydroxychloroquine in advanced non-small-cell lung cancer. J Thorac Oncol.

2012 Oct;7(10):1602-8. doi: 10.1097/JTO.0b013e318262de4a. PubMed PMID: 22878749; PubMed Central PMCID: PMCPMC3791327.

19. Zeh HJ, Bahary N, Boone BA, et al. A Randomized Phase II Preoperative Study of Autophagy Inhibition with High-Dose Hydroxychloroquine and Gemcitabine/Nab-Paclitaxel in Pancreatic Cancer Patients. Clin Cancer Res. 2020 Jul 1;26(13):3126-3134. doi: 10.1158/1078-0432.CCR-19-4042. PubMed PMID: 32156749; PubMed Central PMCID: PMCPMC8086597.

20. Kimmelman AC. The dynamic nature of autophagy in cancer. Genes Dev. 2011 Oct 1;25(19):1999-2010. doi: 10.1101/gad.17558811. PubMed PMID: 21979913; PubMed Central PMCID: PMCPMC3197199.

21. Mahalingam D, Mita M, Sarantopoulos J, et al. Combined autophagy and HDAC inhibition: a phase I safety, tolerability, pharmacokinetic, and pharmacodynamic analysis of hydroxychloroquine in combination with the HDAC inhibitor vorinostat in patients with advanced solid tumors. Autophagy. 2014 Aug;10(8):1403-14. doi: 10.4161/auto.29231. PubMed PMID: 24991835; PubMed Central PMCID: PMCPMC4203517.

22. Frese KK, Tuveson DA. Maximizing mouse cancer models. Nat Rev Cancer. 2007 Sep;7(9):645-58. doi: 10.1038/nrc2192. PubMed PMID: 17687385.

23. Amaravadi RK, Yu D, Lum JJ, et al. Autophagy inhibition enhances therapy-induced apoptosis in a Myc-induced model of lymphoma. J Clin Invest. 2007 Feb;117(2):326-36. doi: 10.1172/JCI28833. PubMed PMID: 17235397; PubMed Central PMCID: PMCPMC1765515.

24. Komatsu M, Waguri S, Koike M, et al. Homeostatic levels of p62 control cytoplasmic inclusion body formation in autophagy-deficient mice. Cell. 2007 Dec 14;131(6):1149-63. doi: 10.1016/j.cell.2007.10.035. PubMed PMID: 18083104.

25. Duran A, Linares JF, Galvez AS, et al. The signaling adaptor p62 is an important NF-kappaB mediator in tumorigenesis. Cancer Cell. 2008 Apr;13(4):343-54. doi: 10.1016/j.ccr.2008.02.001. PubMed PMID: 18394557.

26. Yang S, Wang X, Contino G, et al. Pancreatic cancers require autophagy for tumor growth. Genes Dev. 2011 Apr 1;25(7):717-29. doi: 10.1101/gad.2016111. PubMed PMID: 21406549; PubMed Central PMCID: PMCPMC3070934.

27. Sflomos G, Dormoy V, Metsalu T, et al. A Preclinical Model for ERalpha-Positive Breast Cancer Points to the Epithelial Microenvironment as Determinant of Luminal Phenotype and Hormone Response. Cancer Cell. 2016 Mar 14;29(3):407-422. doi: 10.1016/j.ccell.2016.02.002. PubMed PMID: 26947176.

28. Dobrolecki LE, Airhart SD, Alferez DG, et al. Patient-derived xenograft (PDX) models in basic and translational breast cancer research. Cancer Metastasis Rev. 2016 Dec;35(4):547-573. doi: 10.1007/s10555-016-9653-x. PubMed PMID: 28025748; PubMed Central PMCID: PMCPMC5396460.

29. Li X, Pan B, Ma J, et al. Breast cancer organoids model treatment response of HER2 targeted therapy in HER2-mutant breast cancer. Annals of Oncology. 2019;30:v768-v769. doi: 10.1093/annonc/mdz268.022.

30. Campaner E, Zannini A, Santorsola M, et al. Breast Cancer Organoids Model Patient-Specific Response to Drug Treatment. Cancers (Basel). 2020 Dec 21;12(12). doi: 10.3390/cancers12123869. PubMed PMID: 33371412; PubMed Central PMCID: PMCPMC7770601.

31. Bleijs M, van de Wetering M, Clevers H, et al. Xenograft and organoid model systems in cancer research. EMBO J. 2019 Aug 1;38(15):e101654. doi: 10.15252/embj.2019101654. PubMed PMID: 31282586; PubMed Central PMCID: PMCPMC6670015.

32. Yang L, Liu B, Chen H, et al. Progress in the application of organoids to breast cancer research. J Cell Mol Med. 2020 May;24(10):5420-5427. doi: 10.1111/jcmm.15216. PubMed PMID: 32283573; PubMed Central PMCID: PMCPMC7214171.

33. Fan H, Demirci U, Chen P. Emerging organoid models: leaping forward in cancer research. J Hematol Oncol. 2019 Dec 29;12(1):142. doi: 10.1186/s13045-019-0832-4. PubMed PMID: 31884964; PubMed Central PMCID: PMCPMC6936115.

34. Sasmita AO, Wong YP. Organoids as Reliable Breast Cancer Study Models: An Update. Int J Oncol Res. 2018;1(2). doi: 10.23937/ijor-2017/1710008.

35. Amaravadi RK, Lippincott-Schwartz J, Yin XM, et al. Principles and current strategies for targeting autophagy for cancer treatment. Clin Cancer Res. 2011 Feb 15;17(4):654-66. doi: 10.1158/1078-0432.CCR-10-2634. PubMed PMID: 21325294; PubMed Central PMCID: PMCPMC3075808.

36. Rosenfeld MR, Ye X, Supko JG, et al. A phase I/II trial of hydroxychloroquine in conjunction with radiation therapy and concurrent and adjuvant temozolomide in patients with newly diagnosed glioblastoma multiforme. Autophagy. 2014 Aug;10(8):1359-68. doi: 10.4161/auto.28984. PubMed PMID: 24991840; PubMed Central PMCID: PMCPMC4203513.

37. Maycotte P, Gearheart CM, Barnard R, et al. STAT3-mediated autophagy dependence identifies subtypes of breast cancer where autophagy inhibition can be efficacious. Cancer Res. 2014 May 1;74(9):2579-90. doi: 10.1158/0008-5472.CAN-13-3470. PubMed PMID: 24590058; PubMed Central PMCID: PMCPMC4008672.

38. Barnard RA, Wittenburg LA, Amaravadi RK, et al. Phase I clinical trial and pharmacodynamic evaluation of combination hydroxychloroquine and doxorubicin treatment in pet dogs treated for spontaneously occurring lymphoma. Autophagy. 2014 Aug;10(8):1415-25. doi: 10.4161/auto.29165. PubMed PMID: 24991836; PubMed Central PMCID: PMCPMC4203518.

39. Wong H, Choo EF, Alicke B, et al. Antitumor activity of targeted and cytotoxic agents in murine subcutaneous tumor models correlates with clinical response. Clin Cancer Res. 2012 Jul 15;18(14):3846-55. doi: 10.1158/1078-0432.CCR-12-0738. PubMed PMID: 22648270.

40. Kerbel RS. Human tumor xenografts as predictive preclinical models for anticancer drug activity in humans: better than commonly perceived-but they can be improved. Cancer Biol Ther. 2003;4(Suppl 1):S134-9.

41. Collins KP, Witta S, Coy JW, et al. Lysosomal Biogenesis and Implications for Hydroxychloroquine Disposition. J Pharmacol Exp Ther. 2021 Feb;376(2):294-305. doi: 10.1124/jpet.120.000309. PubMed PMID: 33172973; PubMed Central PMCID: PMCPMC7841421.

42. Munster T, Gibbs JP, Shen D, et al. Hydroxychloroquine concentration-response relationships in patients with rheumatoid arthritis. Arthritis Rheum. 2002 Jun;46(6):1460-9. doi: 10.1002/art.10307. PubMed PMID: 12115175.

43. Lee JY, Vinayagamoorthy N, Han K, et al. Association of Polymorphisms of Cytochrome P450 2D6 With Blood Hydroxychloroquine Levels in Patients With Systemic Lupus Erythematosus. Arthritis Rheumatol. 2016 Jan;68(1):184-90. doi: 10.1002/art.39402. PubMed PMID: 26316040.

44. Wang P, Du Y, Wang J. Indentification of breast cancer subtypes sensitive to HCQ-induced autophagy inhibition. Pathology - Research and Practice. 2019;215(10). doi: 10.1016/j.prp.2019.152609.

45. Xie X, White EP, Mehnert JM. Coordinate autophagy and mTOR pathway inhibition enhances cell death in melanoma. PLoS One. 2013;8(1):e55096. doi: 10.1371/journal.pone.0055096. PubMed PMID: 23383069; PubMed Central PMCID: PMCPMC3559441.

46. Arnaout A, Robertson SJ, Pond GR, et al. A randomized, double-blind, window of opportunity trial evaluating the effects of chloroquine in breast cancer patients. Breast Cancer Res Treat. 2019 Nov;178(2):327-335. doi: 10.1007/s10549-019-05381-y. PubMed PMID: 31392517.

47. Gao L, Zhao X, Lang L, et al. Autophagy blockade sensitizes human head and neck squamous cell carcinoma towards CYT997 through enhancing excessively high reactive oxygen species-induced apoptosis. J Mol Med (Berl). 2018 Sep;96(9):929-938. doi: 10.1007/s00109-018-1670-5. PubMed PMID: 30022281.

48. Wang W, Liu L, Zhou Y, et al. Hydroxychloroquine enhances the antitumor effects of BC001 in gastric cancer. Int J Oncol. 2019 Aug;55(2):405-414. doi: 10.3892/ijo.2019.4824. PubMed PMID: 31268153; PubMed Central PMCID: PMCPMC6615922.

49. Lin YC, Lin JF, Wen SI, et al. Chloroquine and hydroxychloroquine inhibit bladder cancer cell growth by targeting basal autophagy and enhancing apoptosis. Kaohsiung J Med Sci. 2017 May;33(5):215-223. doi: 10.1016/j.kjms.2017.01.004. PubMed PMID: 28433067.

Chapter Three

Autophagy dependency in osteosarcoma and subsequent clinical implications

Summary

The survival rates of osteosarcoma (OSA), a type of bone cancer, have not improved in almost 40 years. Recently, other cancer types have been shown to be differentially dependent on autophagy, a lysosomal recycling pathway that cancer cells use to survive in the tumor microenvironment and during chemotherapy. Here, autophagy dependency was determined in canine OSA using a genetic knockout screen. All cell lines tested were initially intermediately to very dependent on autophagy. However, some cells were able to survive following loss of the autophagy gene ATG7 despite this dependency. Different tumor cells adapted to the loss of autophagy in varying ways including differing lysosomal activity and macropinocytosis regulation. However, generally, the ATG7 deficient clones were commonly enriched for extracellular matrix receptor interaction, focal adhesion, and PI3K-Akt signaling. Further, ATG7 deficient clones were not all sensitized to standard OSA chemotherapy. Overall, targeting autophagy in OSA patients with autophagy dependent tumors is a promising strategy. However, other therapies may be necessary to target cancer cells that adapt to autophagy inhibition following initial autophagy treatment.

Introduction/Motivation

Osteosarcoma (OSA) is a rare type of bone cancer in people that mainly affects children, teenagers, and young adults. The five-year survival rate is 25-30% for patients with metastatic disease upon diagnosis [1]. However, even without metastatic disease at initial presentation, the five-year survival rate is only 60% [1]. Survival rates have not improved in almost four decades due to chemoresistance, high dose chemotherapy toxicity, lung metastasis even during chemotherapy treatments, and no ideal treatment regimen for progressive or recurrent/refractory disease [1, 2, 3, 4].

Although OSA accounts for less than 1% of all diagnosed human cancer incidents in the United States [5], it is one of the most common cancers in dogs. Genome wide profiling studies have shown that the dog OSA gene expression profile is indistinguishable from the human pediatric OSA gene expression profile. Clinically and pathologically, human pediatric and canine OSA also appear the same. Further, dog OSA is more similar to human OSA than any other human cancer is to human OSA [6]. Dogs get naturally occurring OSA just as humans do while being exposed to similar environmental risk factors. They are a more outbred population than inbred laboratory animals, have faster progression of disease compared to human malignancies that allows for more rapid collection of data, and are a good clinical model for drug testing and approval due to a lack of gold standard treatment regimens and lower research costs [6, 7]. Comparative oncology between humans and dogs is a valuable resource that can advance osteosarcoma patient survival in both groups.

Macroautophagy (referred to as “autophagy” here) is a lysosomal degradation pathway by which cellular components are recycled to maintain homeostasis and cell functioning. There are over 30 autophagy-related genes (ATGs) in the autophagy cascade, many of whose functions are well known within the autophagic pathway [8, 9, 10, 11] (Figure 3.1). Environmental stressors such as nutrient deprivation and hypoxia induce autophagy. It is upregulated during cell remodeling and differentiation and consequently has implications in many diseases including cancer [8, 12, 13]. Certain cancers are more innately dependent on autophagy than others as observed in breast cancer [14] and in pancreatic cancer [15]. A CRISPR screen knocking out multiple genes across the autophagic pathway in multiple human cancer types including breast, brain, fibrosarcoma, colorectal, lung, and OSA also revealed dependence or independence on autophagy but showed that cells that were initially dependent on autophagy survived following the inability to use autophagy [16]. These studies suggest that cancers that are dependent on autophagy will respond to pharmacologic autophagy inhibition but will probably require combination treatments to be efficacious long-term. Further, autophagy plays a complex role in many types of cancer including OSA [17, 18]. It is important for the development, growth, and invasion of human OSA cell lines as evidenced by genetic knockdown or chemical inhibition of key autophagy genes including ATG4B [19] or Beclin-1 [20]. Autophagy is also elevated in OSA cisplatin- and Taxol-resistant cells [21, 22, 23]. It is induced in human OSA cells by factors known to mediate drug resistance such as GFRA1 [24], HSP90AA1 [25], and HMGB1 [26]. The results of these studies indicate that inhibiting autophagy in combination with standard chemotherapies used to treat OSA is

an attractive strategy. However, it is unknown whether all OSA patients would benefit from autophagy inhibition either as a single agent or with combination treatment.

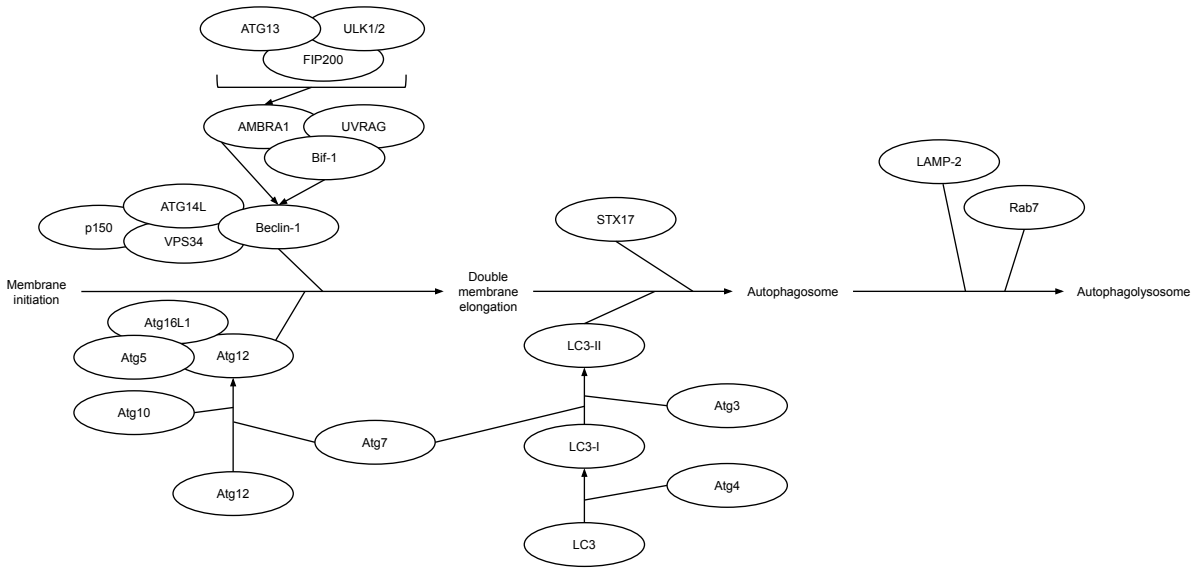

Figure 3.5 Proteins throughout the autophagy cascade. More than 30 autophagy-related proteins have important functions during the entire process of autophagy.

Here, autophagy dependency in canine OSA was determined using a CRISPR screen revealing that OSA was intermediately to highly dependent on autophagy. Several ATG7 null ($ATG7^{-/-}$) clones that could no longer use canonical autophagy had variable responses to serum starvation, autophagy inhibition, doxorubicin, and carboplatin, indicating that only some OSA patients will benefit from autophagy inhibition combined with typical OSA treatment regimens. Gene expression analysis of $ATG7^{-/-}$ clones revealed potential therapeutic targets when cells cannot use autophagy. Overall, these results implicate the importance of determining which patients will benefit from autophagy inhibition and provide insight into novel treatments for OSA.

Materials and Methods

Guide RNA Design, Creation, and Validation

Guide RNAs (gRNAs) targeting autophagy genes for the canine genome were designed from upstream exon sequences (the first four or five exons) of genes of interest using the MIT Zhang lab gRNA design (crispr.mit.edu, no longer available). Two to four gRNAs were designed per gene. Following previous reports of designing and making gRNAs from Liang et al [27], forward gRNA primers were created with the T7 promoter sequence (TAATACGACTCACTATAG) followed by the first 19 base pairs of the gRNA sequence. If the gRNA sequence did not start with G, a G was added after the T7 promoter sequence and before gRNA sequence. Reverse primers were created with the last 19 base pairs of the gRNA sequence followed by the first 15 base pairs of the tracrRNA sequence (GTTTTAGAGCTAGAA). The forward and reverse complement sequences of the gRNAs were ordered from Integrated DNA Technologies (idtdna.com).

PCR was performed with GoTaq Flexi DNA polymerase (0.25 μL, 1.25 U) (Promega, PRM8295) to amplify the tracrRNA constant region from the CRISPR-Lenti V2 plasmid (10 ng/μL) using forward primer GTTTTAGAGCTAGAAATAGCAAG (0.5 μM), reverse primer AAAAGCACCGACTCGGTGCCAC (0.5 μM), 1.5 mM $MgCl_2$, 1X GoTaq Flexi Buffer, and 0.2 mM of each dNTP in 50 μL total. Thermal cycling conditions were 95°C for 2 min for initial denaturation followed by 35 cycles of 95°C for 30 s for denaturation, 50°C for 30 s for annealing, and 72°C for 30 s for elongation followed by 72°C for 5 min for a final elongation step. Product size (80 bp) was validated against a 1 kb DNA ladder (Fisher Scientific, BP2573100) on a 2% agarose (Fisher Scientific,

16500100) gel in 1X TAE buffer run at 80V for 50 min. PCR product was purified using the Wizard SV Gel and PCR Clean-Up System (Promega, PRA9281) and final concentration of product was determined on a Nanodrop and diluted to 17.1 ng/μL in water.

Nested PCRs were performed to incorporate the gRNA target sequence in between the T7 promoter and the tracrRNA constant region. Briefly, 0.5 μM of the T7 promoter forward primer (TAATACGACTCACTATAG) and 0.5 μM of the tracrRNA reverse primer (AAAAGCACCGACTCGGTGCCAC) along with 15 nM of gRNA forward primer and 15 nM of gRNA reverse primer (**Table 4.1**), plus 0.25 μL GoTaq Flexi DNA polymerase, 1X GoTaq Flexi Buffer, 17.1 ng/μL of tracrRNA product from previous PCR, 1.5 mM $MgCl_2$, and 0.2 mM of each dNTP were mixed in 50 μL total then thermal cycling conditions were 95°C for 2 min for initial denaturation followed by 35 cycles of 95°C for 30 s for denaturation, 50°C for 30 s for annealing, and 72°C for 30 s for elongation followed by 72°C for 5 min for a final elongation step. Product size (115 bp) was checked on a 2% agarose gel in 1X TAE buffer run at 80V for 50 min. Product was purified using the Wizard SV Gel and PCR Clean-Up System and concentration was determined on a Nanodrop.

To make the gRNAs, in vitro transcription was performed using the Ambion T7 kit (AM1354). Briefly, dTPs, 1X reaction buffer, and enzyme were combined with 500 ng of gRNA PCR product to a total of 20 μL and incubated at 37°C for 4 hr. Then 1 μL DNAse was added for 15 min at 37°C. RNA was purified using an Ambion RNA extraction kit (AM1908). Purified RNA was analyzed on the Nanodrop then diluted to 10 ng/μL in TE buffer and stored in aliquots at -80°C until use in transfections.

To validate that gRNAs would work, genomic DNA regions of 300 to 800 base pairs long that contained the gRNA sequence were amplified from the canine genome. 0.15 μM forward and reverse primers (**Table 4.2**), 100 ng genomic canine DNA or 25 ng plasmid canine DNA, 1.5 mM $MgCl_2$, 0.2 mM of each dNTP, 1X GoTaq Flexi Buffer, and 0.25 μL GoTaq Flexi DNA polymerase were combined in 50 μL total. Thermal cycling conditions included 95°C for 2 min for initial denaturation followed by 35 cycles of 95°C for 30 s for denaturation, 50°C for 30 s for annealing, and 72°C for 30 s for elongation followed by 72°C for 5 min for a final elongation step. A small amount of product was checked for size by resolving on a 2% agarose gel in 1X TAE buffer at 80V for 50 min. Product was purified using the QIAquick PCR Purification Kit (Qiagen, 28104). To perform Cas9 in vitro cleavage assays to ensure the gRNAs target the canine genome in the correct place, 150 ng Cas9, 50 ng gRNA, 60 ng target DNA product, and 1X NEB buffer 3.1 (Fisher Scientific, NC0458502) in 10 μL was incubated together at 37°C for 1 hr. The solution was then heated to 65°C for 10 min to inactivate Cas9. The entire product was resolved on a 1.5% agarose gel in 1X TAE buffer run at 80V for 50 min.

Table 4.1 gRNA primers

gRNA	Forward Primer	Reverse Complement Primer
ATG5 #1	TAATACGACTCACTATAGGTGCT TCGAGATGTGTGGT	TTCTAGCTCTAAAACAACCACAC ATCTCGAAGCA
ATG5 #2	TAATACGACTCACTATAGGAAGA GTAAGTTATTTGACG	TTCTAGCTCTAAAACACGTCAAA TAACTTACTCT
ATG7 #1	TAATACGACTCACTATAGGTCGG CTAGACGAAGCTCCG	TTCTAGCTCTAAAACTCGGAGCT TCGTCTAGCCG
ATG7 #2	TAATACGACTCACTATAGGCTGC CAGCTCGCTTAACG	TTCTAGCTCTAAAACACGTTAAG CGAGCTGGCAG
FIP200 #1	TAATACGACTCACTATAGGAGAG TGTGCACCTACAGTG	TTCTAGCTCTAAAACGCACTGTA GGTGCACACTC

FIP200 #2	TAATACGACTCACTATAGGAAGG TAGTTTTCGGAATAG	TTCTAGCTCTAAAACGCTATTCC GAAAACTACCT
STX17 #1	TAATACGACTCACTATAGGATAG TAATACCAACAGAC	TTCTAGCTCTAAAACAGTCTGTT GGTATTACTAT
STX17 #2	TAATACGACTCACTATAGGCCGT TCCAATATTCGAGAA	TTCTAGCTCTAAAACTTTCTCGA ATATTGGAACG
AMBRA1 #1	TAATACGACTCACTATAGGTTCT CGCCCCCATAGTAT	TTCTAGCTCTAAAACGATACTAT GGGGGCGAGAA
AMBRA1 #2	TAATACGACTCACTATAGGAAGG TAGAGCGTGGACTAT	TTCTAGCTCTAAAACGATAGTCC ACGCTCTACCT
ATG3 #1	TAATACGACTCACTATAGGTAGT CCACCACTGTCCAAC	TTCTAGCTCTAAAACTGTTGGAC AGTGGTGGACT
ATG3 #2	TAATACGACTCACTATAGGTGAA GGCATATCTACCAA	TTCTAGCTCTAAAACGTTGGTAG ATATGCCTTCA
ATG13 #1	TAATACGACTCACTATAGGTGAT TGTCCAGGCTCGAC	TTCTAGCTCTAAAACAGTCGAGC CTGGACAATCA
ATG13 #2	TAATACGACTCACTATAGGCACA TCGATCTCCCGACTG	TTCTAGCTCTAAAACGCAGTCGG GAGATCGATGT
BECN1 #1	TAATACGACTCACTATAGGGACA CGAGCTTCAAGATC	TTCTAGCTCTAAAACGGATCTTG AAGCTCGTGTC
BECN1 #2	TAATACGACTCACTATAGGCCAT TTCTTGAAACTCGC	TTCTAGCTCTAAAACGGCGAGTT TCAAGAAATGG
BECN1 #3	TAATACGACTCACTATAGGCTTC CCCACCATATAAGGA	TTCTAGCTCTAAAACCTCCTTAT ATGGTGGGGAA
BECN1 #4	TAATACGACTCACTATAGGTCCC GCTACCCGGTGGCAT	TTCTAGCTCTAAAACAATGCCAC CGGGTAGCGGG
LAMP2 #1	TAATACGACTCACTATAGGATAG TGGTGCAATTCGGAT	TTCTAGCTCTAAAACGATCCGAA TTGCACCACTA
LAMP2 #2	TAATACGACTCACTATAGGCGTG AACATCCCAATAGTA	TTCTAGCTCTAAAACGTACTATT GGGATGTTCAC
ULK2 #1	TAATACGACTCACTATAGGCCTT CGCCGTGGTCTTCCG	TTCTAGCTCTAAAACCCGGAAGA CCACGGCGAAG
ULK2 #2	TAATACGACTCACTATAGGATGC GAATACCACTGACG	TTCTAGCTCTAAAACACGTCAGT GGTATTCGCAT
VPS34 #1	TAATACGACTCACTATAGGCTAT ATCTACAGTTGTGAC	TTCTAGCTCTAAAACGGTCACAA CTGTAGATATA
VPS34 #2	TAATACGACTCACTATAGGCTTT GTAGGATGTTCTCAC	TTCTAGCTCTAAAACGTGAGAAC ATCCTACAAAG
ATG12 #1	TAATACGACTCACTATAGGTTTT TCTTGGTGTCGCCAG	TTCTAGCTCTAAAACGCTGGCGA CACCAAGAAAA
ATG12 #2	TAATACGACTCACTATAGGAGCG AACCCGAACCATTC	TTCTAGCTCTAAAACTGAATGGT TCGGGTTCGCT
PTEN #1	TAATACGACTCACTATAGGAAAG ACTTGAAGGCGTATA	TTCTAGCTCTAAAACGTATACGC CTTCAAGTCTT
PTEN #2	TAATACGACTCACTATAGGGTTT GATAAGTTCTAGCT	TTCTAGCTCTAAAACCAGCTAGA ACTTATCAAAC

PCNA #1	TAATACGACTCACTATAGGTACC GCTGCGACCGCAAC	TTCTAGCTCTAAAACAGTTGCGG TCGCAGCGGTA
PCNA #2	TAATACGACTCACTATAGGAACA AGTAATGTCGATAAG	TTCTAGCTCTAAAACCCTTATCG ACATTACTTGT
FOXO3A #1	TAATACGACTCACTATAGGTCGA GAGCTCGCCCGACAA	TTCTAGCTCTAAAACTTTGTCGG GCGAGCTCTCG
FOXO3A #2	TAATACGACTCACTATAGGCCGG CGGCGGGCTGTCTCC	TTCTAGCTCTAAAACTGGAGACA GCCCGCCGCCG
GFP #1	TAATACGACTCACTATAGGTGAA CCGCATCGAGC	TTCTAGCTCTAAAACTTCAGCTC GATGCGGTTCA
GFP #2	TAATACGACTCACTATAGGGAGC GCACCATCTTC	TTCTAGCTCTAAAACTGAAGAAG ATGGTGCGCTC

Table 4.2 Genomic DNA primers

gRNA	Left Primer	Right Primer	Product Size (bp)
ATG5 #1	AGCTTCACTTTGGCTGTGG T	GCCTCCAGGTTCTTAGCTT C	506
ATG5 #2	GCTTCTCATTGTGCCATCT T	CATTTCAGTGGTGTGCCTT C	810
ATG7 #1	GGGATTATGTCAGGGAAG GA	CCTAAACTGGAGGGCAGA GA	534
ATG7 #2	GACCAGGAATTTGGACAG GA	CCATGGATAAGCAACTGAA GG	518
FIP200 #1	GTGTGGCAGACCTCAAGC A	CCGTTCTCCTTCACCCATC	733
FIP200 #2	GACAACCATCCCTTTGTTC C	AGTGCTGGGACGGTATGT GT	577
STX17 #1	CTGACAGTAGAAGTGACC CAACA	TGCACCTGAAGAAGACAG GA	555
STX17 #2	AGGTGGTTGGATTGGTGA AG	CATGGATCTGGTCAAAGAA GG	541
AMBRA1 #1	AGGTACCTGTCTGGGCTG AA	TCTCTTCCTGTGCCTGGTG	600
AMBRA1 #2	TTACCAAGCTAGGCCAAAG A	AAACTCGGTGGATGAAAT GG	526
ATG3 #1	TGGCTGTCAAGATTACACA GGA	CGGTTAAGTATCTGCCTCC AAC	757
ATG3 #2	TGCCCTAGCATACAGCACT T	TGGGCCCTTTCCCTCTAC	501
ATG13 #1	GTTATGGTCATTGGCGTCT T	CCTCTGGGATGTCTTTGAT TG	658
ATG13 #2	AGTAGTCACCTCTCCCACT AGAAA	GGGCAAGGGAGAAATGAA	526

BECN1 #1	CCTGACTCTGGGCTGATAAA	GTCAGAACTGCTTCTTGTTGGA	504
BECN1 #2	GCCTCTGTGGTTTATCAAGTCC	AAGTGATGGGCCAGGTATGT	532
BECN1 #3	CGGAGTGCAGATCCCTTG	CATACTTGGGCCGGTCGT	581
BECN1 #4	CATGGACGTCGGTGCTGT	CGGAGTGCAGATCCCTTG	623
LAMP2 #1	GTTCAGGCCACTTTCCCTTT	CCCTTTCCCTCTGTCCTCTC	523
LAMP2 #2	AGTCCAGCGTAAGCTACAAACA	CTGCAGCTCGTCTTTCCTTC	519
ULK2 #1	GCGACTTCGAGTACAGCAAGAG	CGCTGTGCAAGGAGGAAA	314
ULK2 #2	GCTGGGAGTCATGTTTGGAG	CCCAGTTCTTTATTCCCTCTGT	508
VPS34 #1	AAAGTTGGGCGGGGATTT	GCAGGCTGATAACCATCTTCT	338
VPS34 #2	AATGGGAGAACCATCTGGAA	AGGGAAACTAAGGCCTGGAA	535
ATG12 #1	CGCTCGGAAGAAGAGAGGAG	GGAGGTCTCCCCAGAAACA	453
ATG12 #2	GTTCAGCGTAATAGCCAGTGTT	CTCAGGAAGACCAGGAAGG	534
PTEN #1	CATTATTGCTATGGGGTTTCCT	AAATTAACTTGGTAAGAAGCGTTG	331
PTEN #2	CTAGGGCCTCTTGTGCCTTT	GCCTCTTCCCTCTGATATGTTG	506
PCNA #1	CTGGTCCAGGGCTCCATC	CAAGCCAAAGGGTTCTCATC	534
PCNA #2	TTTGCACGTATATGCCGAGA	GCGGTTGAACATCTACCTTTG	822
FOXO3A #1	CTACGCCGACCTCATCACTC	GCCGCAGACCTACCTCCT	544
FOXO3A #2	GAACTCTATCCGGCACAACC	TTGTCAGAGAGCCCATCATTC	534

Cell Culture and Preparation

All cell lines were maintained at 37°C and 5% CO_2 in DMEM (Corning, 10-017-CV) supplemented with 10% FBS (Peak Serum, PS-FB3), 1X penicillin-streptomycin (Corning, 30-002-CI), and 1 mM sodium pyruvate (Corning, 25-000-CI). Cells were

validated, confirmed mycoplasma negative, and only used for up to 20 passages. The cell lines were all transduced with both Incucyte NucLight Red Lentivirus Reagent with puromycin selection (Essen Bioscience, 4476) and GFP. Cells were sorted for over 99% double positive RFP/GFP cells using a FACSAria III (BD Biosciences) prior to use in experiments.

CRISPR/Cas9 Screen

To perform CRISPR/Cas9 transfections, RFP^+/GFP^+ were used. 300 cells/well were plated in 100 μL in a 96-well plate the day before transfection. The day of the transfection, Cas9 and gRNAs were thawed on ice. Optimem (Fisher Scientific, 31985062) was brought to 37°C. Lipofectamine CRISPRMAX Cas9 Transfection Reagent (Invitrogen, CMAX00008) was brought to room temperature. Based on the Lipofectamine CRISPRMAX Cas9 Transfection Reagent Quick Reference, in one set of tubes, the scaled amounts of gRNAs for GFP, gRNAs for the gene of interest, Cas9, Optimem, and Cas9 Plus reagent of were added in respective order and incubated for 5 min at room temperature. In another set of tubes, scaled amounts of Optimem and CRISPRMAX were mixed then added to the first set of tubes and incubated for 5-10 min. Either 10 or 20 μL of transfection mix was added to each well. Transfection was kept on the cells for 4 hr up to 48 hr depending on the experiment and then was replaced with 200 μL fresh media. Media was subsequently changed every 2-3 days until the end of the assay. Cells were assayed on an Incucyte Zoom (Essen Bioscience) every 3 to 6 hr for 7 to 10 days.

Clone Selection

To select for ATG7$^{-/-}$ clones, cells that had undergone ATG7 and GFP transfection were sorted for RFP positive only cells on a FACSAria III. Then 500 cells were plated in a 15 cm dish. Single colonies were grown for 10 to 14 days then selected and moved to individual wells of a 24-well plate. Once the population was large enough, cells were assessed for ATG7 loss by western blot.

Western Blotting

Cell were isolated for western blot by putting fresh lysis buffer (1% Triton X-100, 150 mM NaCl, 10 mM Tris pH 7.5, 100 mM Na-orthovanadate [Alexis Biochemicals, 400-032-G025], 34.8 μg/mL PMSF [Fluka Biochemica, 78830], and 1x protease inhibitor cocktail [Roche, 11836153001]) directly on the plate. Samples were frozen then thawed on ice and centrifuged at 14,000 rpm for 2 min at 4°C. Supernatant was collected. Protein concentration was determined using the Pierce BCA Protein Assay Kit (Thermo Scientific, 23225). Between 3 and 20 μg of protein was resolved on a 8-16% or 4-20% SDS-polyacrylamide stain-free gel (Bio Rad, 4568106 and 4568095) and transferred onto low autofluorescence PVDF membranes using the Trans-Blot Turbo RTA Mini 0.45 μm LF PVDF Transfer Kit (Bio Rad, 1704274). Membranes were blocked for 1 hour at room temperature in either 5% nonfat dry milk (LC3, p62, FOXO3A, α-tubulin) or 5% BSA (ATG7, α-tubulin) in tris-buffered saline/Tween 80 (TBST) (10 mM Tris pH 7.5, 100 mM NaCl, and 0.1% Tween 80 [Fisher Chemicals, BP338-500]). Blots were probed overnight at 4°C with polyclonal anti-LC3B antibody (Novus Biologicals, NB100-2220) at 1:1,000, monoclonal anti-α-tubulin antibody (Sigma-Aldrich, T5168) at 1:5,000, monoclonal anti-

p62/SQSTM1 antibody (Novus Biologicals, H00008878-M01) at 1:1,000, polyclonal anti-FOXO3A antibody (Abcam, ab23683) diluted to 1 μg/mL, or monoclonal anti-ATG7 antibody (Cell Signaling Technology, 8558S) diluted 1:1,000 in blocking solution. Blots were washed three times in TBST then incubated at room temperature for 1 hour with HRP conjugated secondary antibodies anti-rabbit-HRP (Pierce, 31460) at 1:2,000 for LC3, ATG7, and FOXO3A or anti-mouse-HRP (Pierce, 31430) at 1:2,000 for p62 or 1:5,000 for α-tubulin in blocking solution. Housekeeping controls were α-tubulin or total protein. Blots were washed three times with TBST. Immunodetection was performed using SuperSignal West Dura (Thermo Scientific, 34075) and imaged in a ChemiDoc XRS+ (Bio Rad, Hercules, CA) using Image Labs version 3.0 software.

Drug, Serum Starvation, and LysoTracker Assays

To perform drug and serum starvation assays, cells were imaged once every 24 hr in the Incucyte over the duration of the assay. For Lys05, cells were treated with 8, 4, 2, 1.5, 1, 0.5, or 0 μM Lys05 4-6 hr after plating 500 cells/well in a 96-well plate. For serum starvation assays, 500 cells/well in a 96-well plate were plated in DMEM supplemented with 10% FBS a few hours before replacing the media with DMEM supplemented with 2% FBS (serum starved). For doxorubicin, cells were treated with 2000, 1000, 500, 250,125, 62.5, 31.25, 15.625, 7.1825 or 0 nM doxorubicin 4-6 hr after plating 500-2000 cells/well in a 96-well plate. For carboplatin, cells were treated with 320, 160, 80, 40, 20, 10, 5, 2.5, 1.25 or 0 μM carboplatin 4-6 hr after plating 500-2000 cells/well in a 96-well plate. Cell death was analyzed by including YOYO-1 Iodide (Invitrogen, Y3601) at 100 nM per well. YOYO-1 binds to double-stranded DNA as measure of dead cells in the well or cells that

are dying and have permeable membranes. For LysoTracker assays, 10,000 cells/well were plated in a 96-well plate the day before analyzing. Four hours prior to adding LysoTracker, cells were serum starved and/or treated with 20 μM HCQ. LysoTracker Green (Invitrogen, L7526) was added to wells at a final concentration of 50 nM. Plates were imaged as close to addition of LysoTracker as possible for highest signal.

Macropinocytosis Assays

To analyze macropinocytosis, 400,000 cells were plated in a 6-well plate the day before treatment. Twelve to sixteen hours prior to fluorescent tagging, media was replaced with fresh media, serum free media, or 2 μM Lys05. Cells were incubated with a final concentration of 1 mg/mL dextran-FITC (Invitrogen, D1822) for 30 min at 37 C. Cells were put on ice, washed three times with cold PBS, then trypsinized. Cells were washed one more time with PBS then fixed with 4% PFA for 15 min. Cells were washed once with PBS then re-suspended in PBS for flow. Flow cytometry was performed for RFP and FITC using a Cytek Aurora 4 laser machine then data processed in FlowJo.

RNA Sequencing

Two days before RNA isolation, 1 million cells were plated on a 10 cm dish. RNA was isolated from cells directly on the plate using the Qiagen RNeasy Mini Kit (74104) and Qiagen QIAshredder (79654). RNA was sent to the Genomics and Microarray Core at the University of Colorado Anschutz Medical Campus for paired end RNA sequencing on an Illumina NovaSeq 6000. Quality filtering and adapter sequence trimming was done using Trimmomatic with a phred score > 20 using the following conditions: TruSeq3-

SE.fa:2:30:10 CROP:130 LEADING:3 TRAILING:3 SLIDINGWINDOW:4:20 MINLEN:50. HISAT2 was used to align sequences to the canine genome (v3.1). Samtools was used to sort and index files then featureCounts was used to quantify transcripts. Downstream analysis included analyzing differentially expressed genes using DESeq2 in R, performing gene set enrichment analysis using GSEA from MSigDB, and analyzing differentially expressed genes in DAVID to identify enriched pathways. Further, gene expression in various pathways was assessed using normalized counts. Pathway scores were calculated similar to the MAPK pathway activity score (MPAS) from Wagle et al [28]. Briefly, these scores were calculated by summing z-scores of genes within the pathway for an individual sample then dividing by the square root of the number of genes in the set. The ATG7$^{-/-}$ clones used for RNA seq were Abrams clone 16, D17 clone 1, Gracie clone 4, and OSA8 clone 3.

Statistical Analysis

All experiments were performed with technical triplicates and a minimum of three biological replicates. Statistical significance was determined with two-tailed unpaired t-tests either between the gene of interest and FOXO3A or PCNA or between the parent and the ATG7$^{-/-}$ clone in GraphPad Prism. Two-way ANOVAs using multiple comparisons were performed on experiments using wild-type versus ATG7$^{-/-}$ cells. Significance is determined by *$p \leq 0.05$, **$p \leq 0.01$, ***$p \leq 0.001$, or ****$p \leq 0.0001$. All error bars represent standard deviation.

Results

gRNAs designed for the canine genome accurately guide Cas9 to cut

Guide RNAs targeted to 12 genes that span the entire autophagy pathway were designed using the canine genome although only 8 of them were used in the subsequent CRISPR screen (Figure 3.2). Two gRNAs targeting different exons were made per gene to give confidence that at least one would work in every cell line. gRNAs against three control genes (FOXO3A, PTEN, and PCNA) were also designed to use as positive and negative controls in subsequent studies. To validate that the gRNAs would work in canine cell lines, genomic DNA product containing the gRNA sequence was amplified. An in vitro Cas9 cleavage assay was performed by combining genomic DNA with Cas9 and gRNAs to show that the respective gRNA precisely tells Cas9 where to cut (**Figure 3.3**).

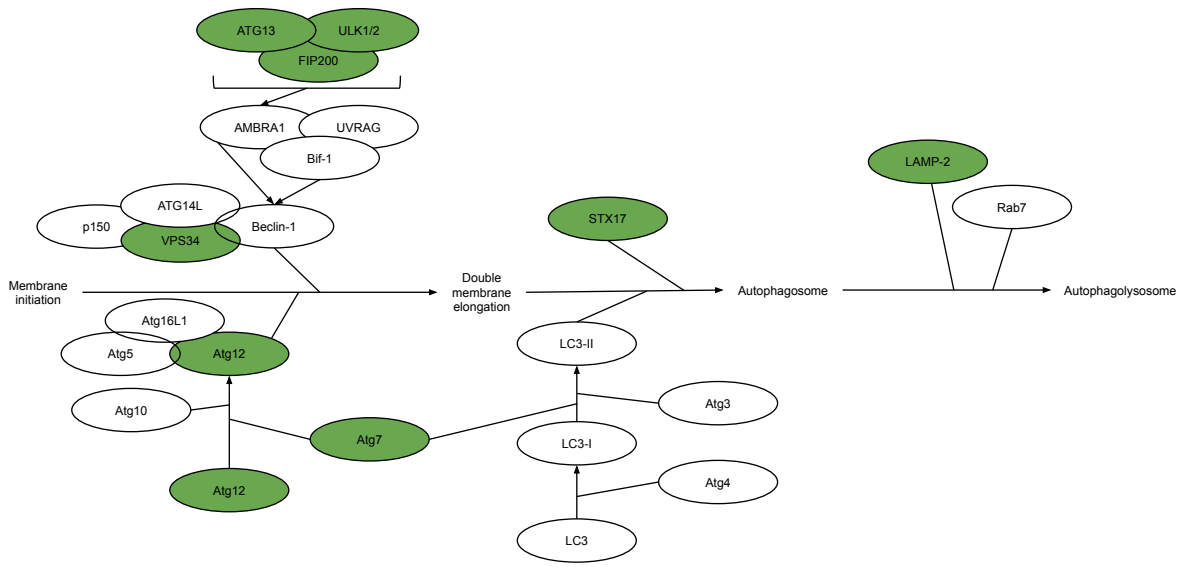

Figure 3.2 Genes targeted in the autophagic pathway. Eight genes (green) were targeted in the autophagic pathway for the CRISPR screen.

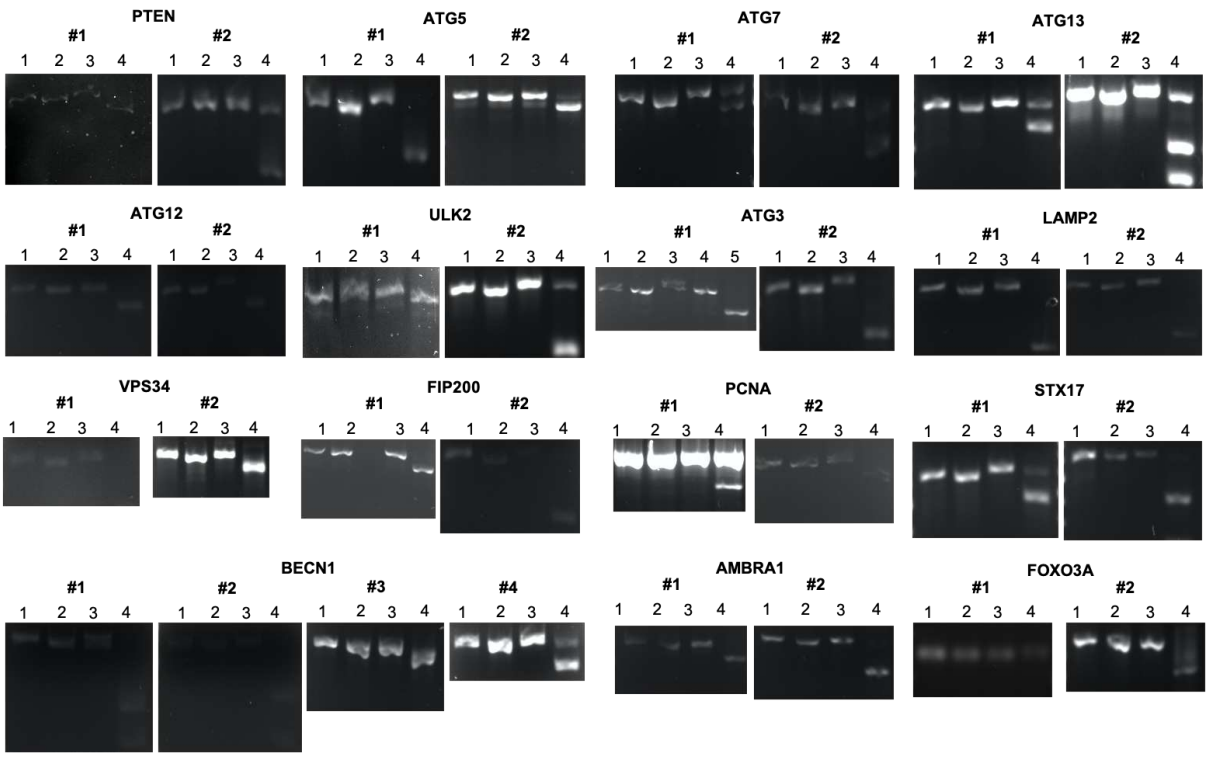

Figure 3.3 Cas9 in vitro cleavage assays to validate gRNAs. To show that a gRNA guides Cas9 to cut DNA, the loss of genomic DNA and/or the gain of bands smaller than the genomic DNA were observed for each gRNA. To verify that cutting of the genomic DNA only occurred when all necessary components are were present, (lane 4, except for ATG3#1 where it is lane 5), control samples with genomic DNA only (lane 1), genomic DNA plus gRNA but no Cas9 (lane 2), or genomic DNA plus Cas9 but no gRNA (lane 3) were analyzed. The gel for ATG3#1 shows that when a gRNA is used whose sequence is not within the genomic DNA sequence, there is no cutting (lane 4).

CRISPR screen reveals variable autophagy dependency in canine OSA

To determine if there is differential autophagy dependency in canine OSA, six cell lines were used in a CRISPR/Cas9 screen. All cell lines had to be optimized to achieve sufficient and dependable transfections. Optimization and subsequent validation of transfections were determined by achieving significant growth differences between FOXO3A and PCNA knockouts using GFP loss measured via the Incucyte as a surrogate for gene knockouts (**Figures 3.4 and 3.5**) following an assay developed by Towers et al

[16]. FOXO3A is a member of the forkhead box class O (FOXO) proteins. It is a transcription factor involved in inducing target genes that affect apoptosis, proliferation, cell cycle progression, survival, and DNA damage. Deregulation of FOXO3A is highly associated with carcinogenesis [29]. Proliferating cell nuclear antigen (PCNA), is vital to DNA replication [30]. Without PCNA, cells cannot survive [31, 32]. FOXO3A is a non-essential gene (negative control) to tumor cells since they are already tumorigenic but PCNA is essential (positive control) since cells require DNA replication to survive. Green object count was subtracted from the red object count to analyze only cells that had taken up the transfection.

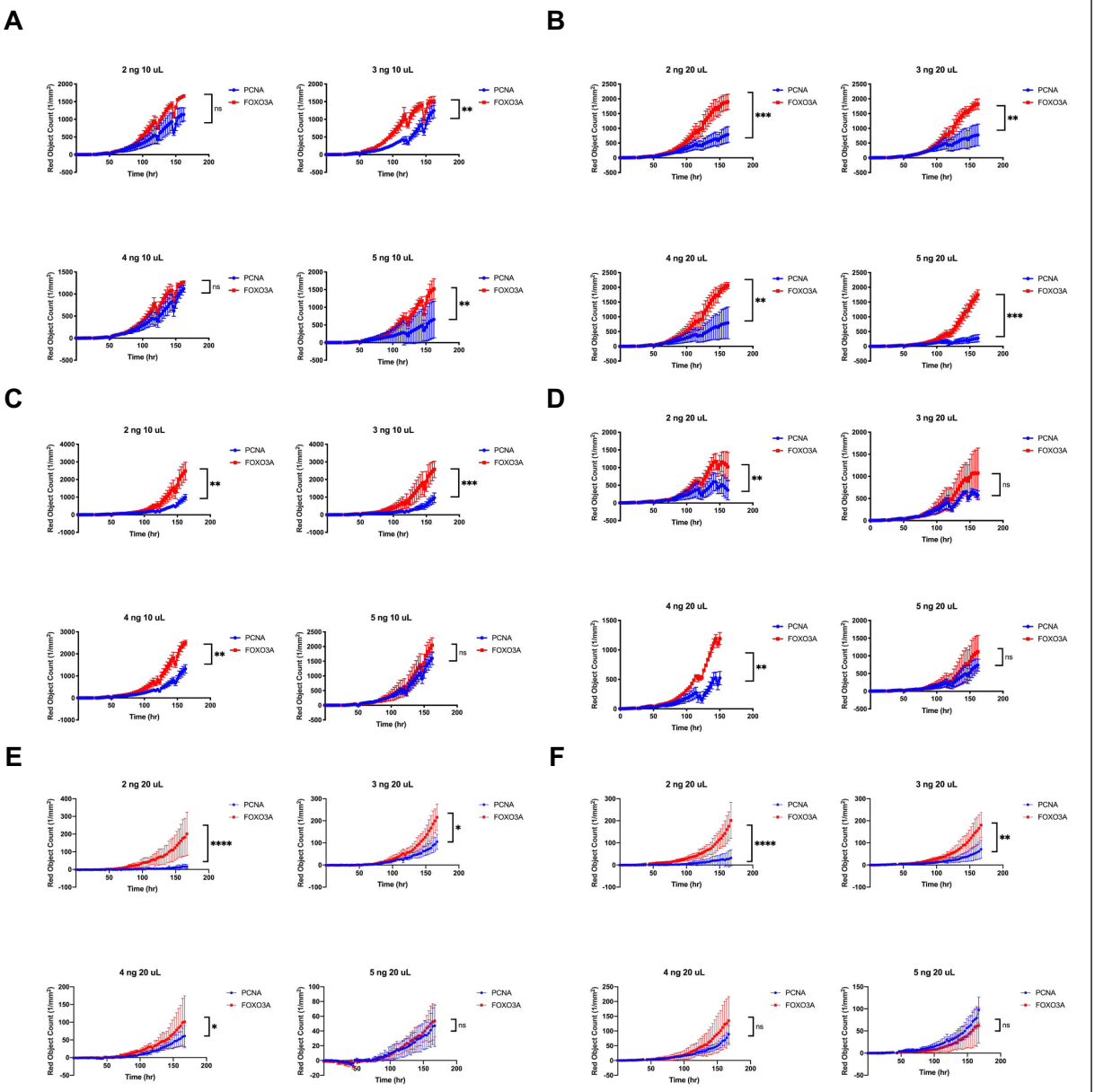

Figure 3.4 CRISPR transfection optimizations. Many optimization experiments were performed to assess growth difference between FOXO3A and PCNA using varying amounts of total gRNA, transfection volumes, and transfection times since all of these factors affect how well the transfection works. These were the final optimization experiments performed where there was significant growth difference between FOXO3A and PCNA in Abrams (**A**), D17 (**B**), Gracie (**C**), OSA8 (**D**), OS2.4 (**E**), and Yamane (**F**). All transfection times were 48 hr.

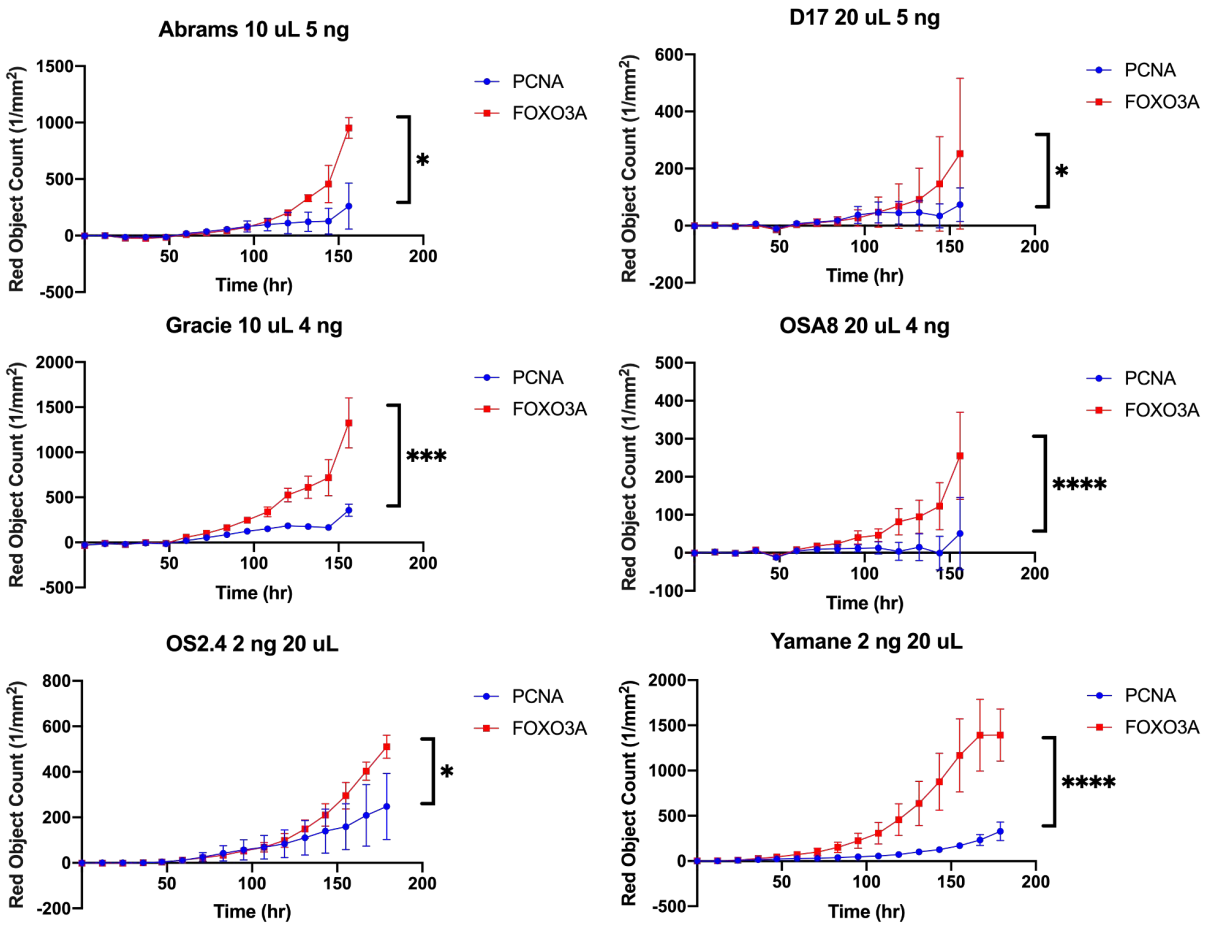

Figure 3.5 CRISPR transfection validations. To validate that transfections would work consistently, experiments were performed using the volume, amount of gRNA, and transfection time that achieved significant growth differences between PCNA and FOXO3A growth in the six cell lines. All transfection times are 48 hr.

Once the transfections were optimized, 8 ATG genes were screened (**Figure 3.6**). Growth differences were determined by significance between PCNA or FOXO3A and the gene of interest at the last time point. A CRISPR knockout score (CKS) was determined for each gene. The area under the curve (AUC) was calculated for all genes. PCNA area was set to 0 by subtracting the AUC of PCNA from its own area and the FOXO3A area was normalized to be 1 after PCNA AUC was subtracted from FOXO3A AUC. PCNA AUC was subtracted from all genes of interest AUC then a normalized CKS of the gene of interest was calculated by taking the ratio of the gene of interest adjusted AUC to

FOXO3A adjusted AUC. Typically, the scores fell between 0 and 1, but sometimes the scores fell below 0 or above 1. This would indicate that an ATG gene was either more essential than PCNA or was less essential than FOXO3A for that cell line, respectively, in this particular assay. CRISPR scores are based on at least three independent transfection replicates with triplicates performed in each replicate (**Figures 3.6 A and 3.7**). A CRISPR score above 0.5 indicates that that gene is not essential to the cells. To determine autophagy dependency, cell lines that had 6 or more genes with CRISPR scores above 0.5 were considered autophagy independent, cell lines that had 3-5 genes with scores above 0.5 were considered intermediately dependent, and cell lines that had 2 or less genes with scores above 0.5 were considered autophagy dependent. The CRISPR scores reveal that some canine OSA lines are more dependent on autophagy than others but none of the cell lines tested were completely autophagy independent (**Figure 3.6 B**).

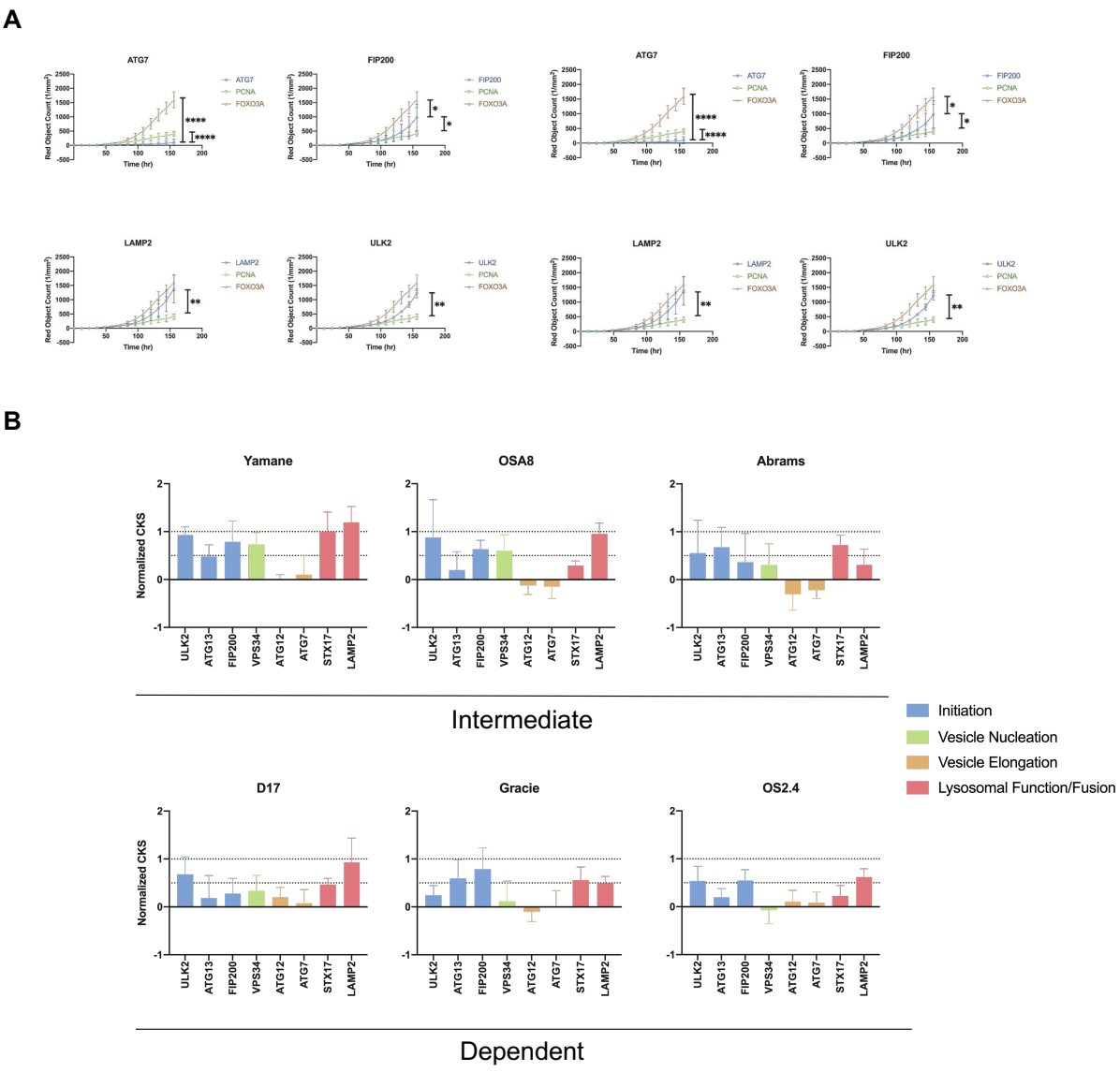

Figure 3.6 CRISPR ATG knockout screen. Representative ATG knockout experiments in Gracie (**A**). Significance is determined by difference in growth at the last time point. A comparison of CRISPR knockout scores between canine OSA cell lines that range from dependent to intermediately dependent on autophagy (**B**).

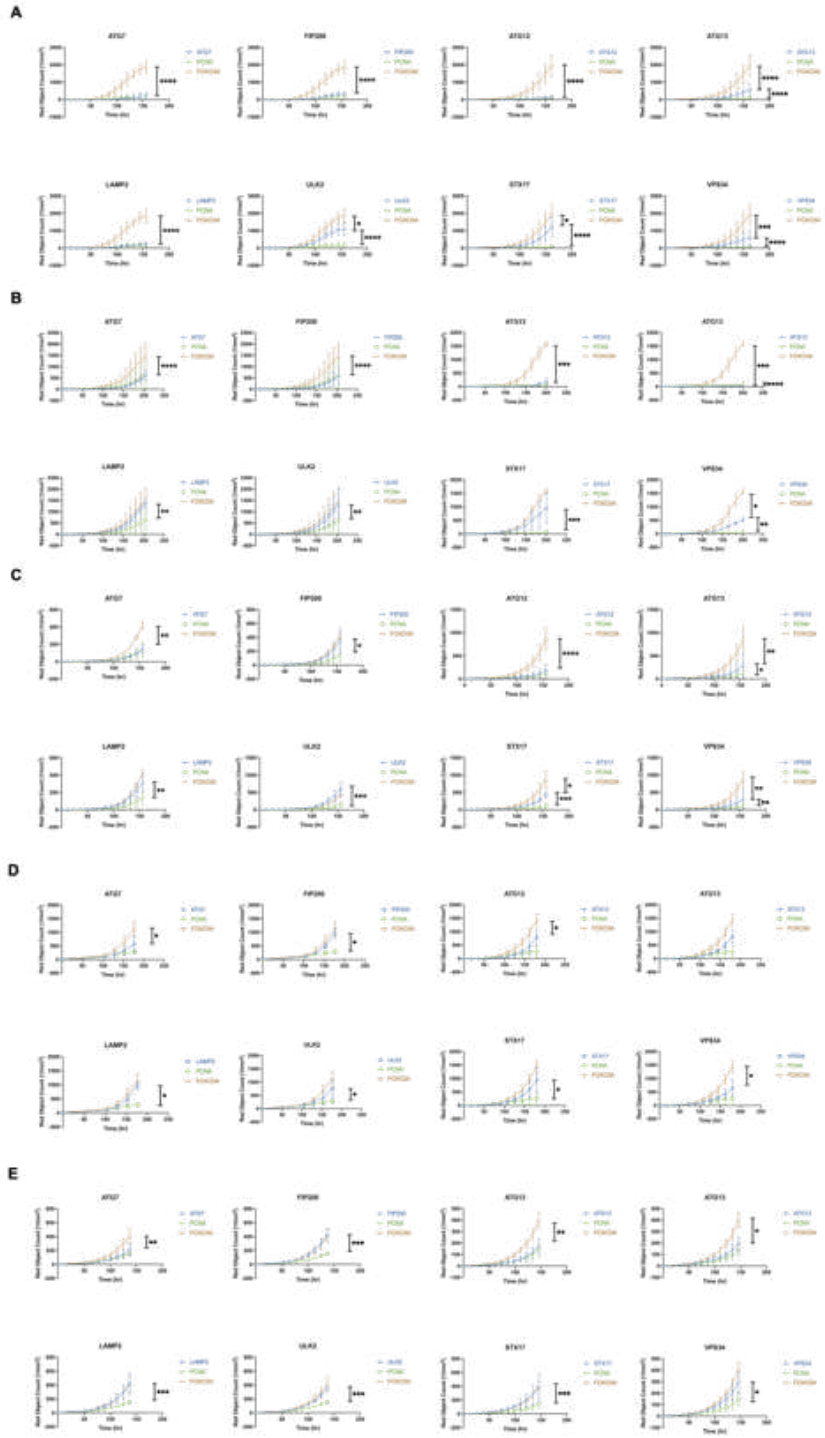

Figure 3.7 ATG CRISPR screen in canine OSA. Plots representative of 3 or more individual experiments in Abrams (**A**), D17 (**B**), OSA8 (**C**), OS2.4 (**D**), and Yamane (**E**).

To validate that GFP loss is a good surrogate for gene loss, cells were sorted for RFP^{+}/GFP^{-} expressing cells then analyzed via western blot for the respective gene lost. There is less expression of FOXO3A or ATG7 in cells that concurrently do not express GFP compared to those where only GFP was knocked out (**Figure 3.8**).

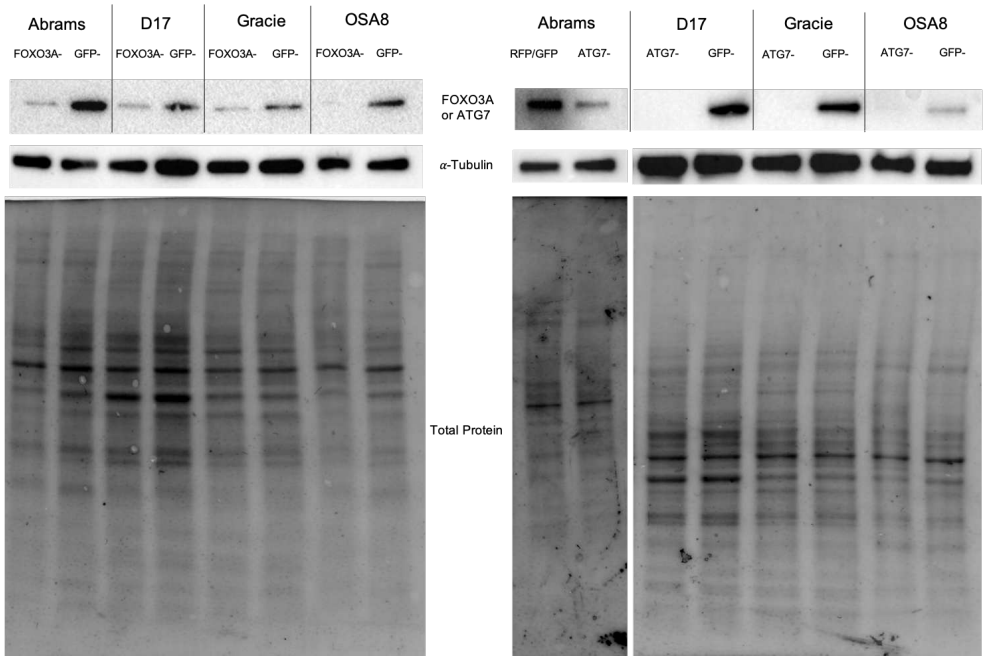

Figure 3.8 Western blots confirm gene knockout is occurring in cells that have lost GFP expression. FOXO3A (left) or ATG7 (right) western blots of cells following live cell sorting for cells only expressing RFP.

ATG7 null clones adapt to survive despite not using canonical autophagy

$ATG7^{-/-}$ clones were generated following sorting of RFP^{+}/GFP^{-} previously transfected with gRNAs for ATG7 and GFP. They were evaluated for ATG7 expression by western blot (**Figure 3.9**). Many of the clones grown out still had ATG7 expression (represented on D17 western blot) which is indicative of false positives in the CRISPR screen. This was expected since ATG7 is an essential gene based on the CRIPSR knockout score being less than 0.5 for all cell lines tested; therefore, most cells that lost

GFP also lost ATG7 and should not survive. The clones that did not express ATG7 did not have any LC3-I to LC3-II turnover (**Figure 3.10**) which is typical of cells that can no longer use autophagy [33]. Gracie ATG7$^{-/-}$ clones also had increased p62 expression compared to the non-genetically modified wild-type (WT) which is consistent with the inability to use autophagy. Abrams, D17, and OSA8 ATG7$^{-/-}$ clones did not show obvious accumulation in p62 expression (**Figure 3.10**). This could be due to the regulation of p62 by other mechanisms [34].

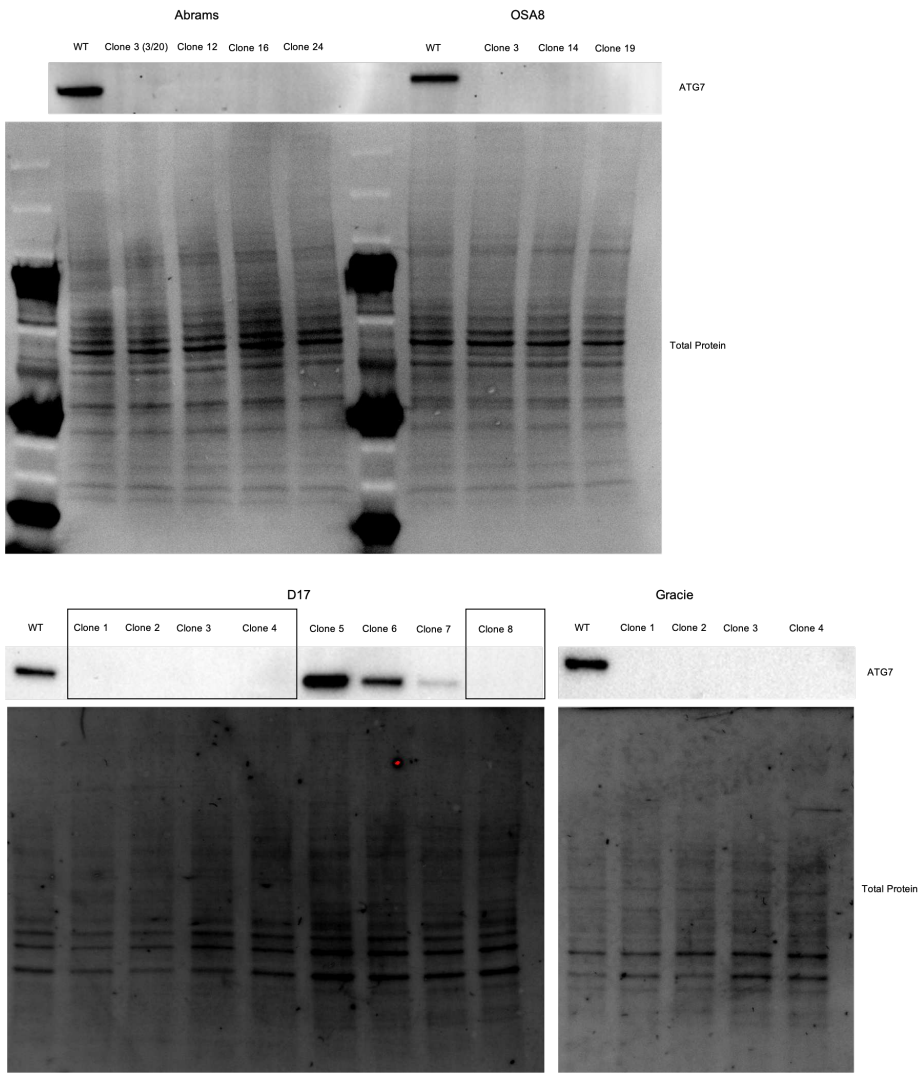

Figure 3.9 Generation of ATG7 knockout clones in four of the canine OSA lines. Western blots of ATG7 confirm that clones have lost ATG7 and do not express it.

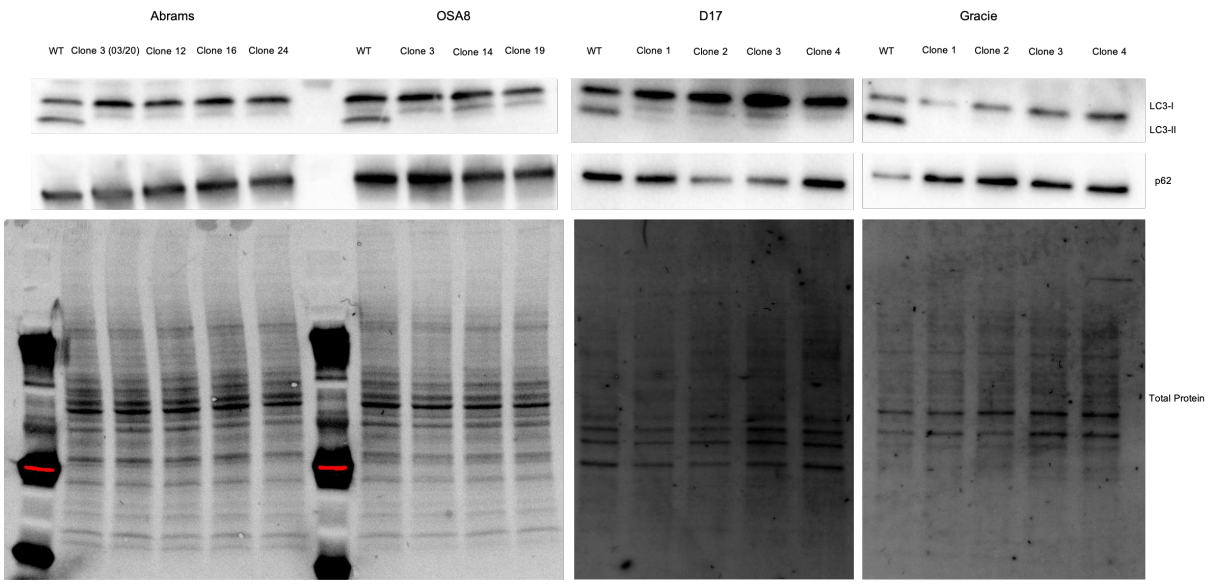

Figure 3.10 ATG7$^{-/-}$ clones do not express LC3-II since they cannot convert LC3-I to LC3-II. Western blots of LC3 show that ATG7$^{-/-}$ clones do not convert LC3-I to LC3-II. p62 western blots are less conclusive.

Since originally ATG7-dependent cells are deficient in canonical autophagy, ATG7$^{-/-}$ clones' growth and response to serum starvation were assessed. Cell growth determined by doubling times showed no difference between WT and ATG7$^{-/-}$ clones (**Figure 3.11 A**). Following serum starvation, Gracie WT was able to grow more than the ATG7$^{-/-}$ clones up to 96 hr before growth became similar to the clones (**Figure 3.11 B**). This suggests Gracie ATG7$^{-/-}$ clones are not able to survive this type of stress without the use of autophagy. Surprisingly, D17 ATG7$^{-/-}$ clones were able to grow significantly more than the WT despite stress from serum starvation (**Figure 3.11 B**). Further, D17 ATG7$^{-/-}$ clones did not experience any cell death while the WT were close to 100% dead at the end of 7 days (**Figure 3.12**). Abrams and OSA8 ATG7$^{-/-}$ clones respond similarly to WT following serum starvation (**Figure 3.11 B**). This suggests these clones have adapted by modifying signaling in other cellular pathways to circumvent their lack of ability to use autophagy. Overall, these results indicate that not all OSA will have the same

cellular responses without the ability to use autophagy despite starting as intermediately to very autophagy dependent.

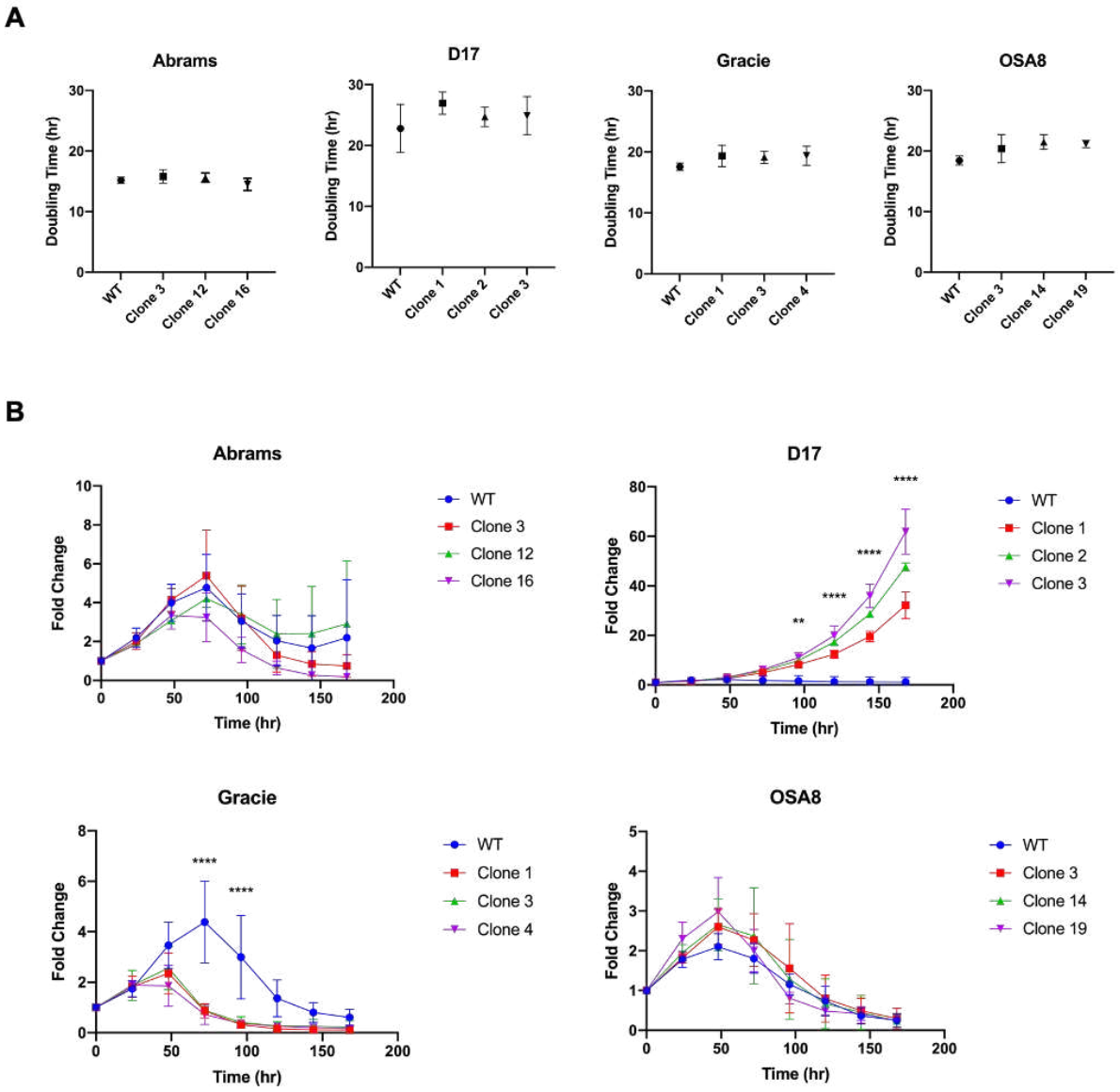

Figure 3.11 ATG7$^{-/-}$ clone growth is not different than WT in full serum but serum starved conditions lead to variable responses. Doubling times of ATG7$^{-/-}$ clones are not different from WT (**A**). Growth following serum starvation (**B**). Death following serum starvation (**C**).

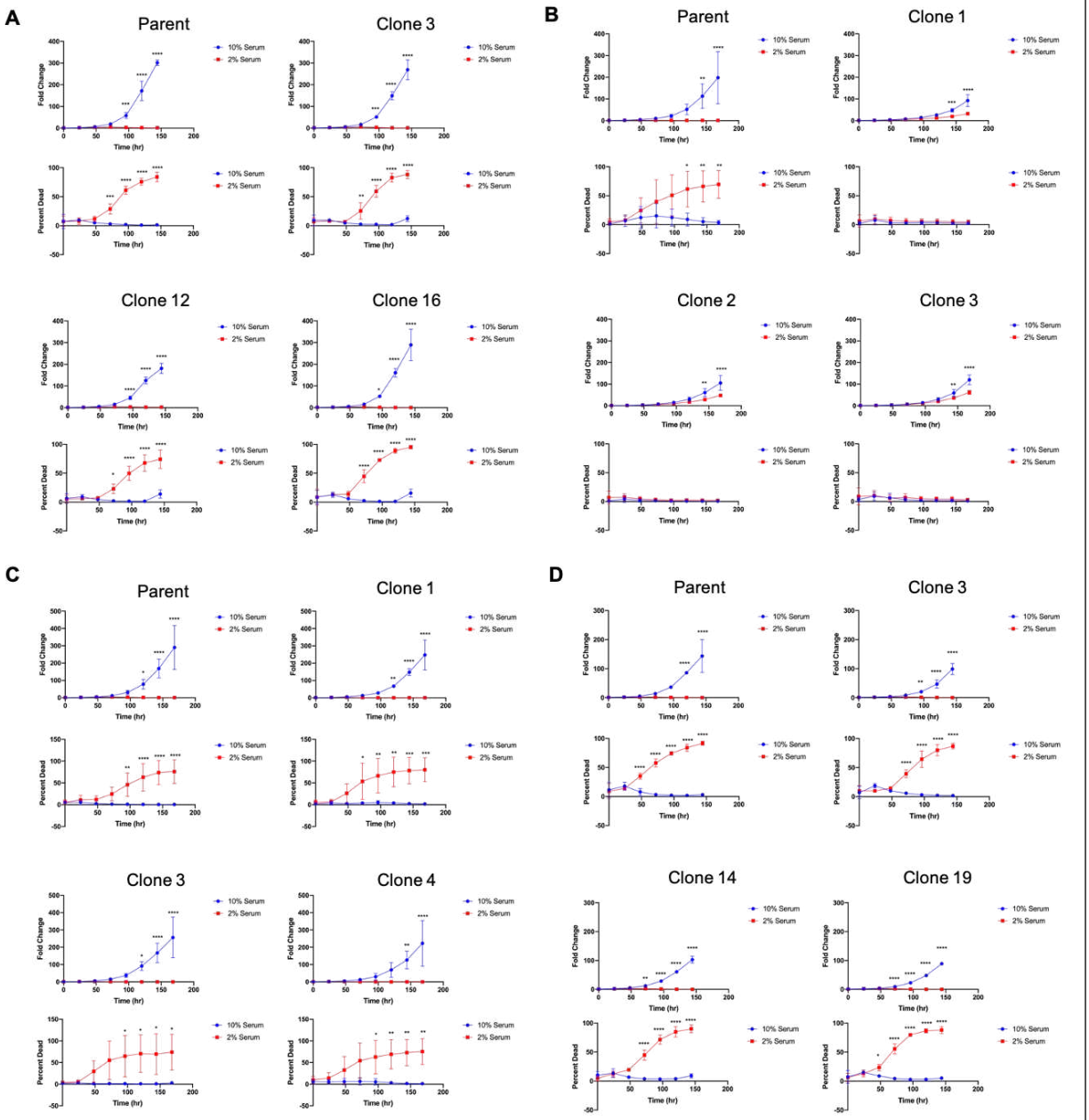

Figure 3.12 Serum starvation of ATG7 clones. Abrams (**A**), D17 (**B**), Gracie (**C**), OSA8 (**D**). Top plots for each cell line are fold change growth and bottom plots are percent dead.

The lysosomal activity of the cells was also assessed using LysoTracker in the IncuCyte to determine if ATG7$^{-/-}$ clones are upregulating the lysosomal pathway despite not degrading cellular components via autophagy. Overall, D17 generate more lysosomes than Gracie (**Figure 3.13 A**). D17 ATG7$^{-/-}$ clones had significantly more lysosomes

compared to WT, especially following serum starvation (**Figure 3.13 A**). Conversely, Gracie ATG7$^{-/-}$ clones had significantly less lysosomes compared to WT basally and following serum starvation. Further, there was no difference in lysosomal activity in D17 WT following serum starvation or autophagy inhibition via hydroxychloroquine (HCQ) treatment but there were significant differences between conditions in the ATG7$^{-/-}$ clones (**Figure 3.13 B**). The opposite effect was observed in Gracie; serum starvation and HCQ treatment significantly changed the lysosomal activity in WT while those effects were abolished in the ATG7$^{-/-}$ clones (**Figure 3.13 C**). When analyzing gene expression in WT vs ATG7$^{-/-}$ clones using 105 genes from the lysosomal gene set from the GSEA, D17 and OSA8 ATG7$^{-/-}$ clones had significantly higher expression, suggesting they are upregulating the lysosomal pathway compared to WT basally (**Figure 3.13 D**). Abrams and Gracie ATG7$^{-/-}$ clones were not significantly different from WT though they trended toward lower lysosomal pathway expression compared to WT. These results are consistent with LysoTracker where D17 ATG7$^{-/-}$ clones have higher lysosomal activity versus WT while Gracie ATG7$^{-/-}$ clones have lower lysosomal activity compared to WT. Although lysosomal activity was not assessed in Abrams or OSA8, this data suggests that Abrams ATG7$^{-/-}$ clones will behave more similarly to Gracie and OSA8 ATG7$^{-/-}$ clones will behave more similarly to D17.

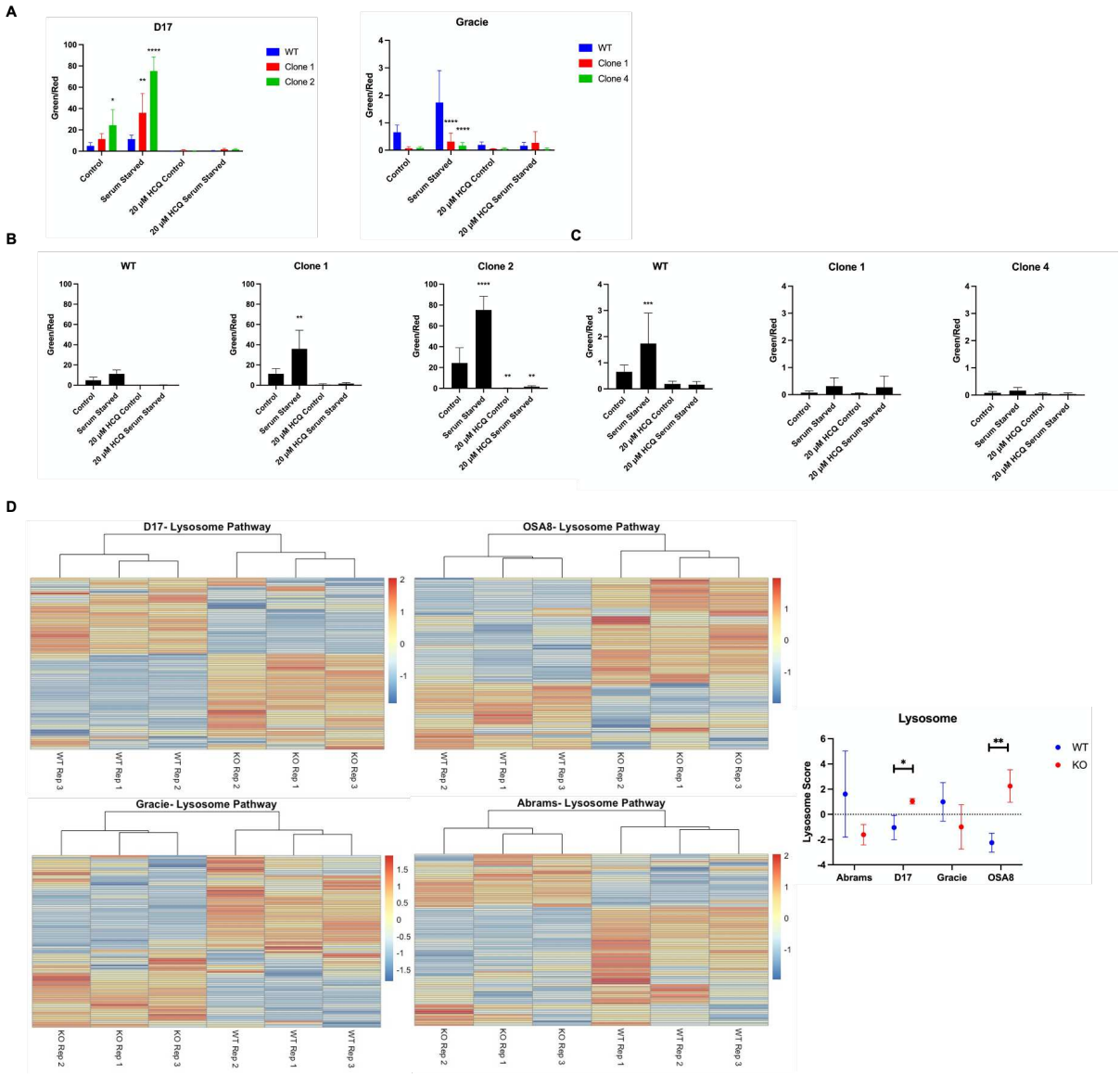

Figure 3.13 ATG7$^{-/-}$ clones use the lysosomal pathway differently compared to WT. Lysosome activity quantified in WT versus ATG7$^{-/-}$ clones following imaging on an IncuCyte where lysosome activity (green) was normalized to cell count (red) (**A**). D17 lysosomal activity in WT and two clones (**B**). Gracie lysosomal activity in WT and two clones (**C**). Lysosomal pathway gene expression in WT and clones (**D**). Statistical significance is between WT and clones in each condition, the condition compared to control in each individual cell line, or WT vs KO in each cell line.

Different ATG7$^{-/-}$ clones had different enriched pathways compared to their respective WT (**Figure 3.14**). Notably, when analyzing RNA seq counts in GSEA against the hallmarks of cancer, three of the clones had significant enrichment in epithelial to

mesenchymal transition, while Gracie the ATG7$^{-/-}$ clone significantly downregulated the epithelial to mesenchymal transition pathway. Three of the clones also had enrichment in KRAS signaling although Abrams and D17 significantly downregulated KRAS while OSA8 upregulated it. For a more targeted analysis, significantly differentially expressed genes between WT and the respective ATG7$^{-/-}$ clone were analyzed in DAVID, a tool that allows functional annotation to understand biological meaning behind large lists of genes, by looking at functional annotation clustering of these significantly differentially expressed genes in KEGG pathways (**Table 3.1**). When analyzing significantly downregulated genes in the ATG7$^{-/-}$ clones compared to WT, extracellular matrix receptor interaction, focal adhesion, and PI3K-Akt signaling was significantly enriched in Abrams, D17, and OSA8. This cluster was also significantly enriched based on the upregulated differentially expressed genes in Abrams and D17 as well. D17 also had a cluster consisting of extracellular matrix receptor interaction and protein digestion and absorption in the downregulated differentially expressed genes. OSA8 had a cluster containing PI3K-Akt signaling, Ras signaling, and MAPK signaling when analyzing the downregulated genes. Interestingly, Gracie had no functional annotation clustering in either up- or downregulated genes. Overall, these results suggest that these autophagy deficient cells are upregulating the PI3K-Akt signaling axis and that this could be a potential target for autophagy inhibited or deficient tumors.

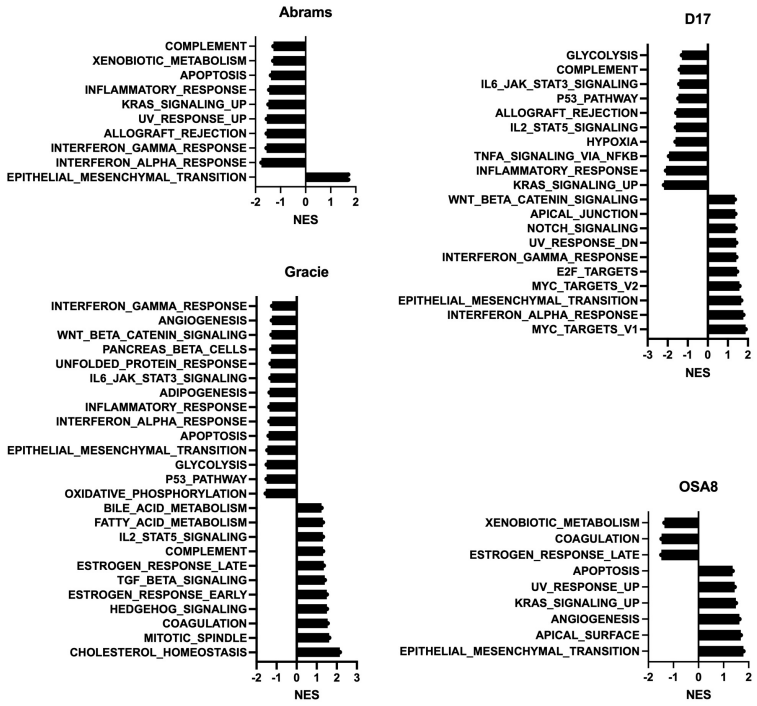

Figure 3.14 Pathway enrichment analysis in WT vs ATG7$^{-/-}$ clones. GSEA on all genes expressed following RNA seq in the ATG7$^{-/-}$ clones.

Table 3.1. Functional annotation clustering of significantly up- or downregulated genes.

Cell Line	UP	DOWN
Abrams	Extracellular matrix receptor interaction, focal adhesion, PI3K-Akt signaling	Extracellular matrix receptor interaction, focal adhesion, PI3K-Akt signaling
D17	Extracellular matrix receptor interaction, focal adhesion, PI3K-Akt signaling	Extracellular matrix receptor interaction, protein digestion and absorption
Gracie	None	None
OSA8	None	Extracellular matrix receptor interaction, focal adhesion, PI3K-Akt signaling; PI3K-Akt signaling, Ras signaling, MAPK signaling

ATG7–/– clones do not respond differently to autophagy inhibition

Since ATG7 knockout cells do not have the capability of using autophagy, their sensitivity to Lys05 was compared to the WT. Lys05 is an autophagy inhibitor that causes deacidification of lysosomes [35, 36]. Interestingly, at the concentrations used, there was no difference in the number of cells that were growth inhibited at 96 hr or 144 hr following treatment between ATG7$^{-/-}$ clones and WT except for OSA8 clone 3 compared to parent (**Figure 3.15 A**). Cell death was also not different between the ATG7$^{-/-}$ clones and WT (**Figure 3.15 B**). Lys05 targets PPT1 in the lysosome causing autophagy inhibition [35], and therefore PPT1 was assessed using RNA seq data between WT and ATG7$^{-/-}$ clones. All ATG7$^{-/-}$ clones have less PPT1 expression (**Figure 3.15 C**). Since lysosomal activity was diminished following treatment with a lysosomal inhibitor (**Figure 3.13**), this data suggests Lys05 may have another mechanism of action in these cells.

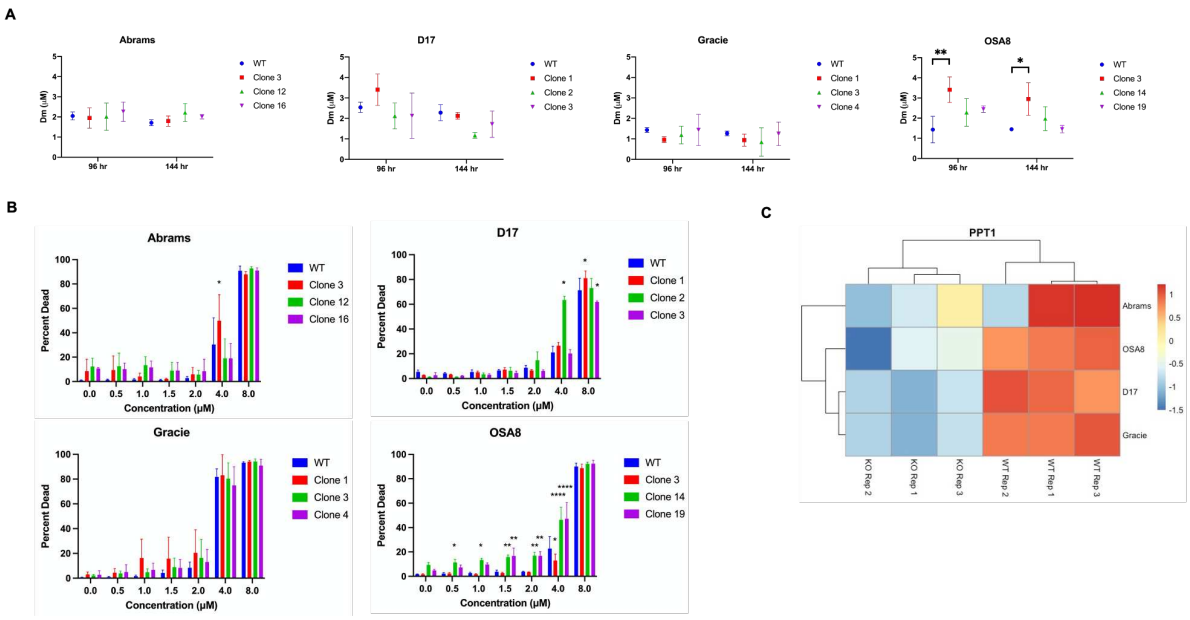

Figure 3.15 ATG7$^{-/-}$ clones are still sensitive to the autophagy inhibitor Lys05. Median dose effect of Lys05 at 96 hr and 144 hr (**A**). Cell death following Lys05 treatment for 144 hr (**B**). PPT1 expression from ATG7$^{-/-}$ clones versus WT from RNA seq (**C**). Statistical significance is WT compared to ATG7$^{-/-}$ clones.

Blocking autophagy at the lysosomal step with an inhibitor that affects more than just autophagy can also inhibit other metabolic scavenging pathways such as macropinocytosis (MP) [37]. Macropinocytosis is the non-specific uptake of fluid into large cytoplasmic vesicles via the lysosome-dependent degradation pathway [38]. It has been found that inhibiting autophagy causes an increase in macropinocytosis [39]. Therefore, macropinocytosis was assessed in the ATG7$^{-/-}$ clones to determine if they upregulate it compared to WT. Basally, D17 WT and ATG7$^{-/-}$ clones had higher levels of macropinocytosis than Gracie. Interestingly, under normal growth conditions, one of the D17 ATG7$^{-/-}$ clones had significantly increased macropinocytosis compared to WT and this effect was further enhanced under serum starved conditions (**Figure 3.16 A**). In contrast, Gracie ATG7$^{-/-}$ clones did not change their usage of macropinocytosis compared to WT. Neither the Gracie clones nor WT upregulated macropinocytosis in serum starved conditions. However, Lys05 inhibited macropinocytosis in all cells regardless of autophagy status. Gene expression of macropinocytosis-related genes from the Gene Ontology database was consistent with these results (**Figure 3.16 B**). Abrams and D17 ATG7$^{-/-}$ clones had a higher macropinocytosis score compared to WT while Gracie and OSA8 clones did not.

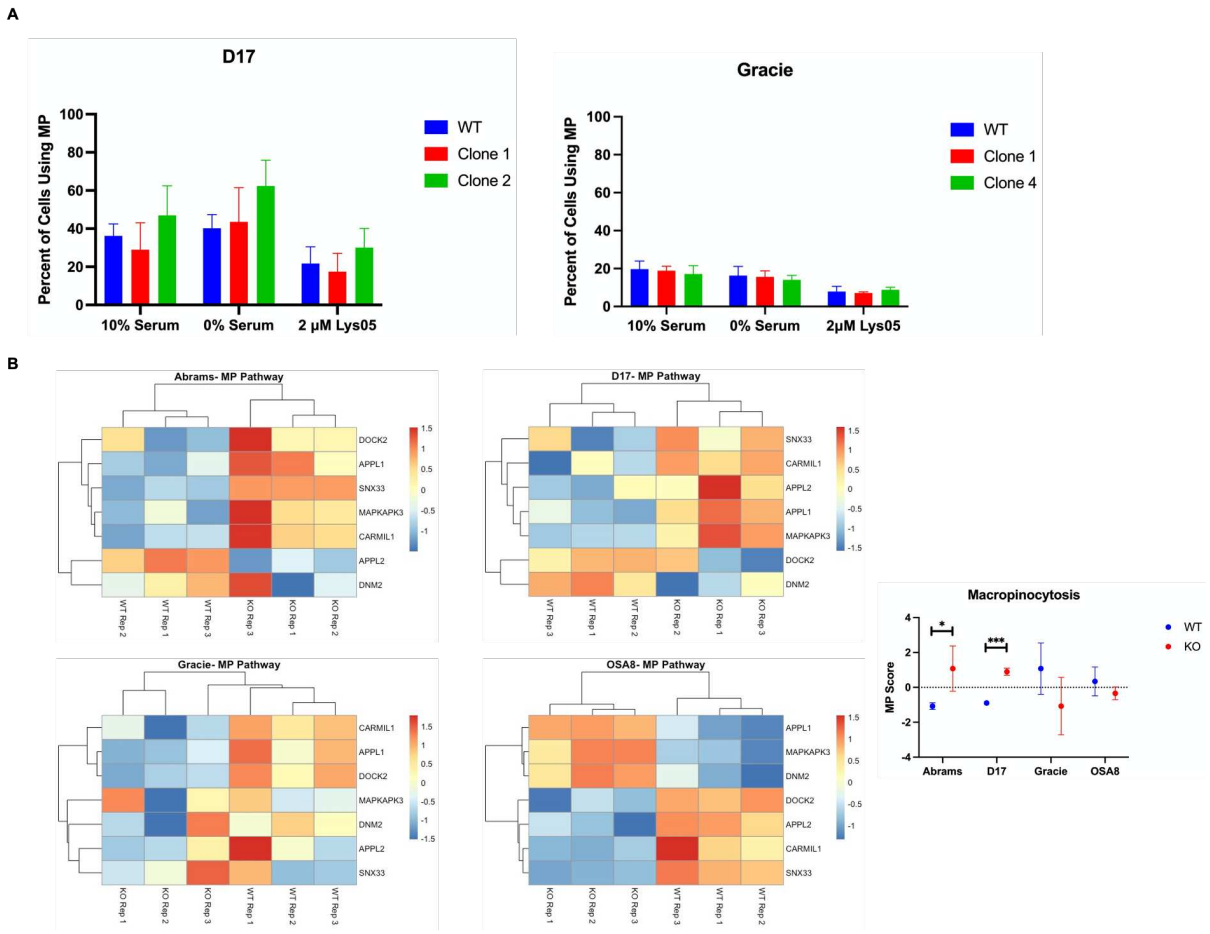

Figure 3.16 ATG7$^{-/-}$ clones do not upregulate macropinocytosis in the same way. Macropinocytosis measured by flow cytometry following uptake of dextran-FITC (**A**). Macropinocytosis gene expression scores from RNA seq (**B**). Statistical significance is WT compared to ATG7$^{-/-}$ clone.

ATG7 deficient clones are overall not sensitized to OSA chemotherapies

Doxorubicin and carboplatin are first line treatments for canine OSA patients [40]. There are reports of doxorubicin or carboplatin treatment upregulating autophagy and subsequent combination autophagy inhibition with carboplatin or doxorubicin re-sensitizes OSA to the chemotherapy in human OSA cell lines [41, 42, 43]. Therefore, ATG7$^{-/-}$ clones were assessed for sensitivity to doxorubicin and carboplatin by monitoring cell growth and cell death. The ATG7$^{-/-}$ clones of the different cell lines had varying

responses to both cell growth (**Figure 3.17 A**) and death (**Figure 3.17 B**). Abrams ATG7$^{-/-}$ clones were not growth inhibited compared to WT and actually had higher Dm's than WT, indicating they grew better than WT. However, a few of the clones did have more cell death than WT at 72 hr. Conversely, two of the D17 ATG7$^{-/-}$ clones were significantly growth inhibited at 48 hr but cell death was not different between the clones and WT. Gracie ATG7$^{-/-}$ clones growth inhibition trended less than WT but was not significant. Cell death was significantly different in WT and clones at just 500 nM at 72 hr. Neither OSA8 ATG7$^{-/-}$ clone growth nor cell death was different compared to control. Overall, this indicates that loss of autophagy reduces cell growth in some OSA tumors but can actually have the opposite effect in other OSA tumors following doxorubicin treatment. Results were slightly different following carboplatin treatment. Cell growth was not significantly different between ATG7$^{-/-}$ clones and WT in any cell lines following 72 hr (**Figure 3.18 A**). Cell death was also not different in D17 or OSA8 (**Figure 3.18 B**). However, cell death was significantly higher in Abrams ATG7$^{-/-}$ clones compared to WT at almost all concentrations tested. Gracie also had some significant difference in cell death at higher concentrations of carboplatin. These results indicate that the loss of autophagy causes increased cell death vulnerability to carboplatin. Taken together, this data suggests that acquired autophagy resistance through the loss of ATG7 causes tumors to respond differently to standard OSA chemotherapies and does not make all OSA tumors more sensitive to DNA damaging drugs.

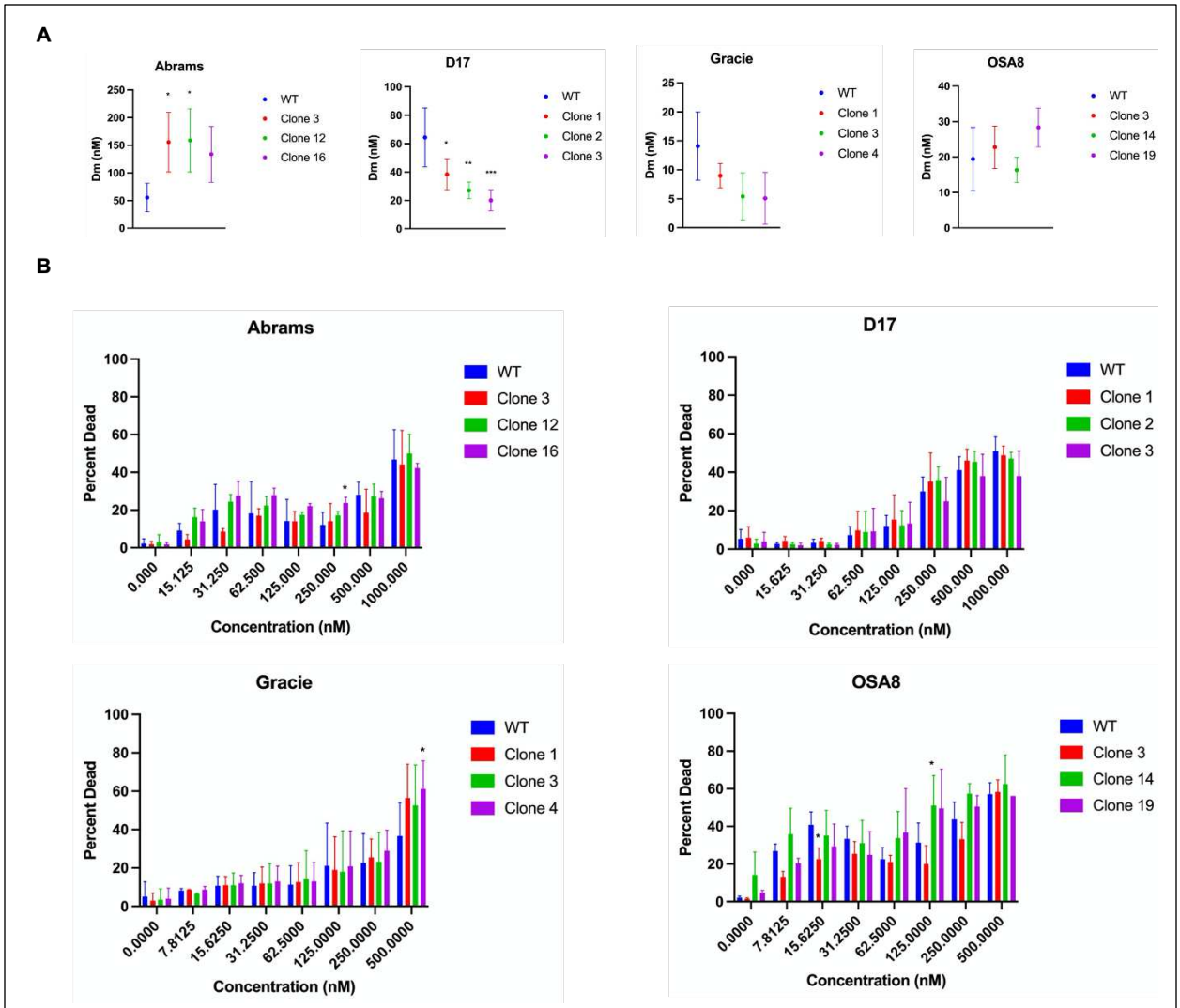

Figure 3.17 ATG7$^{-/-}$ clones have varying responses to doxorubicin. Cells affected measured by growth at 48 hr (**A**). Percent of cells dead following doxorubicin treatment at 72 hr (**B**). Statistical significance is between WT and the clone at that respective concentration.

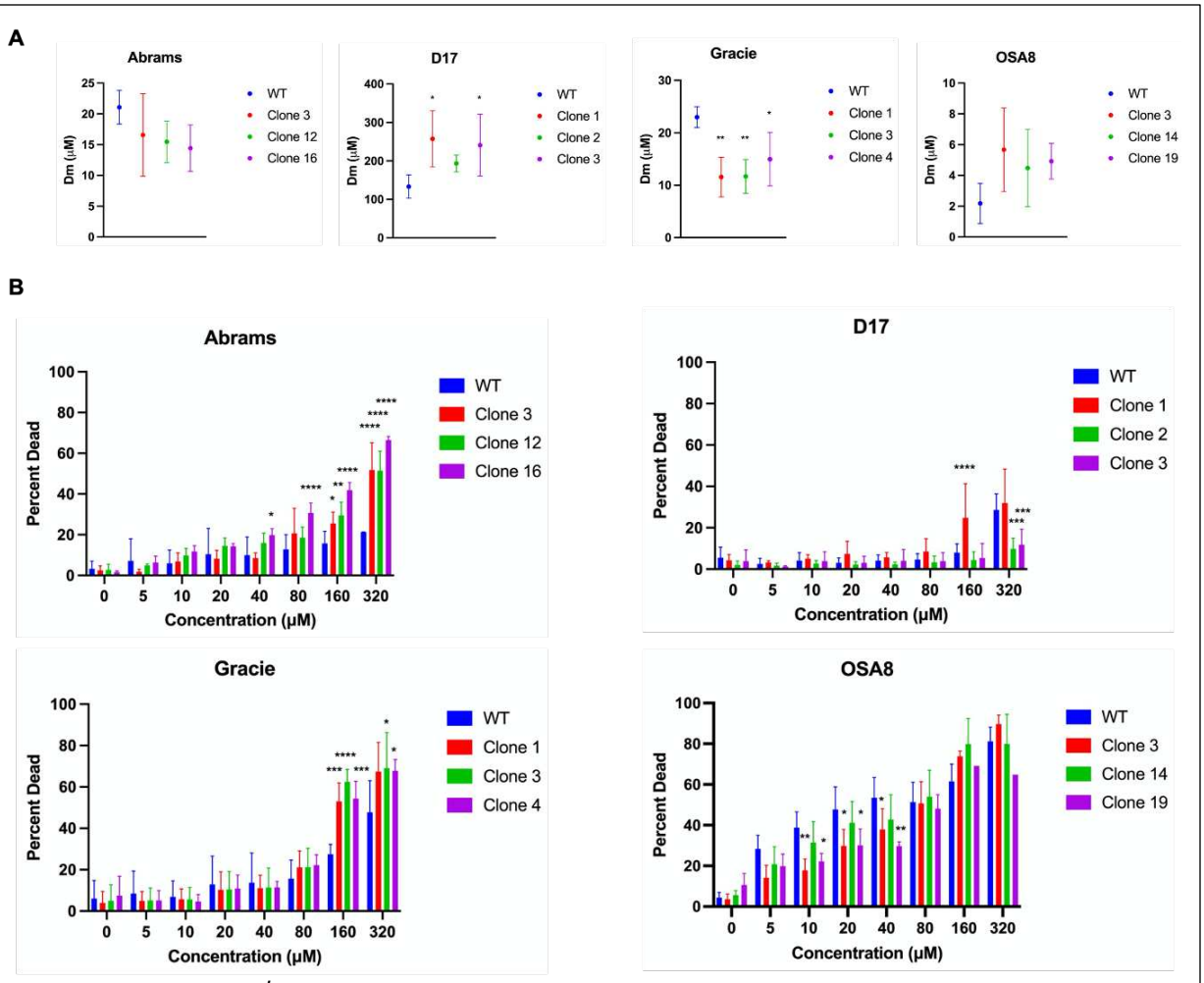

Figure 3.18 ATG7$^{-/-}$ clones have varying responses to carboplatin. Cells affected measured by growth at 72 hr (**A**). Percent of cells dead following carboplatin treatment at 72 hr (**B**). Statistical significance is between WT and the clone at that respective concentration.

Canine and human OSA are sensitive to HCQ

Since canine and human OSA have many similarities, both canine and human OSA cell lines were tested for their sensitivity to HCQ to determine if both species are affected by autophagy inhibition at the same toxicity. Both human and canine OSA are differentially sensitive to HCQ after 96 hr (**Figure 3.19**). This indicates that human OSA may behave similarly to canine OSA since their sensitivities to HCQ are not different.

Further, the highest achievable concentration of HCQ in patients treated with 200 to 400 mg HCQ corresponds to between 10 and 20 μM [44, 45, 46] *in vitro* and these data imply that most OSA tumors will be sensitive to HCQ at clinically relevant concentrations, suggesting targeting autophagy in OSA may be a promising treatment.

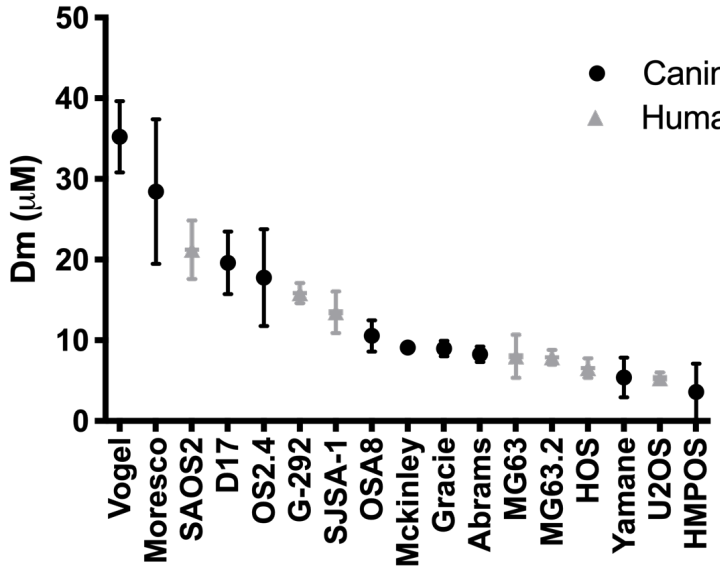

Figure 3.19 HCQ sensitivity in osteosarcoma cell lines. There is a difference in sensitivity to HCQ across canine and human osteosarcoma which indicates that human osteosarcoma will also have differential dependency on autophagy.

Discussion

Autophagy is implicated in cancer in multiple ways. For one, certain cancers have differential autophagy dependency where some tumors of the same cancer type are dependent on autophagy for survival while autophagy is dispensable for other tumors of the same cancer type to survive. Autophagy is also a mechanism of resistance to many cancer treatments and therefore targeting autophagy could be beneficial for patients who are no longer responsive to their therapies. Since OSA survival rates have not improved

in almost four decades, autophagy was explored by genetic and pharmacologic means in OSA. Here, autophagy dependency was determined in six canine OSA cell lines using a CRISPR knockout screen of eight autophagy genes that span the entire pathway. All cell lines tested were intermediately to extremely dependent on autophagy when assessed within the first 5-7 days of autophagy gene loss (**Figure 3.6**). This is the first screen in autophagy demonstrating that many OSA tumors are likely to be initially dependent on autophagy. Interestingly, all cell lines were dependent on ATG7 and ATG12 to survive. This suggests that the formation of the autophagosome membrane is essential for OSA cells. Further, the most autophagy dependent cell lines were also dependent on ULK2 and VPS34. Recently, ULK2 downregulation has been implicated in cancer progression in glioma [47] and chemotherapy sensitivity in non-small cell lung cancer [48], contrary to what the screen revealed here. This may be because the tumors with downregulation of ULK2 are not dependent on autophagy to start. However, the essentiality of VPS34 in autophagy dependent tumors is encouraging since there are small molecule inhibitors that target VPS34 [49, 50]. VPS34 inhibitors have also been shown to synergize with chemotherapy treatment, suggesting this combination may be especially beneficial for autophagy dependent tumors [51]. Towers et al. performed this autophagy CRISPR screen in many cancer types including one human OSA cell line which was also found to be intermediately dependent on autophagy, implicating OSA autophagy dependency [16]. Further, both canine and human OSA are responsive to autophagy inhibition at clinically achievable doses. (**Figure 3.19**), implying that human OSA will behave similarly to canine OSA in autophagy dependency studies.

Although OSA was initially dependent on autophagy, there were some cells that were able to survive despite the loss of functional canonical autophagy. These cells were no longer able to convert LC3-I to LC3-II (**Figure 3.10**) and grew at rates similar to their WT counterparts (**Figure 3.11**). This suggests that under selective pressure, initially autophagy dependent cells adapt to survive. This adaptation to survival will not be the same for all OSA. Although it was previously found that cells that cannot use autophagy are dependent on proteasomal degradation via the NRF2 pathway [16], that was not the mechanism of survival based on RNA seq differences between WT and ATG7$^{-/-}$ clones (data not shown). Instead, all but one of the ATG7 deficient clones upregulated PI3K-Akt signaling (**Table 3.1**). There is potential for treatment of OSA patients with combined autophagy and PI3K-Akt inhibition. This has combination has shown promise in breast cancer cells [52], hepatocellular carcinoma [53], and in glioma and prostate cancer cells [54] *in vitro* and *in vivo*.

Interestingly, all of the ATG7 deficient clones were still sensitive to the autophagy inhibitor Lys05 (**Figure 3.15**). This suggests these clones are still using scavenging processes that involve lysosomal degradation because all clones still died at the higher concentrations of Ly05. Since Lys05 can affect any cellular mechanism that requires lysosomes and it has been recently shown that autophagy inhibition causes increased macropinocytosis [39], ATG7 deficient clones from two cell lines were tested for macropinocytosis uptake. Overall, one cell line had much lower overall macropinocytosis and further did not increase macropinocytosis following autophagy inhibition or in serum starved conditions while the other cell line had high basal macropinocytosis that was enhanced after serum starvation but blocked with autophagy inhibition (**Figure 3.16**). This

indicates that Lys05 and other lysosomal inhibitors are likely blocking function of other lysosomal scavenging pathways even when cells are able to use autophagy. Upregulation of macropinocytosis at levels sufficient to accelerate tumor proliferation was recently reported breast cancer and supports the idea that blocking multiple lysosomal degradation pathways may be beneficial [55]. The cell line with lower macropinocytosis had much lower lysosomal activity than the cell line with high macropinocytosis (**Figure 3.13**), suggesting that tumor cells can be dependent on lysosomal degradation via autophagy but not on other lysosomal scavenging pathways.

The various clones from different OSA tumors responded differently to standard OSA chemotherapies including doxorubicin and carboplatin (**Figures 3.17 and 3.18**). Surprisingly, most of the ATG7 deficient clones were not more sensitive to either doxorubicin or carboplatin despite the inability to use autophagy as a survival mechanism. Although there is some evidence that autophagy is a mechanism of resistance in OSA in response to doxorubicin and carboplatin [41, 42, 43], this data suggests that autophagy deficiency through the loss of ATG7 will not be the mechanism of resistance in many OSA tumors. However, since the ATG7 deficient clones were still sensitive to lysosomal inhibition via Lys05, combination therapy of autophagy inhibition that is a lysosomal inhibitor plus a DNA damaging agent such as doxorubicin or carboplatin may be more effective. Further, cycling autophagy inhibition with chemotherapy may also be efficacious to both prevent resistance to autophagy inhibition and to mechanistically change signaling pathways that tumor cells use to evade chemotherapy.

Overall, identifying the subset of patients with autophagy dependent tumors can enhance the use of autophagy inhibitors as single therapy agents in clinic for these

patients. Further, understanding whether tumors become resistant to chemotherapies because of autophagy explicitly or because of other lysosomal degradation pathways may help direct the use of autophagy-specific inhibitors such as those that inhibit VPS34 or non-specific autophagy inhibitors such as HCQ as single therapy or as combination therapies. Elucidating these mechanisms in OSA is especially relevant as there is currently a clinical trial combining HCQ with gemcitabine and docetaxel in OSA (clinicaltrials.gov). Autophagy dependency and targeting chemotherapy resistance due to autophagy are promising aspects in OSA but more work is needed to understand in what context autophagy inhibition is most advantageous.

References

1. Zhang Y, Yang J, Zhao N, et al. Progress in the chemotherapeutic treatment of osteosarcoma. Oncol Lett. 2018 Nov;16(5):6228-6237. doi: 10.3892/ol.2018.9434. PubMed PMID: 30405759; PubMed Central PMCID: PMCPMC6202490.

2. Lamplot JD, Denduluri S, Qin J, et al. The Current and Future Therapies for Human Osteosarcoma. Curr Cancer Ther Rev. 2013 Feb;9(1):55-77. doi: 10.2174/1573394711309010006. PubMed PMID: 26834515; PubMed Central PMCID: PMCPMC4730918.

3. Moore DD, Luu HH. Osteosarcoma. In: Peabody TD, Attar S, editors. Orthopaedic Oncology: Primary and Metastatic Tumors of the Skeletal System: Springer International Publishing; 2014. p. 65-92.

4. O'Farrill JS, Gordon N. Autophagy in Osteosarcoma. In: Kleinerman MD, Eugenie S, editors. Current Advances in Osteosarcoma: Springer International Publishing; 2014.

5. Harrison DJ, Geller DS, Gill JD, et al. Current and future therapeutic approaches for osteosarcoma. Expert Rev Anticancer Ther. 2018 Jan;18(1):39-50. doi: 10.1080/14737140.2018.1413939. PubMed PMID: 29210294.

6. Varshney J, Scott MC, Largaespada DA, et al. Understanding the Osteosarcoma Pathobiology: A Comparative Oncology Approach. Vet Sci. 2016 Jan 18;3(1). doi: 10.3390/vetsci3010003. PubMed PMID: 29056713; PubMed Central PMCID: PMCPMC5644613.

7. Mueller F, Fuchs B, Kaser-Hotz B. Comparative Biology of Human and Canine Osteosarcoma. Anticancer Research. 2007;27(1A):155-164. doi: 10.3390/vetsci3010003.

8. Ravikumar B, Sarkar S, Davies JE, et al. Regulation of mammalian autophagy in physiology and pathophysiology. Physiol Rev. 2010 Oct;90(4):1383-435. doi: 10.1152/physrev.00030.2009. PubMed PMID: 20959619.

9. Yang ZJ, Chee CE, Huang S, et al. The role of autophagy in cancer: therapeutic implications. Mol Cancer Ther. 2011 Sep;10(9):1533-41. doi: 10.1158/1535-

7163.MCT-11-0047. PubMed PMID: 21878654; PubMed Central PMCID: PMCPMC3170456.

10. Mizushima N, Yoshimori T, Ohsumi Y. The role of Atg proteins in autophagosome formation. Annu Rev Cell Dev Biol. 2011;27:107-32. doi: 10.1146/annurev-cellbio-092910-154005. PubMed PMID: 21801009.

11. Bernard A, Klionsky DJ. Toward an understanding of autophagosome-lysosome fusion: The unsuspected role of ATG14. Autophagy. 2015 Apr 3;11(4):583-4. doi: 10.1080/15548627.2015.1029220. PubMed PMID: 25920502; PubMed Central PMCID: PMCPMC4502729.

12. Yang Z, Klionsky DJ. Eaten alive: a history of macroautophagy. Nat Cell Biol. 2010 Sep;12(9):814-22. doi: 10.1038/ncb0910-814. PubMed PMID: 20811353; PubMed Central PMCID: PMCPMC3616322.

13. De Duve C, Wattiaux R. Functions of lysosomes. Annu Rev Physiol. 1966;28:435-92. doi: 10.1146/annurev.ph.28.030166.002251. PubMed PMID: 5322983.

14. Maycotte P, Gearheart CM, Barnard R, et al. STAT3-mediated autophagy dependence identifies subtypes of breast cancer where autophagy inhibition can be efficacious. Cancer Res. 2014 May 1;74(9):2579-90. doi: 10.1158/0008-5472.CAN-13-3470. PubMed PMID: 24590058; PubMed Central PMCID: PMCPMC4008672.

15. Yang S, Wang X, Contino G, et al. Pancreatic cancers require autophagy for tumor growth. Genes Dev. 2011 Apr 1;25(7):717-29. doi: 10.1101/gad.2016111. PubMed PMID: 21406549; PubMed Central PMCID: PMCPMC3070934.

16. Towers CG, Fitzwalter BE, Regan D, et al. Cancer Cells Upregulate NRF2 Signaling to Adapt to Autophagy Inhibition. Dev Cell. 2019 Sep 23;50(6):690-703 e6. doi: 10.1016/j.devcel.2019.07.010. PubMed PMID: 31378590; PubMed Central PMCID: PMCPMC7233142.

17. Camuzard O, Santucci-Darmanin S, Carle GF, et al. Role of autophagy in osteosarcoma. J Bone Oncol. 2019 Jun;16:100235. doi: 10.1016/j.jbo.2019.100235. PubMed PMID: 31011524; PubMed Central PMCID: PMCPMC6460301.

18. Liao YX, Yu HY, Lv JY, et al. Targeting autophagy is a promising therapeutic strategy to overcome chemoresistance and reduce metastasis in osteosarcoma. Int J Oncol. 2019 Dec;55(6):1213-1222. doi: 10.3892/ijo.2019.4902. PubMed PMID: 31638211; PubMed Central PMCID: PMCPMC6831203.

19. Akin D, Wang SK, Habibzadegah-Tari P, et al. A novel ATG4B antagonist inhibits autophagy and has a negative impact on osteosarcoma tumors. Autophagy. 2014;10(11):2021-35. doi: 10.4161/auto.32229. PubMed PMID: 25483883; PubMed Central PMCID: PMCPMC4502682.

20. Li Q, Song C, Lao L, et al. Knockdown of autophagy-related protein 6, Beclin-1, decreases cell growth, invasion, and metastasis and has a positive effect on chemotherapy-induced cytotoxicity in osteosarcoma cells. TUMOR BIOL. 2015;36(4):2531-2539. doi: 10.1007/s13277-014-2868-y.

21. Jiang K, Zhang C, Yu B, et al. Autophagic degradation of FOXO3a represses the expression of PUMA to block cell apoptosis in cisplatin-resistant osteosarcoma cells. Am J Cancer Res. 2017;7(7).

22. Guan J, Yuan Z, He J, et al. Overexpression of caveolin-1 reduces Taxol resistance in human osteosarcoma cells by attenuating PI3K-Akt-JNK dependent autophagy. Exp Ther Med. 2016 Nov;12(5):2815-2822. doi: 10.3892/etm.2016.3713. PubMed PMID: 27882079; PubMed Central PMCID: PMCPMC5103709.

23. Mukherjee S, Dash S, Lohitesh K, et al. The dynamic role of autophagy and MAPK signaling in determining cell fate under cisplatin stress in osteosarcoma cells. PLoS One. 2017;12(6):e0179203. doi: 10.1371/journal.pone.0179203. PubMed PMID: 28598976; PubMed Central PMCID: PMCPMC5466322.

24. Kim M, Jung JY, Choi S, et al. GFRA1 promotes cisplatin-induced chemoresistance in osteosarcoma by inducing autophagy. Autophagy. 2017 Jan 2;13(1):149-168. doi: 10.1080/15548627.2016.1239676. PubMed PMID: 27754745; PubMed Central PMCID: PMCPMC5240831.

25. Xiao X, Wang W, Li Y, et al. HSP90AA1-mediated autophagy promotes drug resistance in osteosarcoma. J Exp Clin Cancer Res. 2018 Aug 28;37(1):201. doi: 10.1186/s13046-018-0880-6. PubMed PMID: 30153855; PubMed Central PMCID: PMCPMC6114771.

26. Huang J, Ni J, Liu K, et al. HMGB1 promotes drug resistance in osteosarcoma. Cancer Res. 2012 Jan 1;72(1):230-8. doi: 10.1158/0008-5472.CAN-11-2001. PubMed PMID: 22102692.

27. Liang X, Potter J, Kumar S, et al. Rapid and highly efficient mammalian cell engineering via Cas9 protein transfection. J Biotechnol. 2015 Aug 20;208:44-53. doi: 10.1016/j.jbiotec.2015.04.024. PubMed PMID: 26003884.

28. Wagle MC, Kirouac D, Klijn C, et al. A transcriptional MAPK Pathway Activity Score (MPAS) is a clinically relevant biomarker in multiple cancer types. NPJ Precis Oncol. 2018;2(1):7. doi: 10.1038/s41698-018-0051-4. PubMed PMID: 29872725; PubMed Central PMCID: PMCPMC5871852.

29. Liu Y, Ao X, Ding W, et al. Critical role of FOXO3a in carcinogenesis. Mol Cancer. 2018 Jul 25;17(1):104. doi: 10.1186/s12943-018-0856-3. PubMed PMID: 30045773; PubMed Central PMCID: PMCPMC6060507.

30. Boehm EM, Gildenberg MS, Washington MT. The Many Roles of PCNA in Eukaryotic DNA Replication. Enzymes. 2016;39:231-54. doi: 10.1016/bs.enz.2016.03.003. PubMed PMID: 27241932; PubMed Central PMCID: PMCPMC4890617.

31. Lin A, Giuliano CJ, Sayles NM, et al. CRISPR/Cas9 mutagenesis invalidates a putative cancer dependency targeted in on-going clinical trials. Elife. 2017 Mar 24;6. doi: 10.7554/eLife.24179. PubMed PMID: 28337968; PubMed Central PMCID: PMCPMC5365317.

32. DeWeirdt PC, Sangree AK, Hanna RE, et al. Genetic screens in isogenic mammalian cell lines without single cell cloning. Nat Commun. 2020 Feb 6;11(1):752. doi: 10.1038/s41467-020-14620-6. PubMed PMID: 32029722; PubMed Central PMCID: PMCPMC7005275.

33. Yoshii SR, Mizushima N. Monitoring and Measuring Autophagy. Int J Mol Sci. 2017 Aug 28;18(9). doi: 10.3390/ijms18091865. PubMed PMID: 28846632; PubMed Central PMCID: PMCPMC5618514.

34. Sanchez-Martin P, Komatsu M. p62/SQSTM1 - steering the cell through health and disease. J Cell Sci. 2018 Nov 5;131(21). doi: 10.1242/jcs.222836. PubMed PMID: 30397181.

35. Rebecca VW, Nicastri MC, Fennelly C, et al. PPT1 Promotes Tumor Growth and Is the Molecular Target of Chloroquine Derivatives in Cancer. Cancer Discov. 2019 Feb;9(2):220-229. doi: 10.1158/2159-8290.CD-18-0706. PubMed PMID: 30442709; PubMed Central PMCID: PMCPMC6368875.

36. Pasquier B. Autophagy inhibitors. Cell Mol Life Sci. 2016 Mar;73(5):985-1001. doi: 10.1007/s00018-015-2104-y. PubMed PMID: 26658914.

37. Amaravadi RK, Kimmelman AC, Debnath J. Targeting Autophagy in Cancer: Recent Advances and Future Directions. Cancer Discov. 2019 Sep;9(9):1167-1181. doi: 10.1158/2159-8290.CD-19-0292. PubMed PMID: 31434711; PubMed Central PMCID: PMCPMC7306856.

38. King JS, Kay RR. The origins and evolution of macropinocytosis. Philos Trans R Soc Lond B Biol Sci. 2019 Feb 4;374(1765):20180158. doi: 10.1098/rstb.2018.0158. PubMed PMID: 30967007; PubMed Central PMCID: PMCPMC6304743.

39. Su H, Yang F, Fu R, et al. Cancer cells escape autophagy inhibition via NRF2-induced macropinocytosis. Cancer Cell. 2021 May 10;39(5):678-693 e11. doi: 10.1016/j.ccell.2021.02.016. PubMed PMID: 33740421; PubMed Central PMCID: PMCPMC8119368.

40. Misaghi A, Goldin A, Awad M, et al. Osteosarcoma: a comprehensive review. SICOT J. 2018;4:12. doi: 10.1051/sicotj/2017028. PubMed PMID: 29629690; PubMed Central PMCID: PMCPMC5890448.

41. Zhao D, Yuan H, Yi F, et al. Autophagy prevents doxorubicininduced apoptosis in osteosarcoma. Mol Med Rep. 2014 May;9(5):1975-81. doi: 10.3892/mmr.2014.2055. PubMed PMID: 24639013.

42. Miao X-D, Cao L, Zhang Q, et al. Effect of PI3K-mediated autophagy in human osteosarcoma MG63 cells on sensitivity to chemotherapy with cisplatin. Asian Pacific Journal of Tropical Medicine. 2015;8(9):731-738. doi: 10.1016/j.apjtm.2015.07.024.

43. Zhang Z, Shao Z, Xiong L, et al. Expression of Beclin1 in osteosarcoma and the effects of down-regulation of autophagy on the chemotherapeutic sensitivity. J Huazhong Univ Sci Technolog Med Sci. 2009 Dec;29(6):737-40. doi: 10.1007/s11596-009-0613-3. PubMed PMID: 20037818.

44. Wolpin BM, Rubinson DA, Wang X, et al. Phase II and pharmacodynamic study of autophagy inhibition using hydroxychloroquine in patients with metastatic pancreatic adenocarcinoma. Oncologist. 2014 Jun;19(6):637-8. doi: 10.1634/theoncologist.2014-0086. PubMed PMID: 24821822; PubMed Central PMCID: PMCPMC4041680.

45. Goldberg SB, Supko JG, Neal JW, et al. A phase I study of erlotinib and hydroxychloroquine in advanced non-small-cell lung cancer. J Thorac Oncol. 2012 Oct;7(10):1602-8. doi: 10.1097/JTO.0b013e318262de4a. PubMed PMID: 22878749; PubMed Central PMCID: PMCPMC3791327.

46. Zeh HJ, Bahary N, Boone BA, et al. A Randomized Phase II Preoperative Study of Autophagy Inhibition with High-Dose Hydroxychloroquine and Gemcitabine/Nab-Paclitaxel in Pancreatic Cancer Patients. Clin Cancer Res. 2020 Jul 1;26(13):3126-3134. doi: 10.1158/1078-0432.CCR-19-4042. PubMed PMID: 32156749; PubMed Central PMCID: PMCPMC8086597.

47. Shukla S, Patric IR, Patil V, et al. Methylation silencing of ULK2, an autophagy gene, is essential for astrocyte transformation and tumor growth. J Biol Chem. 2014 Aug 8;289(32):22306-18. doi: 10.1074/jbc.M114.567032. PubMed PMID: 24923441; PubMed Central PMCID: PMCPMC4139240.

48. Cheng H, Yang ZT, Bai YQ, et al. Overexpression of Ulk2 inhibits proliferation and enhances chemosensitivity to cisplatin in non-small cell lung cancer. Oncol Lett. 2019 Jan;17(1):79-86. doi: 10.3892/ol.2018.9604. PubMed PMID: 30655741; PubMed Central PMCID: PMCPMC6313100.

49. Norman MZ, Parpal S, Van Moer K, et al. Inhibition of Vps34 reprograms cold into hot inflamed tumors and improves anti-PD-1/PD-L1 immunotherapy. Science Advances. 2020;6.

50. Perez-Hernandez M, Arias A, Martinez-Garcia D, et al. Targeting Autophagy for Cancer Treatment and Tumor Chemosensitization. Cancers (Basel). 2019 Oct 19;11(10). doi: 10.3390/cancers11101599. PubMed PMID: 31635099; PubMed Central PMCID: PMCPMC6826429.

51. Dyczynski M, Yu Y, Otrocka M, et al. Targeting autophagy by small molecule inhibitors of vacuolar protein sorting 34 (Vps34) improves the sensitivity of breast cancer cells to Sunitinib. Cancer Lett. 2018 Oct 28;435:32-43. doi: 10.1016/j.canlet.2018.07.028. PubMed PMID: 30055290.

52. Ji Y, Di W, Yang Q, et al. Inhibition of Autophagy Increases Proliferation Inhibition and Apoptosis Induced by the PI3K/mTOR Inhibitor NVP-BEZ235 in Breast Cancer Cells. Clinical Laboratory. 2015;61(8):1043-1051. doi: 10.7754/clin.lab.2015.150144.

53. Yang J, Pi C, Wang G. Inhibition of PI3K/Akt/mTOR pathway by apigenin induces apoptosis and autophagy in hepatocellular carcinoma cells. Biomed Pharmacother. 2018 Jul;103:699-707. doi: 10.1016/j.biopha.2018.04.072. PubMed PMID: 29680738.

54. Degtyarev M, De Maziere A, Orr C, et al. Akt inhibition promotes autophagy and sensitizes PTEN-null tumors to lysosomotropic agents. J Cell Biol. 2008 Oct 6;183(1):101-16. doi: 10.1083/jcb.200801099. PubMed PMID: 18838554; PubMed Central PMCID: PMCPMC2557046.

55. Jayashankar V, Edinger AL. Macropinocytosis confers resistance to therapies targeting cancer anabolism. Nat Commun. 2020 Feb 28;11(1):1121. doi: 10.1038/s41467-020-14928-3. PubMed PMID: 32111826; PubMed Central PMCID: PMCPMC7048872.

Chapter Four

Conclusions and Future Directions

Conclusions

Autophagy in cancer is complex. It is still not completely clear when to inhibit or enhance autophagy in individual patients. Understanding how and when to modulate autophagy and in what context is important for the most effective anticancer therapy.

Since HCQ is being used in many clinical trials as an autophagy inhibitor, it is vital to understand if and how it is effectively affecting its target. With the equivocal response to HCQ reported so far in clinical trials, relating the pharmacokinetics to the pharmacodynamics helps elucidate how HCQ is working in patients. Here, the pharmacokinetics of HCQ was established *in vivo* in non-tumor bearing mice. The pharmacokinetics of the metabolite DHCQ was also assessed. Since DHCQ is an active metabolite, it contributes to the action of HCQ. It is probably a contributing factor to toxicities sometimes associated with HCQ in clinical trials. With ample pharmacokinetic data for HCQ available in humans, the human equivalent dose in mice was established. This is important since it allows other researchers to use clinically achievable exposures in preclinical studies.

Autophagy inhibition was assessed in multiple tissues in non-tumor bearing mice, and similar to clinical trials, was variable depending on the mouse and tissue analyzed. Although LC3-II expression was increased as a marker for autophagy, p62 was variable

and not consistent across HCQ-treated mice. This suggests better biomarkers are necessary to assess autophagy clinically. Relating the concentration of HCQ and DHCQ measured over time to the pharmacodynamic assessment of autophagic flux by LC3 levels in the liver showed counterclockwise hysteresis which means although HCQ is quickly detected in whole blood, the effect of HCQ on autophagy inhibition is not immediate. Autophagy inhibition was sustained through 72 hr and likely longer than what was analyzed here due to the long half-life of HCQ.

Further, cellular response in 2D cell culture, 3D tumor organoids, and tumor xenografts grown in mice is overall similar following HCQ treatment. This is important because it means that *in vitro* methods can be used to study cellular responses in experiments where it would be hard to assess responses *in vivo*. For instance, some breast cancer cell lines do not grow as tumor xenografts in mice. The methods here establish tumor organoids as a viable option to study cellular responses in these tumors. Importantly, correlating HCQ *in vivo* exposure as measured in patients to *in vitro* exposure also established that effects observed in response to HCQ in *in vitro* experiments are achievable in patients since concentrations of HCQ that are measured in humans are low enough to elicit effects *in vitro*.

HCQ decreased autophagic flux regardless of autophagy dependency status in both 2D cell culture and tumor organoids. However, autophagy dependency made a difference when assessing cell death and cell cycle following HCQ treatment. HCQ failed to cause caspase-dependent cell death *in vitro* or *in vivo* in all tumors tested but it did cause more caspase-independent cell death earlier and decreased cell proliferation in autophagy dependent tumors but not in autophagy independent tumors. This

demonstrates that HCQ can be an effective anticancer therapy in the correct context (i.e., in autophagy dependent tumors) but that it may be better as a combination therapy treatment in most circumstances. Better or more specific autophagy inhibitors should also be considered and tested.

Although breast cancer is known to be differentially dependent on autophagy for survival and this dependency correlates to autophagy inhibition, the same is not known in OSA. Given the lack of advancement in treatments for OSA patients, there is a need for more targeted therapies for OSA, and autophagy is a promising prospect. Here, OSA was revealed to be intermediately to very dependent on autophagy based on an autophagy genetic screen, suggesting autophagy inhibition may be a viable treatment option for many OSA patients. All OSA tumors tested are dependent on ATG7 and ATG12, two genes required for the elongation of the pre-autophagosome membrane. It would be interesting to test if targeting this step of the autophagic pathway preferentially affected tumor cells but not normal cells.

While most OSA cells tested were initially dependent on autophagy for survival, with the correct selective pressure, some tumor cells were able to survive despite loss of canonical autophagy. Overall survival mechanisms have some similarities across different tumors such as increased extracellular matrix receptor interaction, focal adhesion, and PI3K-Akt signaling. However, the various clones responded differently to stressors. This included serum starvation; clones of two of the cell lines did not behave differently compared to the respective wild-type (they all died) but the ATG7 deficient clones of one cell line were not only able to survive, they actively proliferated in the serum starvation conditions and did not die. This indicates these autophagy deficient cells adapt

differently to the loss of autophagy. This was further supported by analyzing the number of lysosomes produced and the ability or lack thereof of the cells to upregulate macropinocytosis. One cell line and its autophagy deficient clones had lower numbers of lysosomes and also did not upregulate autophagy while another cell line and its clone had high basal lysosomal numbers and also upregulated macropinocytosis. This was further complicated by the fact that both cell lines and its autophagy deficient clones were still sensitive to lysosomal inhibition. This demonstrates the biologic complexity of mechanistically changing signaling pathways tumor cells use. Even if the same pathway is diminished, cells have drastically different responses that may be impossible to fully predict.

In contrast to some literature, autophagy deficient OSA cells were not necessarily more sensitive to chemotherapies such as doxorubicin or carboplatin. This was further complicated by differences between analyzing cell growth as a measure of sensitivity compared to evaluating cell death since some autophagy deficient clones were not growth inhibited by did have higher cell death or were growth inhibited but did not experience more cell death. This suggests it is important to design experiments with the correct endpoints to understand how a drug is affecting cells. Assessment of only cell growth or only cell death may not be enough to elucidate what is actually going on.

Another important thing discovered about OSA was there is no pattern of sensitivity to autophagy inhibition by HCQ between human and canine OSA. This suggests that most human OSA will likely be intermediately to very dependent on autophagy assessed by a genetic screen. Taking the results from the breast cancer studies, it further implies that HCQ sensitivity should correlate to autophagy dependency because their HCQ

sensitivities fall within the same ranges as breast cancer. Overall, these studies highlight the complexity of autophagy dependency and autophagy inhibition but shed some light on how to move forward with autophagy inhibition in the clinic.

Future Directions

Overall, there is still much to be learned about autophagy dependency and autophagy inhibition. The use of HCQ as a monotherapy for autophagy inhibition has still not been fully promising in clinical trials and as such, more evidence proving that HCQ and chemotherapy combination therapies will work is important. This should be done in as clinically relevant way as possible. Therefore, combination studies using tumor organoids would be advantageous since it is a model that more closely mimics *in vivo* and patient responses. Applying the same types of experiments used here can provide insight and expand upon the probable advantage of HCQ treatment as a combination therapy. Further, this model can be used to study how cells involved in the tumor microenvironment affect autophagy inhibition alone or in combination treatments due to the straightforwardness of co-culturing cells in organoids.

One of the issues the experiments here exposed is the difference between specific autophagy inhibition such as genetic knockout of autophagy genes versus inhibition of autophagy using an agent that has autophagy independent functions such as lysosomal inhibitors. This was apparent when ATG7 deficient cells were not sensitized to carboplatin or doxorubicin when those chemotherapies cause upregulation of autophagy as a mechanism of resistance. Therefore, combination studies should be performed to determine if autophagy inhibition by autophagy specific inhibitors (such as a VPS34

inhibitor) are sufficient to re-sensitize tumors to therapy or if there is an advantage to using lysosomal inhibitors in combination therapies. It may be found that lysosomal inhibition is more effective than specific autophagy inhibition or that in certain contexts specific autophagy inhibition works, but if lysosomal inhibition works all the time, it is worth pursuing more potent lysosomal inhibitors for autophagy inhibition in the clinic. Further, given that initially autophagy dependent cells were able to survive despite loss of autophagy, investigating cyclic therapy of autophagy inhibition with other therapies may help prevent autophagy resistance and also provide enough blockage of autophagy to keep patients sensitive to their therapies.

There is still more work to be done to elucidate the complexity of autophagy in OSA patients. Some immediate experiments that can explored is a more in-depth analysis of the RNA seq data from the ATG7 deficient clones. Some of this data should also be validated *in vitro* and *in vivo* to strengthen some of the conclusions drawn from this bioinformatic analysis. Further, performing the autophagy CRISPR screen in human OSA lines would be a nice supplement to the work done in canine OSA and would provide further evidence for autophagy dependency in OSA. Correlating the autophagy dependency determined by a genetic screen here to pharmacologic autophagy inhibition is also important to make a stronger case for clinical trials using autophagy inhibition in OSA patients. It would be advantageous to generate an autophagy dependency signature to predict what patients would potentially benefit from autophagy inhibition. Ideally, all of this eventually lays the groundwork for positive outcomes from clinical trials targeting autophagy inhibition.